MINISTRY OF NATIONAL EDUCATION

THE ANNALS OF "DUNAREA DE JOS" UNIVERSITY OF GALATI

Fascicle IX
METALLURGY AND MATERIALS SCIENCE

YEAR XXXV (XXXX)
March 2017, no. 1

ISSN 1453-083X

2017
GALATI UNIVERSITY PRESS

EDITORIAL BOARD

Table of Contents

THE ANNALS OF "DUNAREA DE JOS" UNIVERSITY OF GALATI
FASCICLE IX. METALLURGY AND MATERIALS SCIENCE
Nº. 1 - 2017, ISSN 1453-083X

LEAN MANUFACTURING – STREAMLINING PROCESSES AND ELIMINATING WASTE APPLIED TO THE ROMANIAN AUTOMOTIVE INDUSTRY

Ovidiu AMBRUS
TRW Automotive Systems, Timisoara, Romania
email: ovidiu.ambrus@trw.com

ABSTRACT

Lean Manufacturing is currently the most important management method for the production companies. The method is used in conjunction with the quality instrument referred to as "6 sigma", derived from the Toyota production system, and was adapted by Womack and Jones, in 1995, for the western companies, referring to the basic capabilities of the companies. Lean Manufacturing means dividing the production system into flexible assembly lines or cells, streamlining and reducing the time for complex operations. Also, implies using workers highly qualified for certain operations, well-made products, a wider range of interchangeable parts. All the above mentioned is achieved through excellent quality, which is a must, reducing costs by improving the production process, international markets and world competition.

These concepts were applied by the author at TRW (Romanian company from automotive domain), with significant results.

KEYWORDS: manufacturing, lean manufacturing, cost, optimization, Romanian automotive industry

1. Introduction

The elements of the activity provided are not static, but Lean methodology offers stability and reduces variation, the essential elements for a continuous improvement. Therefore, the transition from one standard to another, from one product or process to another is done smoothly.

Lean Manufacturing, or production at minimum costs, is a production philosophy defining the reduction of time from customer demand to product delivery, by eliminating waste. The implementation of LEAN principles has become a survival strategy in a production environment in which the COST reduction is a market reality. If the current results of your company do not meet your expectations, you can find solutions to many of your problems, by joining the Lean world. If you want to implement improved long-term production management methods to help you identify the corporate waste and increase the production capacity while reducing the production costs, by reading this module you can get acquainted with several Lean Manufacturing concepts, which, after implementation, will result in:

1) significant reduction in human effort in the production area – enabling reduction of workforce used;

2) reduction in finished products defects by half – huge impact on inventory& stocks;

3) reduction in the production preparation time to one third – enabling more production on the same equipment;

4) reduction to one tenth or less of the unfinished production.

2. Terminology used

According to Taichi Ohno's classification [1], the 7 types of waste in production are:

1. Overproduction: production ahead of the demand of the downstream process/customer. It is the worst form of waste, as it is the direct originator of the other 6 types of waste.

2. Waiting: operators interrupt their work during the breakdown of machinery, equipment or delays in the materials/ drawings/ parts needed for processing.

3. Transportation: moving parts and products that are not actually required, as for instance from the processing line to storage and back to the shop floor –

to the next process, while it would be more efficient to set the next process in the immediate vicinity of the first processing station [2].

4. Over Processing: performing some unnecessary or incorrect operations because of inappropriate tools or by lack of attention.

5. Inventory: holding a larger inventory than the minimum required for the pull production system to operate.

6. Motion: operators move more than it is required – e.g. looking for parts, equipment, documents, repeated movement of tools, etc.

7. Repairing: inspection, reprocessing, scraps.

Efficiency: Meeting exact customer requirements with the minimum amount of resources. Apparent efficiency versus true efficiency: Taichi Ohno distinguishes between the apparent efficiency and the true efficiency by an example with some workers producing 100 units daily. If improvements to the process boost the output to 120 units daily, there is an apparent 20 percent gain in efficiency. But this is true only if demand also increases by 20 percent. If demand remains stable at 100 units, the only way to increase the efficiency of the process is to figure out how to produce the same number of units with less effort and capital.

The following figures show an example of efficiency for a working cell [3], implemented into TRW Automotive Timisoara:

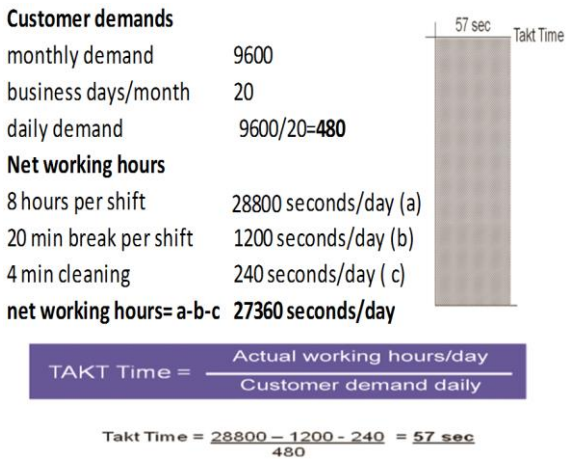

Fig. 1. *Calculating takt time based on customer's requirements* [3]

Starting from the original given customer's demands, given the working days in each region/country, the daily demands can be easily calculated. Furthermore, given the working schedule per shift and considering the regulated breaks and downtimes (cleaning, 5 S...), the needed takt time in order to satisfy customer's demands is calculated above.

Next step is to calculate the planned cycle, which has to be always lower than the takt time, including potential or accepted wastes, as shown in Figure 2 [3].

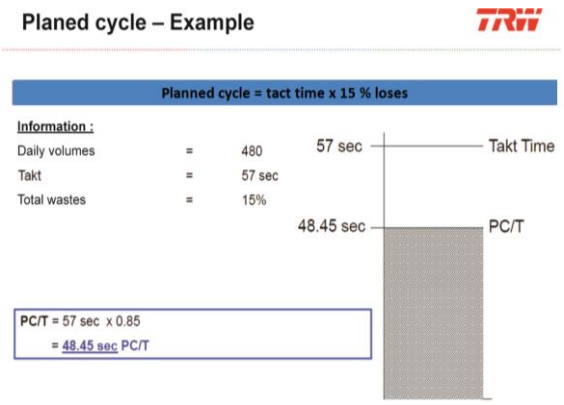

Fig. 2. *Planned cycle definition at TRW Automotive* [7]

The essential step in this exercise is to recognize and eventually eliminate waste contributors. In order to be able to perform this activity, the task or job has to be split in the smallest possible elements (called 'work elements' according to Jeffrey K. Liker and David Meier's [4] definition of Lean. These simple elements sum up the activity per each workbench or each operator, summarizing both 'value- add operations' [4] and 'non-value add' ones as waiting, walking, pulling and so on.

The figure below (Fig. 3) is a typical example of a production system before a Lean evaluation was performed: each operator's tasks are given based on some time measurements, but there are some obvious issues: one operator (operator 3) will constantly delay the overall takt time, while his given time is higher than the needed takt, all other operators have to perform tasks which are not utilizing their available time in a rigorous manner. As a result, the line or cell will constantly run behind the takt, while it will still assume certain inefficiency.

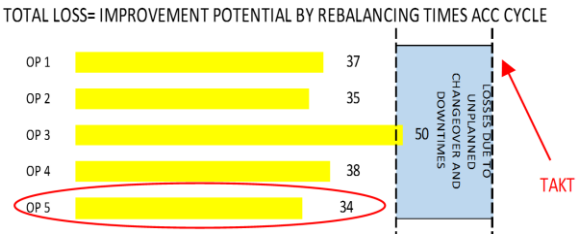

Fig. 3. *Analysis of total wastes at TRW Automotive* [7]

The main elements contributing to the improvement of cell performance/waste elimination are:

1) Ergonomics - the science concerned with the improvement of operator performance in relation to:

- work;
- equipment;
- environment.

Are ergonomics and human factors the same thing?

Essentially yes, they are different terms with the same meaning but one term may be more likely to occur in one country or in one industry than another. They can be used interchangeably but itis pretty cumbersome to read "ergonomics and human factors".

So, what is ergonomics (or human factors)?

"Ergonomics is about designing for people, wherever they interact with products, systems or processes. We don't usually notice good design (unless perhaps, it is exceptional) because it gives us no reason to, but we do notice poor design. The emphasis within ergonomics is to ensure that designs complement the strengths and abilities of people and minimize the effects of their limitations, rather than forcing them to adapt. In achieving this aim, it becomes necessary to understand and design for the variability represented in the population, spanning such attributes as age, size, strength, cognitive ability, prior experience, cultural expectations and goals. Qualified ergonomists are the only recognized professionals to have competency in optimizing performance, safety and comfort" [5].

The 4 principles of saving movement (ergonomics) [6]:

a. Elimination – reduction of the number of movements;

b. Combination – more than 2 movements at a time;

c. Reduction – distance of movement;

d. Smoothness – rhythmic movements.

2) Product flow – ideally in a U-shape, with no 'recurrences' or 'loops'.

3) Configuration and definition of the station should be as simple as possible.

4) Simple delivery of materials to stations.

5) Flexible operators (with various levels of expertise).

By eliminating the 7 waste methods or re-balancing cell (moving the operations from one station to another so that waste should disappear or get minimized), significant results are obtained, as presented in below figure (Fig. 4): while the imposed takt time is kept, with no risks of slowing down the line or not meeting customer's needs, the jobs attributed to different operators were re-organized, in such a way that the value add operations were optimally combined, the non-value add operations were streamlined. As an effect, one of the operators (operator 5) which used to be needed before Lean optimization is now released from the cell. This means a high efficiency of the cell obtained – basically 20% fewer resources for the same output and no need for a higher skill set of the operators.

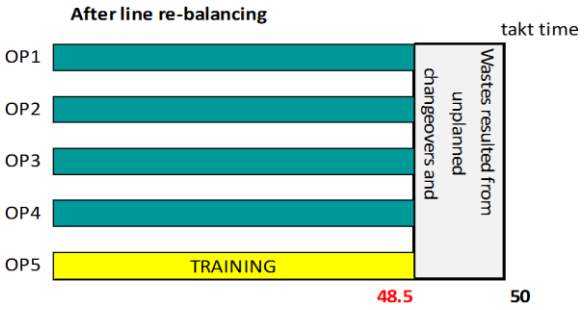

Fig. 4. *Analyzing total wastes after re-balancing at TRW Automotive*

3. Discussion: Production system. Push vs. Pull

One of the major changes driven by Lean methodology is related to the change of mentality regarding the production systems. The business terms push and pull originated in logistics and supply chain management, but are also widely used in marketing. Wal-Mart is an example of a company that uses the push vs. pull strategy (Fig. 5).

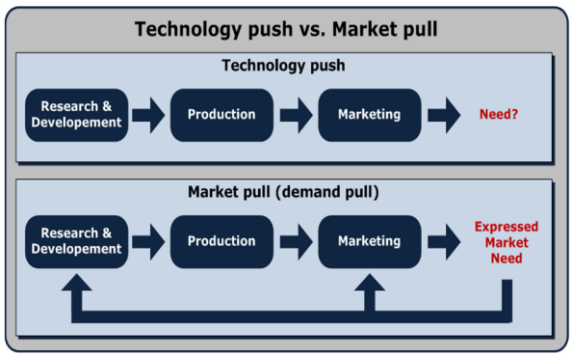

Fig. 5. *Representation of differences between "push" and "pull" systems – technology push vs. market pulling* [6]

A push–pull system in business describes the movement of a product or information between two subjects. On markets, the consumers usually "pull" the goods or information they demand for their needs, while the offerors or suppliers "push" them toward the consumers. In logistics chains or supply chains, the stages are operating normally both in push- and pull-manner. Push production is based on forecast

demand and pull production is based on actual or consumed demand. The interface between these stages is called the push–pull boundary or decoupling point, as it can be seen below in Figure 5.

The two major systems (push system, the 'classical one' and the Lean driven pull system are represented in the pictures below (Fig. 6 and Fig. 7):

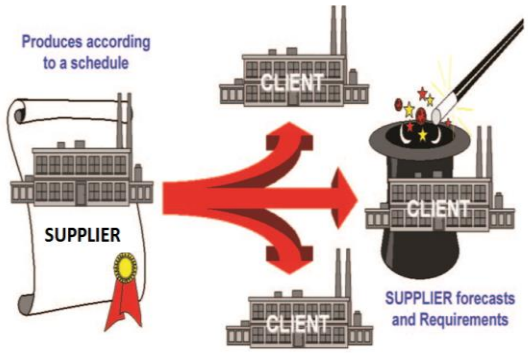

Fig. 6. *Push system characteristics*

The major characteristics of this production system [7]:

- Scheduling production – time, resources, effort needed.
- Difficult control of stocks.
- Problems become invisible – due to the manufacturing batches.
- Increased delivery time.
- Poor quality.
- Complex systems for control.

Pull System means 'pulling' the inventory/demands to the next production step (Fig. 7).

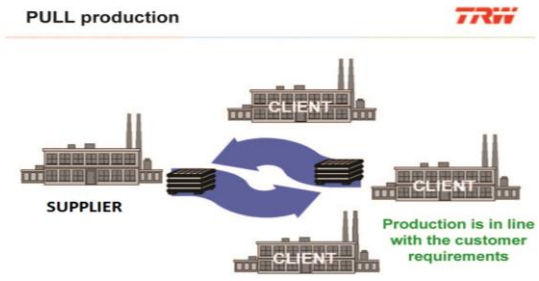

Fig. 7. *Pull system characteristics at TRW Automotive* [6, 15]

The major characteristics of this production system [7, 11]:

- Production is scheduled according to customer's requirements.
- Inventory is controlled and monitored.
- Problems are visible.
- Decreased delivery time.
- Good quality.
- Visual and simple systems for production control.

By implementing the „pull" production system, production becomes more flexible as the members of the work teams "correlate" their progress rate among them, with no need for complex time schedules to standardize work or other laborious analyses to balance work at the workstations. The need for planning and management is reduced as the work teams ensure the continuous flow by self-balancing the workloads – a very simple self-organized form of distributing work, which entails an automatic balancing of the line, at the level of the quickest operator. According to Imai Masaaki, the major benefits of these systems refer to the fact that they:

- are an excellent means of visual control.
- eliminate overproduction.
- indicate priorities.
- simplify production control.
- control the location of materials.
- controls the balancing of operations.
- easily adapt to fluctuation in demands.
- store and move the exact amount of materials required where required.
- avoid stagnation.
- reduce delivery times and wastes.

4. Conclusion

When to use Pull/Push strategy:

a. Push based supply chain strategy, usually suggested for products with small demand uncertainty, as the forecast will provide a good direction on what to produce and keep in inventory, and also for products with high importance of economies of scale in reducing costs [18].

b. Pull based supply chain strategy, usually suggested for products with high demand uncertainty and with low importance of economies of scales, which means, aggregation does not reduce cost, and hence, the firm would be willing to manage the supply chain based on realized demand [18].

These concepts are ready for application in the automotive industry in Romania (TRW - Timisoara) so as to achieve the expected efficiency parameters.

The author, together with a team involved in this process, has carried out a thorough evaluation and analysis of technological processes and manufacturing, and the concepts outlined above are materialized at the level of intercourse.

References

[1]. Taiichi Ohno, *Toyota Production System: Beyond large-scale production.*

[2]. Allen J., Robinson C., Stewart D., *Lean Manufacturing - a plant floor guide*, Society of Manufacturing Engineers, 2001.
[3]. ***, *Lean manufacturing – Methods for cost reduction*, Pilot Project TRW Automotive.
[4]. Jeffrey K. Liker, David Meier, *The Toyota way Fieldbook*.
[5]. James P. Womack, *Lean Thinking: Banish Waste and Create Wealth in Your Corporation*.
[6]. Cananau N., *et al.*, *Total Quality*, EDP, Bucuresti 2009.
[7]. Jeffrey K. Liker, *The Toyota Way: 14 Management Principles from the World's Greatest Manufacturer*.
[8]. ***, *TRW Automotive Lean Guideline*, 2014.
[9]. Stamatis D. H., *Six Sigma and Beyond*, CRC Press, 2003.
[10]. Matt Barney, Tom McCarty, *The New Six SIGMA: A Leader's Guide to Achieving Rapid Business Improvement*, Prentice Hall PTR, 2003.
[11]. Kai Yang, Basem S. El-Haik, *Design for Six Sigma*, McGraw-Hill Professional, 2003.
[12]. Brown Jim, *Leveraging the Digital Factory. Executive Summary*. Industrial Management, vol. 51, july/august 2009.
[13]. Black J. T., Kohser R. A., *DeGarmo's Materials & Processes in Manufacturing*, 10th Edition, Wiley, 2007.
[14]. ***, *Definition of DMADV*, Kuala Lumpur, Malaysia: Lean Sigma Institute, Anonymous, 2005.
[15]. Brue G., Launsby R., *Design for Six Sigma*, New York: McGraw-Hill, 2003.
[16]. Duguay C., Landry S., Pasin F., *From mass production to flexible/agile production*, International Journal of Operations & Production Management, 17(12), p. 1183-1195, 1997.
[17]. Fredriksson B., *Holistic systems engineering in product development*, The Saab-Scania Griffin, November 2006.
[18]. ***, https://books.google.ro/books?id=CuP3VPPUz0wC&pg=PA13&lpg=PA13&dq=%22high+importance+of+economies+of+scale%22&source=bl&ots=IqfGPUHzLk&sig=GXzs3__ZQTQ0D_4ISzX2HPzV06c&hl=ro&sa=X&ved=0ahUKEwilm6O5pJHYAhWQLlAKHYOXAL0Q6AEIJjAA#v=onepage&q=%22high%20importance%20of%20economies%20of%20scale%22&f=false.

THE ANNALS OF "DUNAREA DE JOS" UNIVERSITY OF GALATI
FASCICLE IX. METALLURGY AND MATERIALS SCIENCE
Nº. 1 - 2017, ISSN 1453-083X

LEAN - A PHILOSOPHY HIGHLIGHTING THE VALUE ADDED THROUGH SELF IMPROVEMENT AND WASTE REDUCTION, CONCEPTS PRESENTED FROM THE EXPERIENCE OF THE ROMANIAN AUTOMOTIVE INDUSTRY

Ovidiu AMBRUS
TRW Automotive, Timisoara, Romania
e-mail: ovidiu.ambrus@trw.com

ABSTRACT

The definition of Lean n is: eliminating all sources of error, time and effort that are not necessary starting with the raw materials and up to the final product, from order to delivery and from design to launch. TRW is a Romanian company from the automotive domain, having experience in using new concepts based on the lean manufacturing philosophy.

KEYWORDS: Lean evaluation, flexible production philosophy, reaction time

1. Introduction

The Lean evaluation is performed by taking into account multiple factors, among which the socio-technical system, namely the internal elements (the internal system) and the environment. The Lean evaluation is performed for achieving a mutually defined target. For the Lean evaluation, the inputs of the internal system, the environment and the desired outputs are taken into account. The inputs of the internal system are defined by labor, materials, capital, energy, information, by the correlations, influences and continuous interactions of the internal system with the environment that is in a state of constant change. The environment is represented by society, natural environment, market, technology, government, etc. The desired outputs can be products/services, or undesired outputs such as pollution, losses, wastage.

2. Lean Methods

The Lean evaluation, according to studies published by the well-known expert James P. Womack [1], can be performed through various measurements and analyses, from which data is collected and analyzed, immediate feedback is received for problem control and actions are taken according to the data collected for performance improvement.

The most well-known and used instruments for problem identification are:

1. PDCA (Plan-Do-Check-Act).
2. Analysis - Cause – Effect (Ishikawa).
3. Pareto Analysis (ABC-Analysis, 80/20-Rule).
4. Constraint management.

Fig. 1. *PDCA (Plan-Do-Check-Adjust) diagram* [1]

PDCA (plan–>do–>check–>adjust) is a management method used in business for the control and continuous improvement of processes and products. Also known as the so called "Stewart cycle", it consists in four iterative steps which are described below:

PLAN-ing - Establish the objectives and processes necessary to deliver results in accordance with the expected output (the target or goals). By establishing the output expectations, the completeness and accuracy of the specification are also a part of the targeted improvement. When possible, start on a small scale to test possible effects.

DO – The step of attacking plan implementation, process execution, of making the product or good. It also assumes data collection - used later on for analyses, graphs, charts and conclusions.

CHECKING - Study the actual results (measured and collected in "DO" above) and compare them to the expected results (targets or goals from the "PLAN") to ascertain any differences. Look for deviation in implementation from the plan and also look for the appropriateness and completeness of the plan to enable the execution, i.e., "Do". Charting data can make much easier to see trends over several PDCA cycles and in order to convert the collected data into information. Information is what you need for the next step "ADJUST" [1].

ADJUST - If the CHECK shows that the PLAN that was implemented in DO is an improvement to the prior standard (baseline), then that becomes the new standard for how the organization should ACT going forward. If the CHECK shows that the PLAN that was implemented in DO is not an improvement, then the existing standard will remain in place. In either case, if the CHECK showed something different than expected (whether better or worse), then there is some more learning to be done... and that will suggest potential future PDCA cycles. It should be noted that someone who teach PDCA assert that the ACT involves making adjustments or corrective actions, but generally it would be counterproductive to PDCA thinking to propose and decide upon alternative changes without using a proper PLAN phase, or to make them the new standard (baseline) without going through DO and CHECK steps [1].

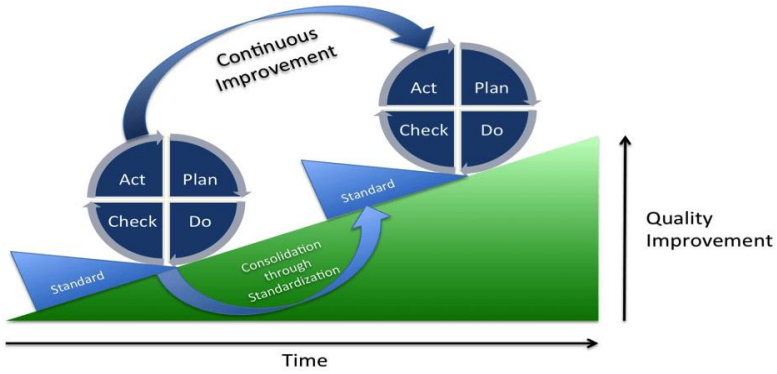

Fig. 2. *Quality improvement cycle through PDCA method* [20]

The fishbone diagram identifies many possible causes for an effect or problem. It can be used to structure a brainstorming session. It immediately sorts ideas into useful categories.

Where can a Fishbone Diagram be used? [2]

First - when we are trying to identify potential root causes of problems;

Second – when analyses performed by the team have become dull and unproductive but it is hard to change them.

Stewart circle comes with a kind of "procedure" -including several steps to be fulfilled, steps listed below:

The effect of the problem- symptom- is to be collected into the center of the whiteboard, circumcised by a box. A horizontal line, the "spine" of the "fish", is to be drawn underneath.

Use the "5 M" approach in order to brainstorm on the top categories of root-causes. "5 M" approach assumes touching all potential areas of root-causes, i.e.:

MAN
METHOD
MACHINE
MATERIAL
MOTHER NATURE (Environment)

Write the categories of causes as branches from the main arrow [1].

Brainstorm on all the possible causes of the problem. Ask: "Why does this happen?" As each idea is given, the facilitator writes it as a branch from the appropriate category. Causes can be written in several places if they relate to several categories [1].

Ask again "why does this happen?" about each cause. Write sub–causes branching off the causes. Continue to ask "Why?" and generate deeper levels of causes. Layers of branches indicate causal relationships [1].

When the group runs out of ideas, focus attention on places of the chart where ideas are few [1].

Fishbone Diagram Example:

For example, under the heading "Machines," the idea "materials of construction" shows four kinds of equipment and then several specific machine numbers.

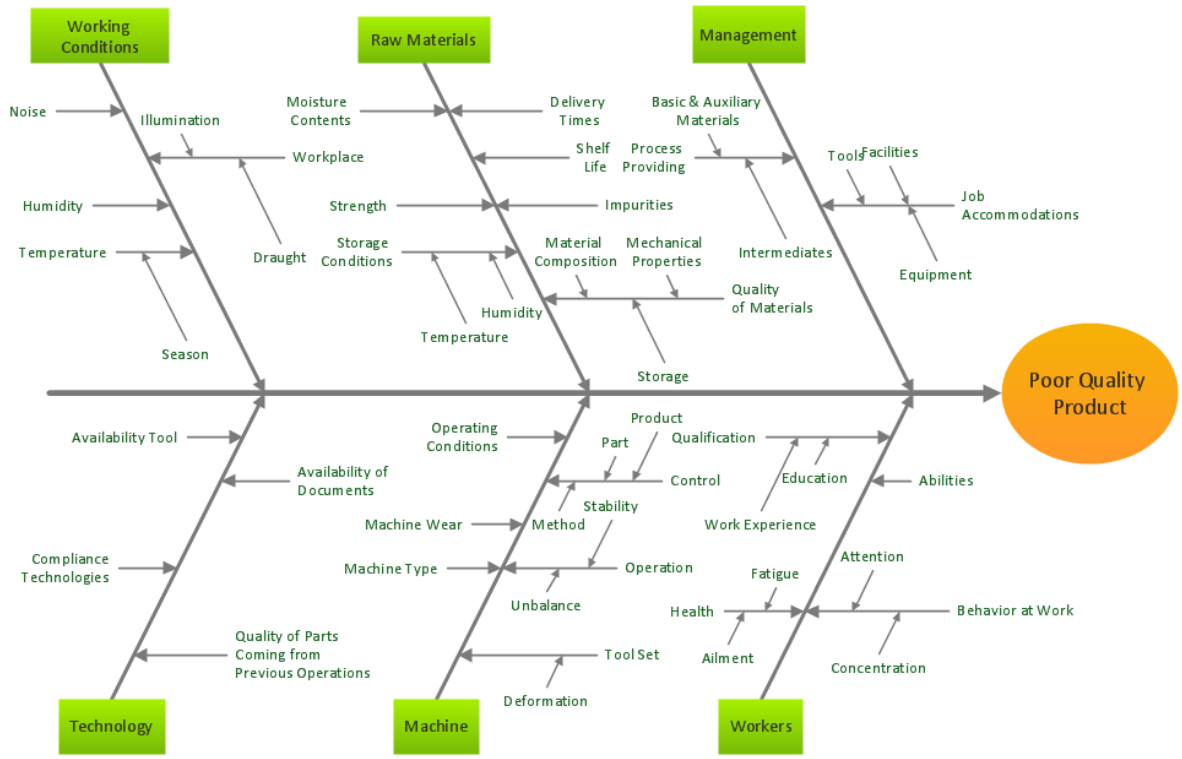

Fig. 3. *Continuous quality improvement example with fishbone diagram at TRW Automotive*

Note that some ideas appear in two different places. "Calibration" shows up under "Methods" as a factor in the analytical procedure, and also under "Measurement" as a cause of lab error. "Iron tools" can be considered a "Methods" problem when taking samples or a "Manpower" problem with maintenance personnel [2].

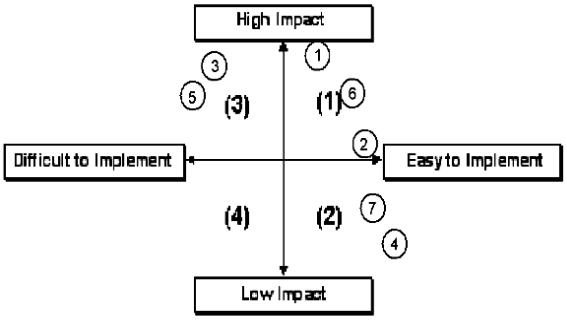

Fig. 4. *Representation of problem identification instruments Lean/6 Sigma according to* [1]

I. The 80:20 Rule to Prioritize

When it comes to simple prioritization techniques, the Pareto technique is one of the simplest one, working under the principle also known as the "80/20 Rule" – which is the concept that 20% of causes generate 80% of results. With this tool, we are trying to find the 20% of work that will generate 80% of the results delivered by all of the work performed.

How can the tool be used? [3]

1. First thing - identify the problems. Use all available source of information in order to describe the issues as accurately as possible.
2. Apply the 5 M technique for each identified problem.
4. Create a measurement/scoring system. This scoring method needs to be adapted to your needs- the most 'burning" issue will get the highest ranking.
5. Group Problems Together by Root Cause [1].
6. Add up the Scores for Each Group. The group with the top score is your highest priority, and the group with the lowest score is your lowest priority [1].
7. Take Action – Now you need to deal with the causes of your problems, dealing with your top-

priority problem or group of problems first. Keep in mind that low scoring problems may not be worth bothering with; solving these problems may cost you more than the solutions are worth taking into consideration [1].

Another method used intensely in the Lean methodology is named 'constraint management'. The principle is the following [4]:

1. A chain is as strong as its weakest link.
2. An interconnected process can produce as much as the weakest link can.
3. Improving the weakest link results in improving the entire system.

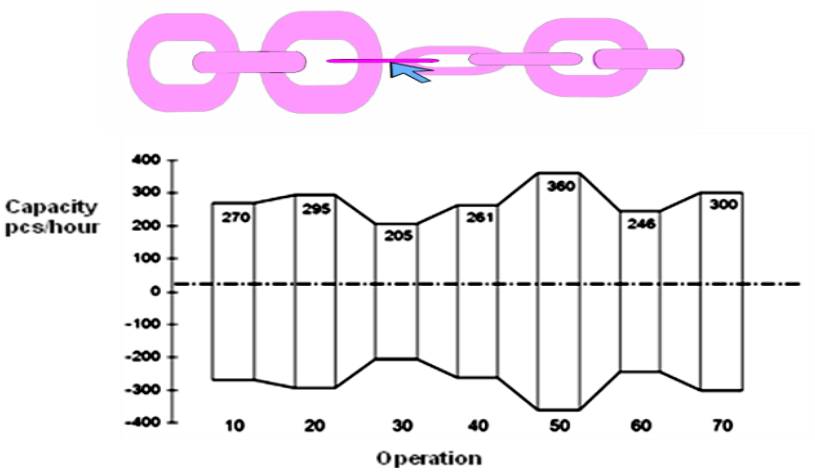

Fig. 5. *'Management of constraints' method representation – used into TRW Automotive Safety Systems, Timisoara*

Steps to follow in this methodology:

1. Identify and highlight the constraints.
2. Exploit the constraints (placing a buffer zone before and after the constraint).
3. Subordinate non-constraints to present constraints.
4. Systematically improve constraints.
5. Return to point no. 1.

The biggest issue in many enterprises is the lack of action based on the collected data, although the data is collected and reported.

A high Lean level means a higher product or service quality, while a lower level defines a low product or service quality.

II. What Exactly Can be Improved in a Plant by Using the Lean Approach

Lean Manufacturing, as it was described before, is a production philosophy that determines time reduction from the customer's order up to the product delivery, through the continuous reduction of losses.

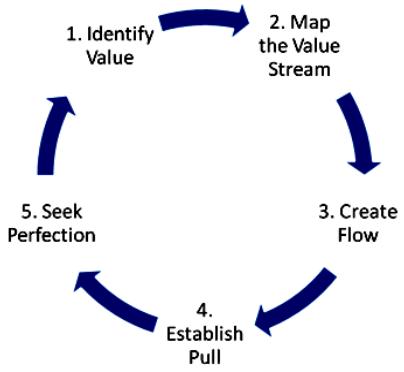

Fig. 6. *Lean universal principles*

There are many definitions, such as:

1. Lean Manufacturing is "a production philosophy that reduces the time from the customer's order until the delivery of the products, through the reduction of losses (of activities that do not add value to the product)" [4].
2. Lean Manufacturing is "A team approach, for the identification and elimination of losses (activities that do not add value to the product) through the continuous improvement of the production flow performed upon the customer's request, targeting perfection" [5].
3. Lean Manufacturing is „a way of thinking and involving in order to completely eliminate losses,

oriented towards customer success… this is obtainable by simplifying and continuously improving all processes and relationships in an atmosphere of mutual trust, respect and complete involvement of employees" [5].

4. Lean: SPC – Statistical Process Control – Control the process before it controls you! Simple controls for the operator, in order to identify the process trends, for the purpose of making educated decision, based on data [12, 14].

III. Concepts Built on the Lean Manufacturing Methodology

A. Cellular manufacturing

The manufacture area is separated in different manufacturing cells. One cell is organized for each product family. The flow is linear and regulated for each product family, but is variable for each product within the family. The machines are located within the manufacturing cell, in a certain order, so that the materials undergo a unique material flow towards the completion of the product. It is advantageous for the machines within the manufacturing cells to be smaller, more dedicated, as they operate more efficiently than the large, multipurpose machine tools.

B. Flexible manufacturing systems (SFF)

A flexible manufacturing system is an integrated computer controlled complex of numerical command machine tools, which includes an automatic transport and handling system for parts and tools, along with automated measurement and testing equipment which, with a minimum amount of manual interventions and setup time, can process any part belonging to a specific family, within the capacity thresholds and according to a predetermined schedule. The entire system is controlled by a DNC computer, usually connected to the plant central (host) computer. SFF are dedicated to specific product families, which must be manufactured in large manufacture volumes, justifying the investment. The obtained advantages are lower costs and a lower inventory of parts in progress. SFF can be designed for various types of manufacture processes: machine cutting, metal molding, assembling, welding, etc.

C. Manufacturing process management (MPM)

Is a process of defining and managing manufacturing processes to be used for the manufacture, assembling and inspection of the final products. MPM allows manufacturers to use product drawings (made in CAD) in order to define the method through which the products will be manufactured and then electronically deliver these manufacturing processes to the workshops. MPM turns „what to manufacture" into „how to manufacture", „when" and „where". MPM represents a „collection of technologies and methods used in order to define the way in which the products will be manufactured". This definition means that MPM is a process through which manufacturing industries will use various types of technology in order to aid product execution, with various machine layouts and methods for the potential layout of the assembly lines.

3. Conclusions

At each level within a manufacturing organization, the goal is to create value for the customer, according to his/her specifications. The "Lean" concept, used in the manufacture field, becomes a way of life: We do not want any losses. The Lean manufacturing targets maximum results, with minimal resource consumption (human effort, equipment, materials, time and space), increasingly and more accurately meeting the customer's needs. It is a flexible manufacturing philosophy which allows enterprises and organizations to react quickly to the evolution of market conditions and customer needs. On this idea, TRW company applied these principles and obtained some results, having now one good reference. I am particularly proud of the clear evidence of the successful implementation of these tools into Quality area. Taking the Fishbone diagram methodology, deep-diving into it, it is quite obvious that conclusions are focusing on the exact root-cause, as in the following example (Fig. 7).

Once the root-cause is determined, it is important to treat each and every potential root-cause rigorously and implement correct actions (Fig. 8 and 9).

Correct implementation and follow up grant spectacular results into the desired area. Figure 10 below shows the evolution of quality issues on a particular area (Airbag production Q issues) in TRW Automotive Timisoara after the implementation of the above-mentioned activities.

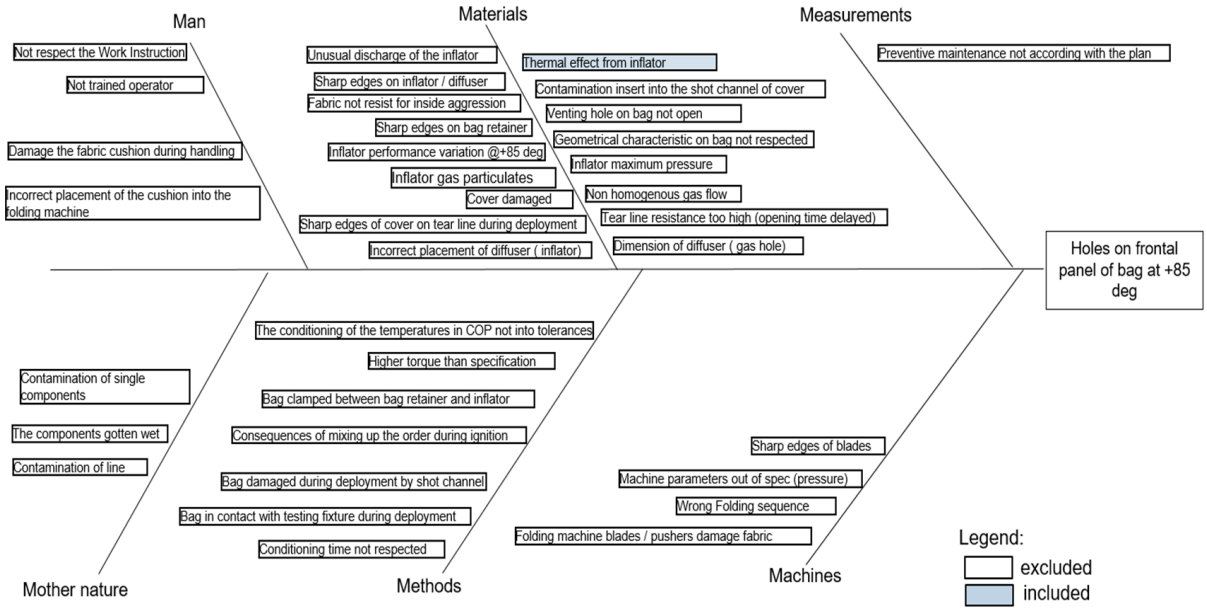

Fig. 7. *Particular example of Fishbone methodology implemented*

Fishbone item	Yes	No	Why
Not respect the Work Instruction		x	Verified shiftily by Layer Process Audit level 1 / Monthly by Layer Process Audit level 2→ The operator respect the Work Instruction
Not trained operator		x	Verified shiftily by Layer Process Audit level 1 / Monthly by Layer Process Audit level 2 → Operator trained - 3 different operators
Damage the fabric cushion during handling		x	Verified shiftily by Layer Process Audit level 1 / Monthly by Layer Process Audit level 2 → The operator respect the Work Instruction and No sharp tools used in the line
Incorrect placement of the cushion into the folding machine		x	Mistake proofing by design (sensors that are ensuring the correct position of bag into the folding machine)
Folding machine blades / pushers damage fabric		x	1. Checked 100 pcs after folding 2. Checked at First Off 3 bags after folding (general procedure) → No damages, no scratches on bags
Wrong Folding sequence		x	Automatic folding sequence
Machine parameters out of spec (pressure)		x	Verified at First Off the pressure records → Pressure into specification
Sharp edges of blades		x	Verified the blades shiftily →No sharp
Contamination of single components		x	Verified the component flow / Incoming procedure -verify 5 parts / each delivery → No risk for contamination
Contamination of line		x	Verified the line → No risk for contamination
The components gotten wet		x	Verified the components and the storage area →No wet components → the components are stored in warehouse → no risk to be wet
Preventive maintenance not according with the plan		x	Verified the preventive maintenance →The preventive maintenance was done according with the plan
The conditioning of the temperatures in COP not into tolerances		x	Verified the temperature diagram for conditioning of module → The conditioning temperature into specification
Higher torque than specification		x	The torque is automatically controlled in the line - Yearly calibration of controller / screw driver
Bag clamped between bag retainer and inflator		x	1. Checked 100 pcs after folding 2. Checked at First Off 3 bags after folding (general procedure) → No damages, no scratches on bags, no bag clamped between bag retainer and inflator
Consequences of mixing up the order during ignition		x	NA (only one stage inflator)
Bag damaged during deployment by shot channel		x	Verified the de-folding behavior of the modules → No bag damaged during deployment by shot channel
Bag in contact with testing fixture during deployment		x	Verified the de-folding behavior of the modules → No contact with testing fixture and no windscreen
Conditioning time not respected		x	Verified the records from conditioning diagram → 4 hours have been respected as conditioning time (specification: min. 4 hours; no upper limit)

Fig. 8. *Particular example of Fishbone methodology implemented- actions at TRW Automotive*

Fishbone item	Yes	No	Why
Incorrect placement of diffuser (inflator)		x	Verified the 9 inflators of NR tests → Correct placement of the diffuser Check with supplier(ZF TRW Aschau) → the position of diffuse is assured 100%
Sharp edges of cover on tear line during deployment		x	Verified the tested parts → No evidences of sharp edges on tear line
Cover damaged		x	Verified the covers → No damages on cover
Inflator gas particulates		x	1. Performed Life dissection of tested inflators of events → no abnormalities found for all 9 inflator of NR results 2. Performed the tank wash test on 3 serial inflators → no abnormalities
Inflator performance variation @+85 deg		x	Verified the Tank pressure curves → The inflators are into specification
Sharp edges on bag retainer		x	Verify the bag retainer - incoming inspection → No sharp edges on bag retainer
Fabric not resist for inside aggression		x	Verified the Quality certificate of fabric →The fabric was according with the specification
Sharp edges on inflator / diffuser		x	Verified the inflators prior to assembly → No sharp edges
Unusual discharge of the inflator		x	Verified the de-folding behavior of the modules → Opening time and bag filling time into specification
Dimension of diffuser (gas hole)		x	Verified the dimension results from ZF TRW Aschau (supplier of inflator) →All values are into the specification
Tear line resistance too high (opening time delayed)		x	1. Verify the opening time → Opening time into specification 2. Verify the tear line thickness of cover → Tear line thickness into specification
Non homogenous gas flow		x	Verified the Tank pressure curves → The inflators are into specification
Inflator maximum pressure		x	Verified the Tank pressure curves → Pressure of inflator into specification (nominal values)
Geometrical characteristic on bag not respected		x	Verify the dimension results from ZF TRW Vigo (supplier of bag) → all values into specification
Venting hole on bag not open		x	Verified all the bags of events and the movies → Venting hole are open and are working as expected according design intend
Contamination insert into the shot channel of cover		x	Verify all the covers of NR tests Verify the covers from stock and ask the supplier to check the covers from stock → No pollution insert into the shot channel cover
Thermal effect from inflator	x		TRW Aschau performed: 1. The mass flow calculation and temperature for suspicions batches were compared it with PPAP data → conclusion: mass flow calculation and temperature for suspicions batches were similar with the mass flow calculation and temperature of PPAP inflator. 2. Analysis over time of mass flow calculation and temperature by comparison , for inflators batch by batch from 2011 until 2017 → conclusion: similar behavior from one batch to the other. Root cause confirmed on the airbag module as thermal effect from inflator.

Fig. 9. *Particular example of Fishbone methodology implemented- actions at TRW Automotive*

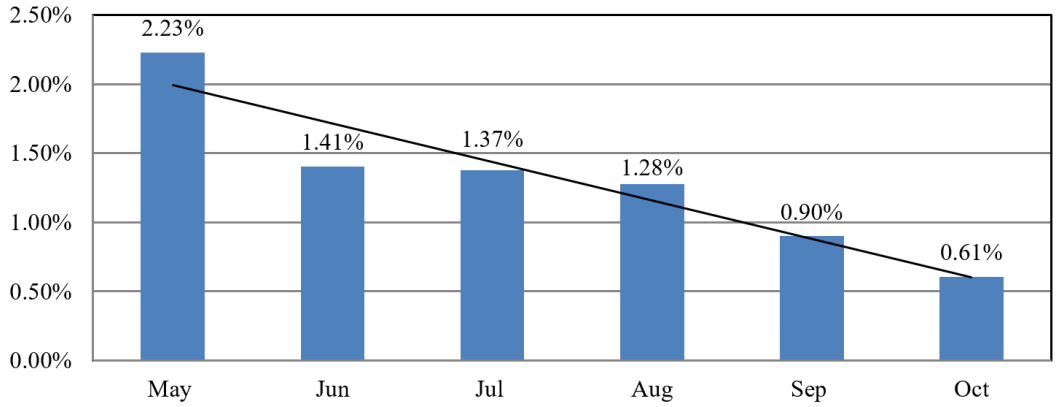

Fig. 10. *Evolution of quality issues (nonconformities) after the implementation of Fishbone driven actions at TRW Automotive*

Thus, the execution processes for products and services requested by the customer must be analyzed according to two fundamental concepts [6]:

1. Added value: Any activity determining an increase in value or utility for the product or service demanded by the market, respectively the activities for which a customer is willing to pay.

2. Loss (non-added value): Any activity that does not add value to the product or service, meaning that it "increases the product's COST without adding VALUE" for the customer. These activities need to be eliminated, simplified, reduced or integrated.

References

[1]. Rother Mike, *Toyota Kata*, New York: MGraw-Hill, ISBN 978-0-07-163523-3, 2010.

[2]. James P. Womack, *Lean Thinking: Banish Waste and Create Wealth in Your Corporation (Hardcover)*.

[3]. Nancy R., *Tague's The Quality Toolbox*, Second Edition, ASQ Quality Press, p. 247-249, 2005.

[4]. Womack J. P., Jones D. T., Roos D., *The Machine That Changed The World: How Lean Production Revolutionized the Global Car Wars*, S. &. Schuster, London, 1990.

[5]. ***, *Lean manufacturing – Methods for cost reduction, Pilot Project TRW Automotive*.

[6]. ***, http://www.lean.ro.

[7]. Art Smalley, *Creating Level Pull: A Lean Production System Improvement Guide For Production Control, Operations, And Engineering Professionals*.

[8]. Matt Barney, Tom McCarty, *The New Six SIGMA: A Leader's Guide to Achieving Rapid Business Improvement*, Prentice Hall PTR, 2003.

[9]. Kai Yang, Basem S. El-Haik, *Design for Six Sigma*, McGraw-Hill Professional, 2003.

[10]. Brown Jim, *Leveraging the Digital Factory*, Executive Summary: Industrial Management, vol. 51, 2009.

[11]. Black J. T., Kohser R. A., *DeGarmo's Materials & Processes in Manufacturing*, 10th Edition, Wiley, 2007.

[12]. ***, *Definition of DMADV*, Kuala Lumpur, Malaysia: Lean Sigma Institute, www.leansigmainstitute.com.
[13]. Brue G., Launsby R., *Design for Six Sigma*, New York: McGraw-Hill, 2003.
[14]. Duguay C., Landry S., Pasin F., *From mass production to flexible/agile production*, International Journal of Operations & Production Management, 17 (12), p. 1183-1195, 1997.
[15]. Fredriksson B., *Holistic systems engineering in product development*, The Saab-Scania Griffin, November, Linkoping, 1994.
[16]. Harry M., Schroeder R., *Six Sigma: The breakthrough management strategy revolutionizing the world's top corporations*, New York: Doubleday, 2000.
[17]. Juran J., *Quality control handbook (3rd ed.)*, New York: McGraw-Hill, 1979.
[18]. McAdam R., Evans A., *The organizational contextual factors affecting the implementation of Six-Sigma in a high technology mass-manufacturing environment*, International Journal of Six Sigma and Competitive Advantage, 1 (1), p. 29-43, 2004.
[19]. Mizuno S., Akao Y., *QFD: The customer-driven approach to quality planning and development*, Tokyo, Japan: Asian Productivity Organization, 1994.
[20]. Moore S., Gibbons A., *Is lean manufacturing universally relevant? An investigative methodology*, International Journal of Operations & Production Management, 17 (9), p. 899-911, 1997.

THE ANNALS OF "DUNAREA DE JOS" UNIVERSITY OF GALATI
FASCICLE IX. METALLURGY AND MATERIALS SCIENCE
Nº. 1 - 2017, ISSN 1453-083X

LEAN MANUFACTURING - PROCESS AUTOMATION AND ELIMINATION OF PRODUCTION LOSSES IN ROMANIAN AUTOMOTIVE INDUSTRY

Ovidiu AMBRUS
TRW Automotive, Timisoara, Romania
e-mail: ovidiu.ambrus@trw.com

ABSTRACT

Lean Manufacturing is currently the most important management method for manufacturing companies. The method, used in conjunction with the quality tool called "six sigma", is based on Toyota Production System and has been adapted by Womack and Jones, in 1995, for Western companies, referring to the real basic capabilities. Lean Manufacturing means flexible assembly cells or lines, more complex works, highly skilled workers, well manufactured products, a much larger variety of interchangeable parts, compulsorily an excellent quality, reduced costs by improving the production process, international markets and global competition [2].

TRW is an example of the practical application of these concepts, in the leather product preparation sector.

KEYWORDS: lean manufactory, automotive industry, process automation

1. Introduction

LEAN manufacturing or lean production is a systematic method for the elimination of waste ("Muda") within a manufacturing system. Lean also takes into account waste created through overburden ("Muri") and waste created through unevenness in workloads ("Mura"). Working from the perspective of the client who consumes a product or service, "value" is any action or process that a customer would be willing to pay for. Manufacturing, or *production at minimum costs*, is a production philosophy which reduces the time period between the customer's order and the product delivery, by *eliminating losses*. Implementation of LEAN principles has become a survival strategy in a production environment where COST reduction is a fact on the market. If you are not content with the current results of your company, you can find answers to many of your problems, by coming into Lean world.

Lean manufacturing pillars may be simply explained by Figure 1.

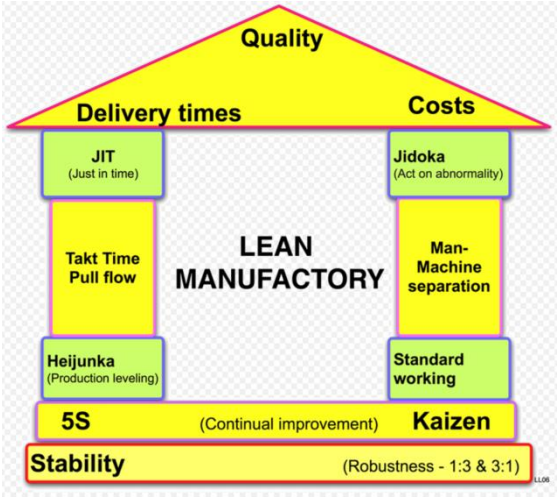

Fig. 1. *Lean Manufacturing pillars* [1]

If you want to introduce long-term production management improvement methods, to help identify losses in the company and increase the productive capacity while reducing production costs, by following this module you can get familiar with some of the Lean Manufacturing concepts, which, after implementation, will lead to:

1) Reducing by half the human effort in the production workshop.

2) Reducing by half the defects of the finished products.

3) Reducing to one-third the time of production preparation.

4) Reducing by half the production space in order to obtain the same results.

5) Reducing to one tenth or less the unfinished production.

2. Terminology used

The 7 losses in production are, according to Taichi Ohno's classification, as follows [3]:

- Overproduction: making too much compared to the downstream/customer process need. It is the most serious form of waste, because it directly determines the other 6 types of losses.

- Waiting: operators interrupt their work due to machinery or equipment failures or delay of materials/drawings/parts required for processing.

- Transport: moving parts and products unnecessarily, such as from the processing line to the warehouse and from here back in the section - to the next processing phase, when it would be more rational for the next process to be located in the close proximity of the first processing station.

- Processing: carrying out unnecessary or incorrect operations because of poor quality equipment or carelessness.

- Inventory: owning an inventory higher than the minimum required for the operation of the pull-type production system.

- Motion: operators make unnecessary movements - like finding parts, equipment, documents, repeatedly moving tools, etc.

- Corrections: inspection, rework, scrap.

Overall, there is a limit of introducing human driven improvements: there is a "barrier" over even extremely skilled operators will not deliver consistent results in terms of efficiency. There is an accepted 10-15% failure ration related to all visual inspection capabilities. Also, there is a natural tendency for operators to "adapt" the process according to their own comfort or the other way around. It is not always possible to design a process/layout/flow in such a way that is comfortable for all operators. There is an answer to all these, called automation.

Automation is the usage of computers or equipment driven/controlled by computers to drive a particular process in order to increase reliability and efficiency, often through the replacement of employees. For a manufacturer, this could entail using robotic assembly lines to manufacture a product.

Automation has been achieved by various means including mechanical, hydraulic, pneumatic, electrical, electronic devices and computers, usually in combination. Complicated systems, such as modern factories, airplanes and ships typically use all these combined techniques. The benefit of automation includes labor savings, savings in electricity costs, savings in material costs, and improvements to quality, accuracy and precision.

3. Case study: implementation of automation and benefits to be considered by TRW Automotive

Project description:

The TRW Automotive factory in Timisoara is producing steering wheels for several customers of TRW. For this task, the company is using 7 die casting machines with 1 cavity or 2-cavity tools.

a) Current situation:

At present, the production is performed using operators. The process steps can change, depending on the steering wheel type. The process steps are [4, 5]:

1. Positioning of the inlay for die casting process (Optional).
2. Armature check.
3. Laser marking.
4. Armature cooling.
5. Positioning of the armature in the trimming press.
6. Positioning of the rim inlays (Optional).
7. Armature hand over to transport buggy.

b) Future state/Project objectives:

The casting process will be changed from a manual to an automatic process. Each of the existing die casting machines will be automated step by step. Each of the sub-processes will be evaluated and the best automation solution will be decided upon:

1. Positioning of the inlay for die casting process will be ensured by a robotic arm.
2. Armature check-gauging (automatic process) and weighting (also automatic).
3. Laser marking.
4. Armature cooling-changed, will introduce a second robot collecting the armatures from the oven.
5. Positioning of the armature in the trimming press - automatic process.
6. Positioning of the rim inlays (Optional) - automatic process.
7. Armature hand over to transport buggy - automatic.

The new process steps will be the following [4]:

1. Armature extraction.
2. Mold lubrication (spraying robot or spraying machine).
3. Part integrity check.
4. NIO armature discard in scrap box (not shown in the picture below).

5. IO armature laser marking.
6. Armature cooling.
7. Positioning of the armature in the trimming press.
8. Place rim inlay in the trimming press (rim inlay robot or linear axis).
9. Pick up inlay for the die casting process (rim inlay robot or linear axis).
10. Return to die casting machine.

Overall changes implemented into each process step, concluded as being most suitable ones, are presented in Figure 7.

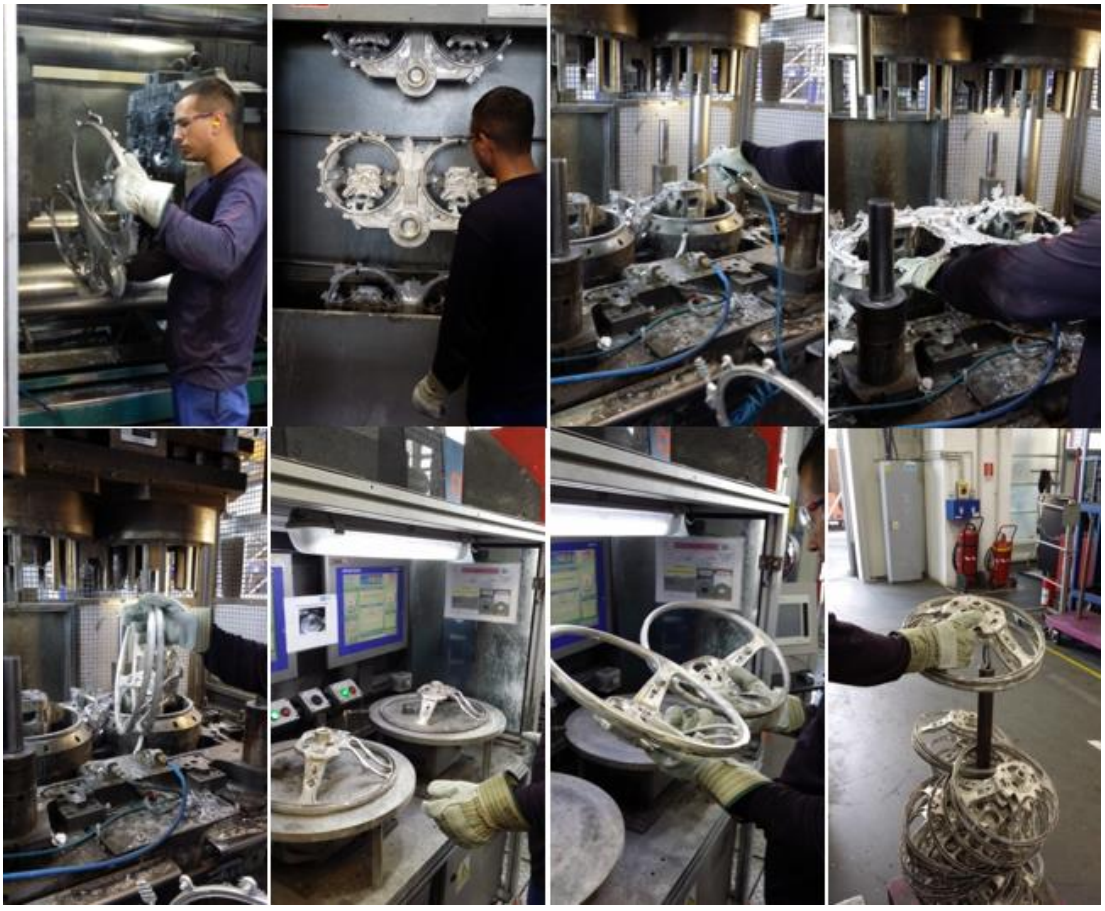

Fig. 1. *The 7 process steps of die casting, performed manually or semi-automatically at TRW Automotive, before the implementation of automation*

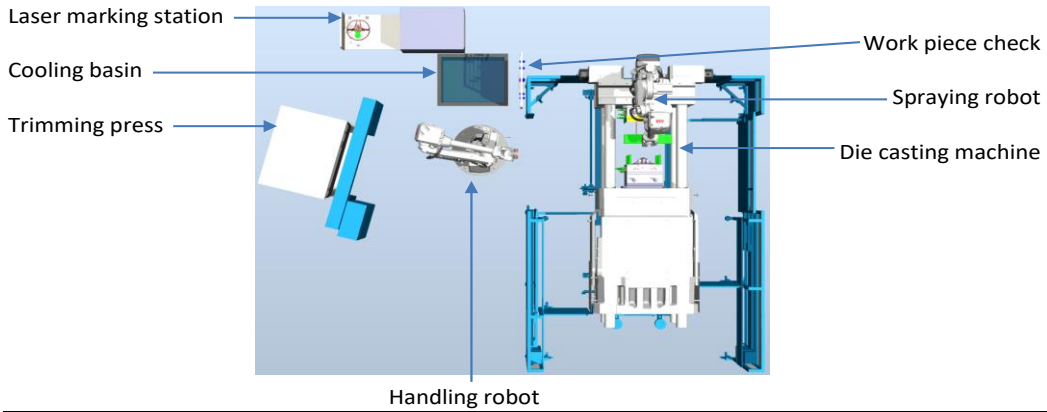

Fig. 2. *New process steps schematics - introduction of the first handling robot*

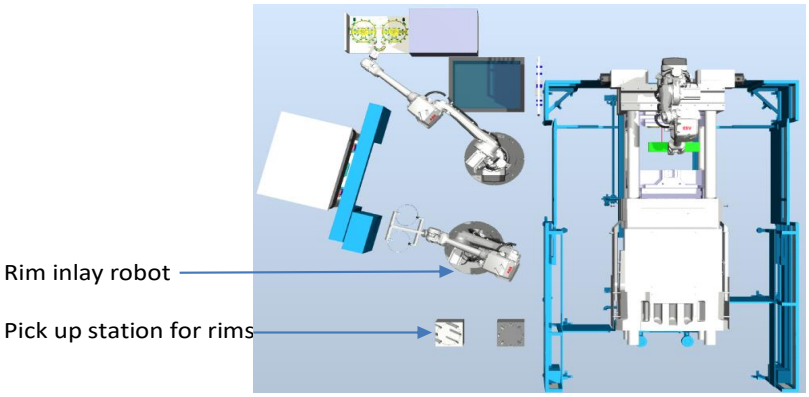

Fig. 3. *New process steps schematics- introduction of the second handling robot*

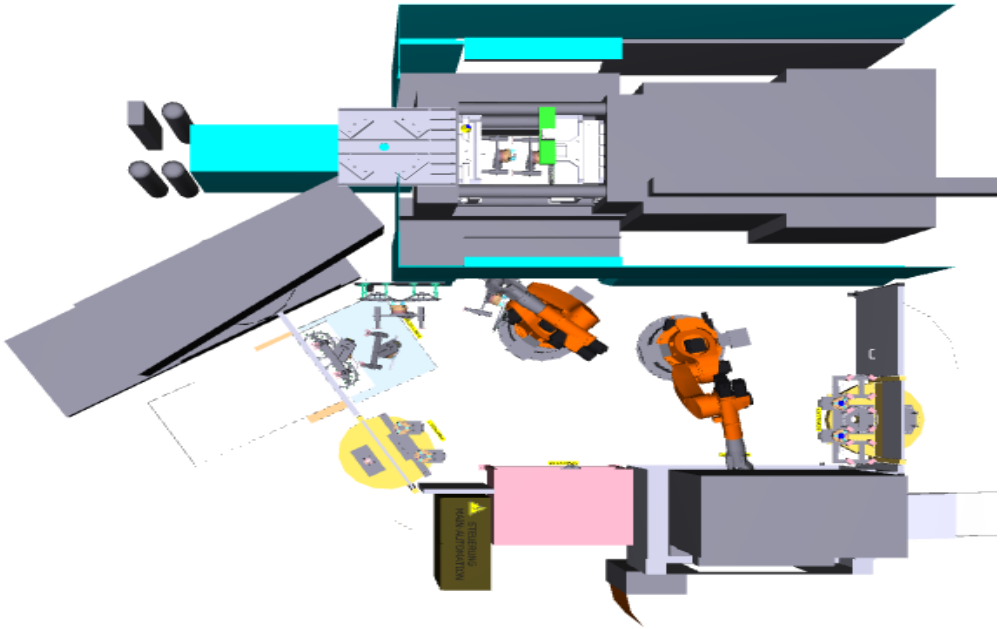

Fig. 4. *New layout of the die casting machine- after the implementation of automation*

Fig. 5. *Activities related to the automation process implementation at first/prototype cell at TRW Automotive*

Fig. 6. *Activities related to the automation process implementation at first/prototype cell at TRW Automotive*

Changes	From	To	Why	effect to product
release agent method	manual	automated	constant/Standard	+
release agent media	Oil	Micro spray (HERA)	Environment/Safety/Standard	0
feeding of inserts	manual	automated	constant/Standard	0
overflow check	manual	automated	constant/Standard	++
cooling	dip into water per elevator	dip into water per robot	standard	0
metal insert verification	manual at weight station	automatic check at overflow detection	constant/Standard	++
weight control	in line shot by shot	First Off/Last Off	no shot to shot variance	0
laser marking	not implemented	single unit traceability	traceability/standard	0
trimm press cleaning	manual	automated	constant/Standard	+

Fig. 7. *Table of changes and benefits on product by the implementation of the automation process on die casting prototype cell*

4. Results and diagnosis

As today's status is running the prototype cell, results are not final and cannot be considered definitive for the entire production. However, so far, several conclusions are totally clear:

- A 30% increase of productivity (output) expected on double cavity machines.
- A 10% improvement of quality - by elimination of human/visual check.
- A reduction by 40% of human operator time; therefore, payment will also decrease for this process.
- A significant improvement in terms of human safety, magnesium being one of the most difficult to control substances in the case of uncontrolled ignition.

Based on all the above-mentioned results, this program could be already considered as extremely successful.

5. Conclusions

Production becomes more flexible because the members of the work brigades "correlate" the pace of advance among them without the need for complex time studies for the workload or other laborious analyses for balancing work in workstations.

TRW company improved the quality and the entire manufacturing process at its products (it is one of the largest manufacturers of automotive wheels), where one important sector is the leather product preparation. Here the quality standards are extremely severe, and the production losses and rejected products are also important.

But by using the above mentioned new ideas from the lean manufacturing philosophy, combined with technological improvements, the quality level has reached the desired standards.

References

[1]. Allen J., Robinson C., Stewart D., *Lean Manufacturing - a plant floor guide*, Society.
[2]. ***, *Lean manufacturing - Methods for reducing costs*, Pilot Project.
[3]. Womack J. P., Jones D. T., Roos D., *The Machine that Changed the World: How Lean Production Revolutionized the Global Car Wars*, S. & Schuster, London, 1990.
[4]. ***, *Lean manufacturing – Methods for cost reduction*, Pilot Project TRW Automotive.

THE ANNALS OF "DUNAREA DE JOS" UNIVERSITY OF GALATI
FASCICLE IX. METALLURGY AND MATERIALS SCIENCE
Nº. 1 - 2017, ISSN 1453-083X

STUDIES AND RESEARCH ON THE PRODUCTION OF TiO_2 AND TiN THIN FILMS BY ASSISTED PHYSICAL VAPOR DEPOSITION MAGNETRON PROCESS

Simona BOICIUC, Petrică ALEXANDRU
"Dunarea de Jos" University of Galati
e-mail: simonaboiciuc@yahoo.com

ABSTRACT

The experimental research carried out in this paper aims at obtaining thin films of TiO_2 and TiN and at characterizing them in terms of morphology, structure, transparency and electrical properties. The films were obtained using a PVD device of sputtering coating, consisting of a vacuum chamber with a capacity of 2 liters, a planar magnetron with ferrite magnets (ϕ40 x 22 x 9), neodymium (ϕ15 x 8), a vacuum pump with sliding blades, a variable DC source voltage of 100-600 volts. The atmosphere used to maintain the plasma during deposition was oxygen and then N_2 rarefied within a pressure range between $3 \cdot 10^{-2}$-$8 \cdot 10^{-3}$ mbar at a flow rate of 1.4 cm^3/min. It was found that the structures and properties of the films are influenced by the parameters used and their color depends on the working atmosphere, the deposition parameters and the layer stoichiometry.

KEYWORDS: TiN, TiO_2, d.c. magnetron, electrical and optical properties

1. Introduction

Thin films are widely applied in many fields of science and technology. The most important applications are registered in microelectronics, optoelectronics and cutting tools industry.

The films of Ti, TiN, TiO_2 can be achieved by physical methods such as PVD (sputtering under DC or RF modes, evaporation with electron beam, thermal evaporation) or by chemical methods such as sol - gel, anodic oxidation, spray pyrolysis, CVD.

There are several PVD deposit methods and choosing one of them depends on: the requirements for the thin layer properties, the maximum temperature the substrate can withstand, procedure compatibility with the processes applied to the substrate before and after deposition and last but not least the production costs, efficiency and large-scale manufacture of the products.

Titanium has superior characteristics compared to other metals, such as low density (4.5 g/cm^3), high melting temperature (Tt = 1660 °C), low coefficient of thermal expansion, high electrical resistivity, elasticity modulus twice lower than that of iron and steel, very low thermal conductivity and excellent paramagnetism.

The hardness of titanium is relatively low (100-225 HB) and is directly proportional to the increase of the impurity concentration. Soluble impurities (interstitial H, C, N and O_2 by substitution) contribute to the increase of titanium hardness, increasing the mechanical strength as well, while plasticity and corrosion resistance decrease [1-4].

Titan has two stable allotropes: Ti α (stable up to 882 °C) with compact hexagonal network/lattice and Ti β (stable between 885-1672 °C) with body-centered cubic network; passing from one phase to another Ti α → Ti β occurs when temperature increases over 882 °C [1-4].

Titanium dioxide (TiO_2) has attracted the interest of many researchers in materials science due to its unique combination of properties: chemical stability, corrosion/photo-corrosion resistance, photocatalytic potential, high dielectric constant (εr ≈ 60-100), high electrical conductivity, sensitivity to UV, favorable energy band, very high refractive index (2.6-2.9), non-toxicity, biocompatibility. These properties make it useful in purifying water and air, in achieving solar cells, photochemical devices, gas sensors (H_2, CO, CO_2, CH_3), capacitors, microelectronic devices, components requiring biocompatible (antibacterial, self - cleaning) properties [1-4].

Thin layers of titanium nitride (TiN) were the first coatings industrially used to increase wear resistance of tools. In the beginning, these layers were

deposited by chemical vapor-phase deposition (CVD). In the 80s industrial-scale deposits began by plasma - assisted physical vapor-phase (PVD). These coatings have been used mainly as a tribological layer for cutting and plastic deformation tools, bearings, seals and as corrosion and erosion resistant layers. TiN is also used as a decorative coating as it possesses excellent infrared reflectance (IR), the reflection spectrum being similar to that of gold, which gives it a golden color [1-4].

TiN crystallizes in the NaCl-type CFC network (a = 4.256 Ä) has a golden color, the density of 5.40 g/cm^3, melting point of 2930 °C, Vickers hardness of 18-21 GPa, the elasticity modulus of 251 GPa, the thermal conductivity 19.2 W/m·°C, thermal expansion of $9.35*10^{-6}$ K^{-1} [2].

TiN oxidizes at 800 °C in atmospheric pressure. The compound is stable at ambient temperature and concentrated at hot acids attack. Depending on the material of the substrate and its roughness, TiN has a coefficient of friction between 0.4-0.9. At low temperatures ~4 K titanium nitride becomes super isolator having resistance to 5 orders of magnitude greater than at ambient temperature [1-4].

Due to the higher biostability of TiN layers, they are used as electrodes in bioelectronic applications in intelligent implants, prosthetic or sensors which must resist to corrosion caused by body fluids, to make medical instruments such as bistoury blades and bone saw. These electrodes have already been applied to sub-retinal prosthesis as well as in biomedical microelectromechanical systems (BioMEMS). TiN thin films are also used in microelectronics as buffer layers (diffusion barrier) to manufacture transistors etc. [1-4].

Film forming can be described through several stages. In the first stage, the atoms sprayed from the target are adsorbed on the substrate surface. Then they diffuse (moving along the surface of the substrate until reaching a stationary position). When adsorbed atoms are grouped, they form nuclei and this stage is called nucleation. Subsequently, these nuclei continue to grow and lead to the formation of a continuous thin film (stage called coalescence).

There are three ways to increase the films based on the interactions between the atoms of the substrate and the deposited atoms: a - 3D island growth (Volmer - Weber); b - 2D layer growth (Frank van de Merwe,) (seen in homoepitaxial growth); c - 3D cluster growth (island) and stratified growth (Stranski - Krastanov) [1-4].

Nucleation and growth mechanisms are even more intense as the power and duration of sputtering deposition are higher.

By increasing deposition temperature, an increase in the roughness and crystallite size occurs.

The most important parameters which may influence the properties of the films are: nitrogen partial pressure, deposition temperature and substrate polarization [4].

The research in this paper is focused on the development of a technology for producing TiO_2, TiN thin films by DC magnetron sputtering process, using oxygen atmosphere and rarified N_2 in a pressure range between $3\cdot10^{-2}$-$8\cdot10^{-3}$ mbar, and on their characterization in terms of morphology, transparency and electrical properties.

2. Experimental conditions

Films were obtained with a PVD installation of sputtering coating, consisting of a vacuum chamber with a capacity of 2 liters, a ferrite magnets planar magnetron (ϕ40 x 22 x 9) neodymium (ϕ15 x 8), a vacuum pump with sliding blade, a variable DC source of 100-600 volts.

As target, use was made of a plate of 99.9% purity titanium, circular diameter of 46.5 mm and thickness of 1 mm.

a. b.

Fig. 1. *Magnetron image: a - without anode; b - with anode glass substrate prepared for deposition*

The support material consisted of glass plates with dimensions of 76 x 25 x 1 mm.

Fig. 1.a illustrates the magnetron with anode and Figure 1.b. the complete picture of the magnetron with anode and glass substrate prepared for deposition.

The installation allows varying the distance magnetron - deposition substrate between 25 and 90 mm and the substrate temperature can be monitored with a chromel-alumel thermocouple.

The atmosphere used to maintain the plasma during deposition was rarefied oxygen in a pressure range between $3 \cdot 10^{-2}$-$8 \cdot 10^{-3}$ mbar and then rarefied N_2 in a pressure range between $3 \cdot 10^{-2}$-$8 \cdot 10^{-3}$ mbar with flow rates of 1.4 cm^3/min.

The microscopic analysis of the obtained films was conducted using an optical microscope Neophot 2 with computerized data acquisition. The transparency of the films was determined with an electronic device that uses a light source and a photoreceptor. Light, after passing through the deposited film, is measured by the photoreceptor and an amplifier and the result is displayed by an analog device.

The electrical properties (resistivity) of the films were measured using the collinear four-point method (probes) using a laboratory facility. In principle, it consists in injecting current through two external points and measuring voltage in two internal points.

The device scheme is illustrated in Fig. 2.

With thin stratures, resistivity is calculated by relation:

$$\rho = \frac{\pi \cdot t}{\ln 2}\left(\frac{U}{I}\right)$$

where: t - film thickness, U - measured voltage, I - current applied.

$$\frac{\rho}{t} = \frac{\pi}{\ln 2}\left(\frac{U}{I}\right)$$ - film surface resistance

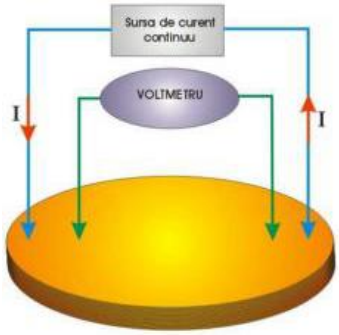

Fig. 2. *Collinear measuring configuration by four - probe method*

The stages of obtaining deposits were:

a. Preparation of the substrate surface.

b. Film deposition by DC magnetron sputtering process.

a. Preparation of the substrate surface

This step consisted in: washing the glass plates (size 76 x 25 x 1 mm) with a special detergent, washing them with water, then with distilled water, ultrasonic cleaning with ethanol followed by drying with compressed air.

b. Film deposition by DC magnetron sputtering process

To obtain the films, a number of regimes were used as presented in Table 1.

Table 1. *Working regimes used in film deposition*

Sample code	Voltage [V]	Current [mA]	Pressure [mbar]	Substrate temperature [°C]	Target-substrate distance [mm]	Deposition time [min]
P1 (Ti) O_2	420	55	5 x 10^{-3}	45	60	60
P2 (Ti) O_2	440	45	1 x 10^{-3}	30	60	120
P3 (Ti) O_2	550	150	5 x 10^{-3}	100	60	30
P4 (Ti) N_2	440	49	1 x 10^{-3}	46	60	180 N_2 ½ of time
P5 (Ti) N_2	450	50	2.5 x 10^{-3}	50	60	60
P6 (Ti) N_2	450	50	2.5 x 10^{-3}	50	60	240
P7 (Ti) N_2	450	50	2 x 10^{-3}	50	60	180

3. Experimental Results

3.1. Microstructural characterization of the deposited films

The macroscopic analysis reveals that the films do not show cracks, are homogenous and adherent as shown in Fig. 3 and 4.

Because of the working atmosphere used (rarefied oxygen in a pressure range between $3 \cdot 10^{-2}$-$8 \cdot 10^{-3}$ mbar, flow rate 1.4 cm^3/min), it is estimated that the film structure corresponding to samples P1, P2, P3 would consist of Ti and TiO_2.

For samples P4, P5, P6, P7 achieved with the addition of N_2, the obtained films have different colors being darker as the duration of maintenance is higher. Because of the working atmosphere used (rarefied N_2 in a pressure range between $3 \cdot 10^{-2}$-$8 \cdot 10^{-3}$ mbar, flow rate 1.4 cm^3/min), samples structure is estimated to consist of Ti and TiN.

The film color depends on the layer stoichiometry, the working atmosphere and the parameters used. It ranged from gray to golden brown (Figure 4).

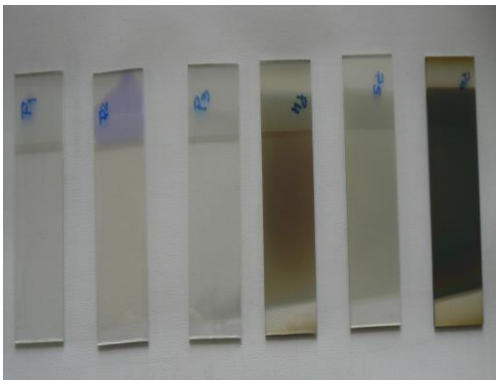

Fig. 3. *Image of films deposited under different regimes*

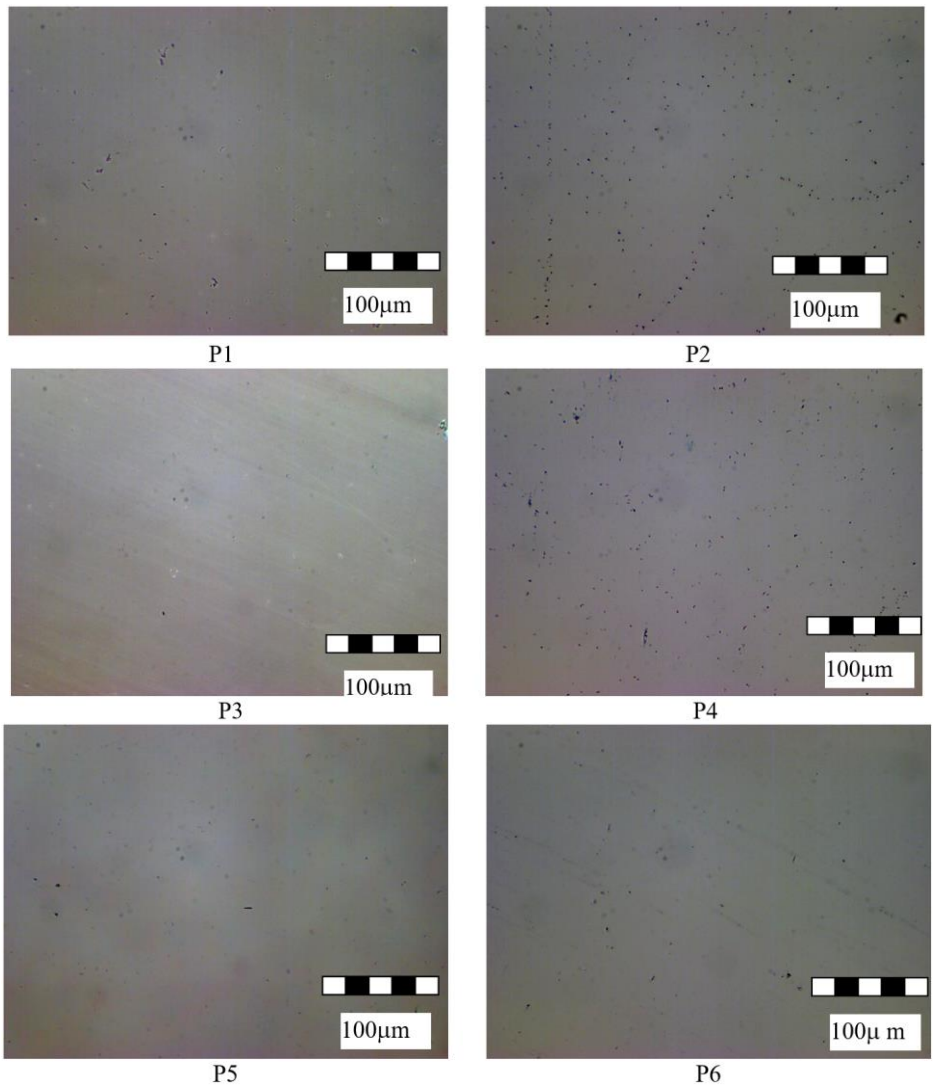

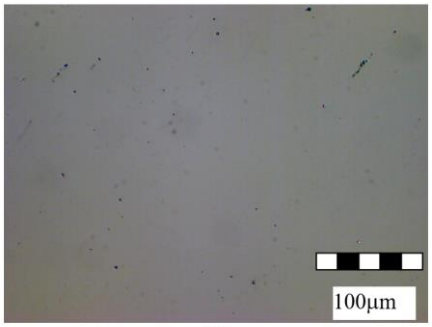

P7

Fig. 4. *Image of films deposited under different regimes*

3.2. Establishing the optical and electrical characteristics of the deposited films

The films corresponding to samples P1, P2, P3 obtained in vacuum have high transparency of about 97% and the surface resistance could not be determined.

The results of transparency and electrical resistance measurements for samples P4, P5, P6, P7 are shown in Table 2.

Table 2 shows that, with increased deposition time, the surface resistance and transparency decrease. This behavior is due on the one hand to increased deposited film thickness, and on the other hand to oxidation and formation of TiN.

This can be observed on the graphs in Fig. 5 and Fig. 6.

Table 2. *Determining transparency and electrical properties of films*

Sample code	Film transparency	Film surface resistance [Ω]	Deposition time [min]
P4 (Ti) N_2	0.3	2806.19	180
P5 (Ti) N_2	0.6	39534.54	60
P6(Ti) N_2	0.0125	693.36	240
P7 (Ti) N_2	0.08125	3939.13	180

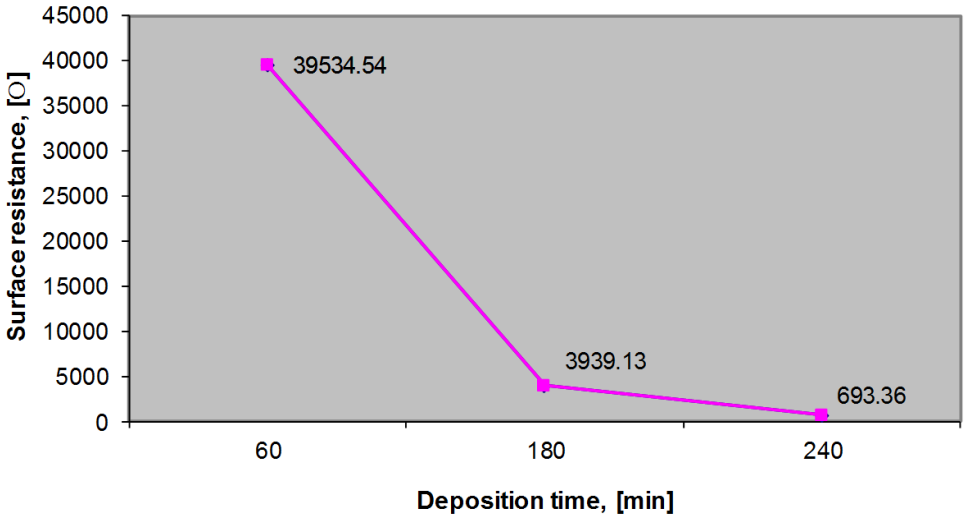

Fig. 5. *Influence of deposition time on the surface resistance of the deposited film*

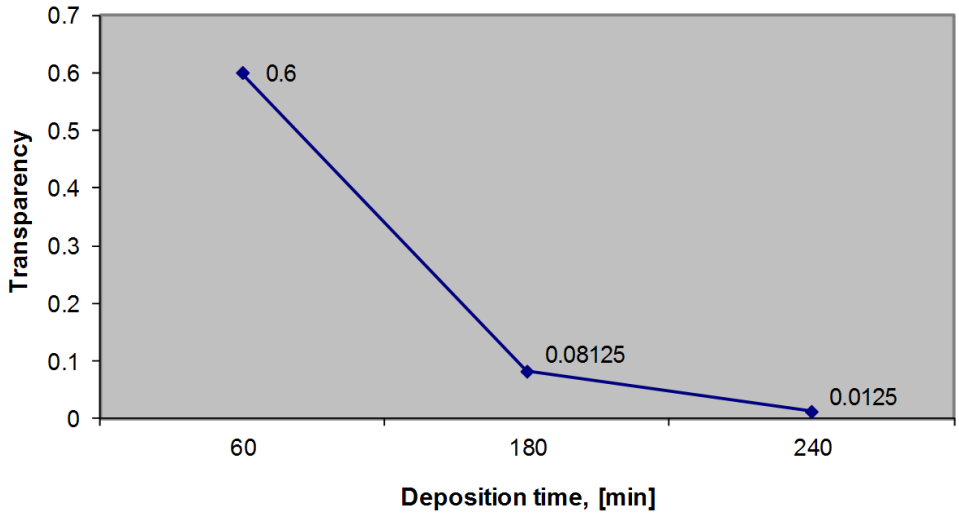

Fig. 6. *Influence of deposition time on the transparency of the deposited film*

3.3. EDX characterization of the deposited film

Figures 7, 8, 9 present the EDX analysis of the film corresponding to samples P2, P5 and P6. It may be noted that with sample P6 where the deposition time was longer, therefore the thickness is higher, the titanium content is higher.

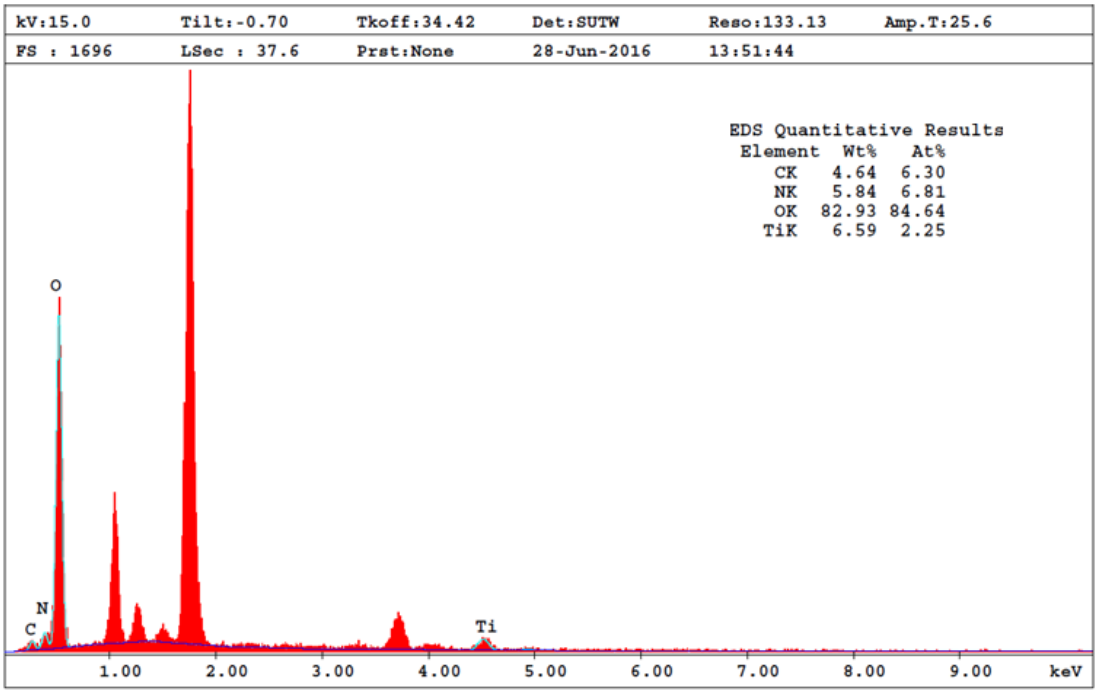

Fig. 7. *EDX analysis of the film corresponding to sample P2*

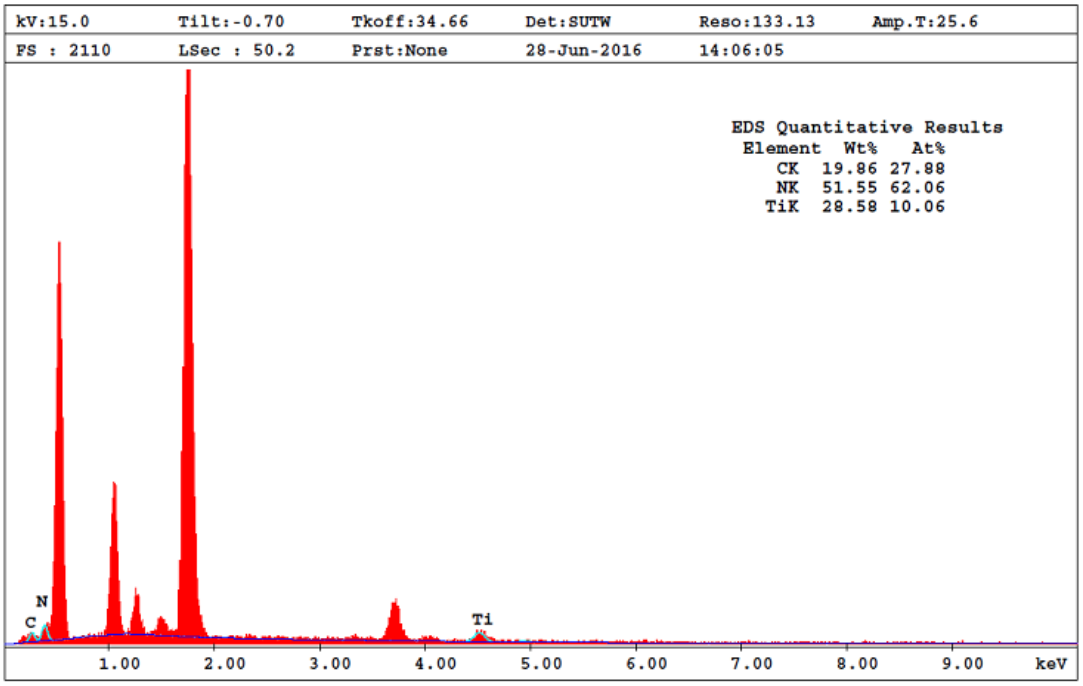

Fig. 8. *EDX analysis of the film corresponding to sample P5*

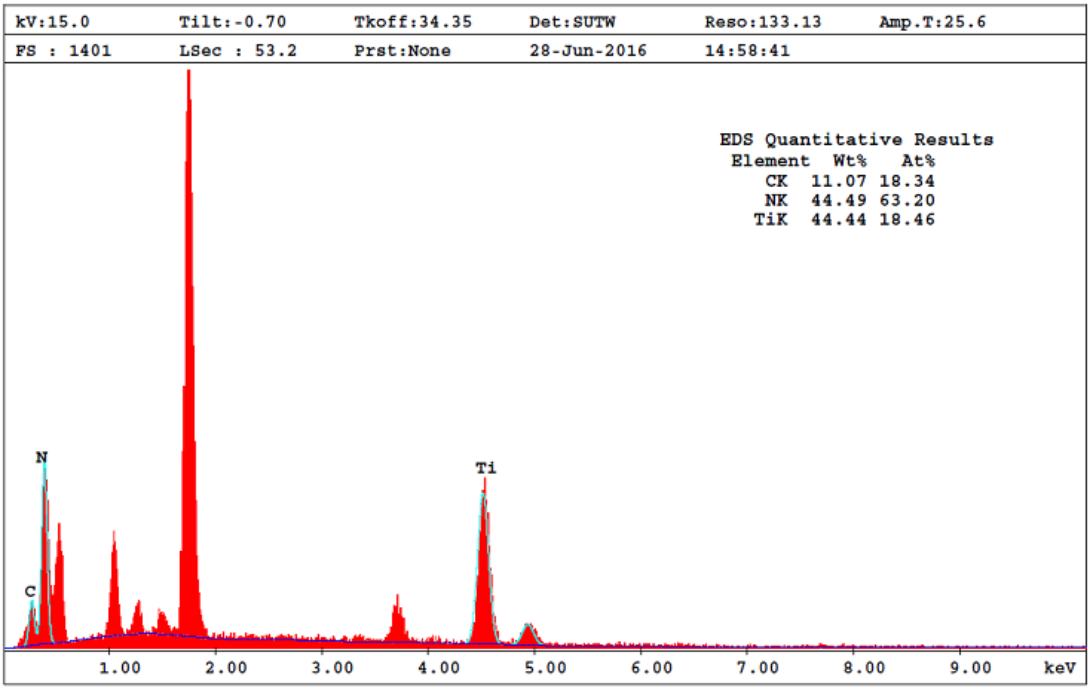

Fig. 9. *EDX analysis of the film corresponding to sample P6*

4. Conclusions

The films of titanium nitride (TiN) deposited by DC magnetron sputtering process, due to its outstanding properties (high hardness, low electrical resistivity, high wear resistance, excellent resistance to corrosion and high thermal stability) are increasingly used in various applications, such as: cutting tools, parts subject to wear and corrosion, microelectronics, decorative layers, diffusion barriers, electrodes in bio-electronics applications, medical devices.

The TiO_2 films are extensively studied as they have excellent photocatalytic, antibacterial (when

exposed to UVA - 320-400 nm) optical, antireflective characteristics.

The experimental research leads to the following conclusions:

- films deposited by DC magnetron sputtering process reveal an economical and simple way of producing coatings with multiple applications;
- it was found that the deposition modes are quite unstable in that there is a tendency to increase voltage and decrease current followed by plasma extinction;
- films were obtained using as atmosphere to maintain plasma, oxygen and then rarefied N_2 in a pressure range between $3 \cdot 10^{-2}$-$8 \cdot 10^{-3}$ mbar, with a flow rate of 1.4 cm^3/min;
- structures and properties of films obtained are influenced by the parameters used;
- the microscopic analysis reveals that the films obtained do not show cracks, are uniform and adherent to mirror surface;
- films color depends on the layer stoichiometry, working atmosphere and parameters used; it ranged from gray to golden brown;
- with increased time of deposition, the surface resistance and transparency decrease (this behavior is due to increasing deposited film thickness and to oxidation and formation of TiN;
- EDX analysis performed on films highlights their chemical composition, i.e. the presence of titanium, oxygen, and nitrogen, in line with the working environment used.

References

[1]. Pitulice Camelia, *Studies and Research Regarding the Biocompatible Materials Used in Prosthesis*, PhD Thesis, Braşov 2013.
[2]. Robert-A. Pato, *Straturi subţiri multifunctionale de nitrura de titan*, Teza de doctorat, Universitatea Tehnica Cluj Napoca, 2011.
[3]. Janika Boltz, *Sputtered tin oxide and titanium oxide thin films as alternative transparent conductive oxides*, Aachen University, 12/12/2011.
[4]. Roquiny Ph., Bodart F., Terwagne G., *Color control of titanium nitride coatings produced by reactive magnetron sputtering at temperature less than 100 °C*, Surface and Coatings Technology, 116-119, p. 278-283, 1999.

THE ANNALS OF "DUNAREA DE JOS" UNIVERSITY OF GALATI
FASCICLE IX. METALLURGY AND MATERIALS SCIENCE
Nº. 1 - 2017, ISSN 1453-083X

INFLUENCE OF SINTERING TEMPERATURE ON THE STRUCTURE OF YTTRIUM BASED PHOSPHOR NANOPARTICLES

Vasilica ŢUCUREANU[1,2,*], Alina MATEI[1], Andrei AVRAM[1], Marian Cãtalin POPESCU[1], Mihai DĂNILA[1], Marioara AVRAM[1], Cãtalin Valentin MĂRCULESCU[1], Bianca Cătălina ŢÎNCU[1], Tiberiu BURINARU[1], Daniel MUNTEANU[2,*]

[1]National Institute for Research and Development in Microtechnologies, IMT-Bucharest,
[2]Transilvania University of Brasov, Department of Materials Science,
[*]Corresponding authors: vasilica.tucureanu@imt.ro, danielmunteanu@unitbv.ro

ABSTRACT

Yttrium-based phosphor materials belonging to the class known as garnets have witnessed a strong return with the development of the first white LEDs. Among these materials, yttrium aluminum garnet doped with cerium has become the best known, being successfully used in generating white light, due to its capacity to convert the blue light emitted by a GaN chip. But its use in optoelectronic applications is subject to the achievement of parameters such as: purity of the crystal phase and particles size in the nanoscale range. In this study, we present a modified sol-gel method for the synthesis of yttrium aluminum garnet doped with cerium (YAG:Ce). In the end, heat treatment will be carried out at various temperatures and the effect of sintering temperature on the crystal phase and morphology will be studied. To highlight the phase transition from amorphous to crystalline state, a Rigaku SmartLab X-ray Diffraction System was used. Moreover, by the X-Ray diffraction pattern we evidenced the presence of the intermediate phases such as the main oxides, the metastable phases with perovskite (YAP) and monoclinic (YAM) structure and finally the garnet phase (YAG). The presence of the dopant in the crystalline structure was demonstrated. The microstructure and morphology evolution of the particles were assessed by using the FEI Nova NanoSEM system. Getting garnet phase and particles with spherical and smooth surfaces at the nanoscale range after a sintering treatment at 1100° C indicates a phosphor applicable in optoelectronics.

KEYWORDS: phosphor, YAG:Ce, sol-gel process

1. Introduction

The international strategy in the field of lighting is aimed at finding new lighting sources with lower power consumption in order to minimize the electricity consumption. For this purpose, the RGB system has been used, a system based on the use of red-green-blue individual LEDs to generate white light. But disadvantages such as the varying degree of LED degradation, circuit complexity, high cost, etc, made this system non-usable for general lighting. However, this white light producing system remains used in the field of video panels [1-3]. Another white light generation system using LED chips, which has proven its viability since 1996, is based on the use of one or more phosphors along with a blue / UV structure. It is expected that these devices based on LEDs will lead to the replacement of classical lighting systems due to advantages such as: low energy consumption, high power efficiency, long life time, high shock resistant, small size, and so on. But in this case, there are problems because the quality of light emitted in a white LED is strongly influenced by the structure and morphology of the luminous material [4, 5].

A phosphor is a material that emits photons at a wavelength greater than the excitement source. Yttrium based phosphor, known as cerium-doped yttrium aluminum garnet (YAG:Ce), is a synthetic crystalline material from garnet family and the most widely used as luminescent material to generate white light in an LED [6, 7]. The only existing method for

obtaining YAG:Ce at an industrial level is the solid-state method between the main oxides at high temperature (1600-1900 °C) and high production cost. High temperature is necessary for crystallization but the phosphors resulting under these conditions have a low production yield due to the large variation in grain size and the presence of secondary phases that act as impurity with consequences on phosphors quality [8, 9]. In order to obtain phosphors with superior optical qualities at a low-cost price, wet methods (method as: sol-gel, coprecipitation, solvo / hydrothermal, spray-pyrolysis etc.), have gained ground. Despite the existence of a very large number of alternative bottom-up methods, obtaining a single phase in garnet form (with a $Y_{3-x}Ce_xAl_5O_{12}$ (YAG) molecular formula) is not a simple task [10-19]. In the crystalline system can coexist the basic oxides (Al_2O_3, Y_2O_3), yttrium aluminum monoclinic (YAM, $Y_4Al_2O_9$), yttrium aluminum perovskite (YAP, $YAlO_3$) and yttrium aluminum garnet (YAG, $Y_3Al_5O_{12}$) [19-21]. Moreover, the presence of cerium ions as secondary cerium oxide (CeO_2, Ce_2O_3) phases in the garnet network leads to the strong degradation of phosphor quality.

The main objective of this investigation was the fabrication of a YAG:Ce by a modified sol-gel method under the presence of DMSO and CTAB for a better control in order to obtain single garnet phase of phosphor at nanometrical scale. The structural and morphological evolution of the phosphor powder has been studied according to the sintering temperature.

2. Experimental procedure for the synthesis and characterization of yttrium based phosphor

In the present paper we proposed a modified sol-gel method for yttrium based phosphor synthesis. The following raw materials were used to synthesize the YAG:Ce phosphor: yttrium oxide (Y_2O_3), aluminum oxide (Al_2O_3), dimethyl sulfoxide (DMSO, $(CH_3)_2SO$), acetylacetone (AcAc, $CH_3COCH_2COCH_3$), cetrimonium bromide (CTAB, $(C_{16}H_{33})N(CH_3)_3Br$), nitric acid ($HNO_3$) (from Sigma Aldrich, all analytical grade). Cerium oxide (CeO_2) at nanoscale was synthesized by coprecipitation method in our labs [22].

The oxides were dissolved in the nitric acid. The solution was stirred continuously and kept at 80° C. While maintaining the system under reflux conditions, AcAc, DMSO and CTAB were added. In the process, we considered the reaction below as ideal, and we used the raw material in stoichiometric report for the preparation of the YAG doped with 5% cerium ion. The chelating agent was added in excess, in a molar ratio 3 times greater than the theoretical reaction.

$$15Al(NO_3)_3 + 8.55Y(NO_3)_3 + 0.45Ce(NO_3)_3 + 15C_5H_8O_2 = 3(Y_{0.95}Ce_{0.05})_3Al_5O_{12} + 75CO_2 + 60H_2O + 36N_2$$

Reaction conditions were maintained for 6 hours, after which the reflux was removed and allowed to stand for several days for bulk polymerization. The quality of the phosphate based on yttrium is strongly influenced by the thermal treatment stage. In our work the annealing has being carried out in two steps. The pre-sintering or slow evaporation was the stage controlled by DMSO and CTAB, used to provide better control over nanoparticle morphology. The utility of DMSO can be explained by the higher boiling temperature of the water which allows a slower evaporation of the liquids from the network., The CTAB also has anchoring capacity or selectivity to various crystal facets. Particular attention has been paid to pre-sintering up to 400 °C when the nitrates and all organic compounds decomposition occur. Temperature was incremented with 4 °C/min and maintained at 400 °C for 24 hours, resulting in the formation of a brown phosphor precursor. The appearance of YAG:Ce yellow phosphors was observed after treatment in air at 1100 °C for 48 hours (4 samples were taken after heat treatment in the range of 900-1100 °C).

To observe the influence of the sintering temperature on the YAG:Ce phosphors structure, Rigaku SmartLab X-ray Diffraction System was used with CuKα radiation in the 2θ range from 20° to 70°. Scherrer's equation was used to calculate the average crystallite size. The dopant presence in the crystalline network was confirmed using energy dispersive X-ray spectroscopy (EDX) for the phosphors elemental composition analysis. EDX spectra were collected with a TESCAN having an EDAX facility, operated at 10 kV. Moreover, using Fourier Transform Infrared (FTIR) spectrometry (Bruker Optics, Tensor 27) and KBr disk technique, we have highlighted the existence of the Ce-O bond in the crystalline network. The spectra were taken in the wavenumber 4000-400 cm^{-1} by averaging 64 scans and with a resolution of 4 cm^{-1}. The microstructure and morphology evolution of the particles were determined using field emission scanning electron microscopy (FE-SEM). The SEM images for the powder samples were taken with an FEI Nova NanoSEM 630 system. In order to increase the image quality, before the SEM examination, the yellow phosphors were dispersed into ethanol, ultra-sonicated for 30 min., dip-cast onto the surface of silicon wafers and coated with a thin gold layer.

3. Results and discussions

The quality of phosphors based on yttrium is determined by its structure and morphology, the purity of the garnet phase, the shape and size of the particles. The XRD diagrams were used in order to study the crystal structures of the phosphor, purity, crystallite size and strain.

The YAG crystal structure has a 160-atom body-centered cubic (bcc) unit cell and Ia-3d (230) space group. From a theoretical point of view, the evolution of a sample of phosphors after the thermal treatment is from raw material (Al_2O_3 -Y_2O_3) to amorphous, YAP, YAM, hexagonal and / or orthorhombic YAP and YAG phase [21]. However, in practice, in the luminescent material several phases coexist, which was seen in the XRD diagrams. All single lines can be indexed (Table 1) for the samples and are attributed to garnet crystal structure and to the intermediate phase caused by incomplete processes [20].

Figure 1 shows X-ray diffraction pattern of the phosphor precursor and for the material after annealing at temperatures of 900-1100 °C.

In the XRD graph of the phosphor precursor (fig 1 [1]) may be observed an amorphous compound. For the phosphor annealed at temperature over 900 °C (fig 1 [2]) the transition from amorphous to crystalline phases, and the existence of the YAP as the predominant phase were observed. The samples annealed at 900-1050 °C (Fig. 1 [3], 1 [4], 1 [5]) revealed the YAG as the predominant phase and the presence of reaction intermediate. XRD analysis (Fig. 1 [6]) for the sample undergoing a heat treatment at 1100 °C shows that this temperature is sufficient to obtain a single phase of garnet. All lines were identified and indexed to the YAG phases, thus confirming the transformation of all intermediates into the garnet structure. The samples sintered over 950 °C, indicate a peak centered at about 2θ = 33.4° which corresponds to the crystalline plane with Miller indices of (420) from YAG structure, suggesting that the predominant phase is the garnet. In the case of the sample annealed at 900 °C we noticed that the main peak is at 2θ = 34.29°, indicating that the main phase is YAP phase. Using the main peak and the Scherrer equation, the average crystallite size was calculated. Figure 2 shows the crystallite size variation as a sintering temperature function, noticing a decrease in the average crystallite size to a certain temperature (1100 °C). The average crystallite size calculated for the YAG:Ce is 36 nm. The possibility of increasing the average size of the crystals appears at high temperature and sintering time.

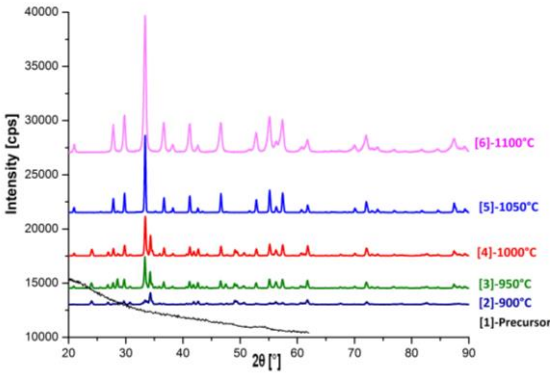

Fig. 1. *X-Ray diffraction pattern of YAG:Ce phosphor samples annealed at different temperature: (1)-precursor, (2) sintering at 900 °C, (3) sintering at 950 °C, (4) sintering at 1000 °C, (5) sintering at 1050 °C and (6) sintering at 1100 °C*

Table 1. *Crystalline planes for yttrium based phosphor after annealing at 900-1100 °C*

Crystalline phase	$2\theta_B$ [°] 1100 °C	$2\theta_B$ [°] 1050 °C	$2\theta_B$ [°] 1000 °C	$2\theta_B$ [°] 950 °C	$2\theta_B$ [°] 900 °C
YAG	20.98, 27.83, 29.72, **33.39**, 36.60, 38.18, 41.21, 42.62, 46.66, 51.66, 52.78, 55.12, 56.28, 57.39, 60.75, 61.75, 70.04, 72.03, 74.03, 76.96, 81.79, 84.64, 87.38, 89.30.	20.96, 27.81, 29.78, **33.40**, 36.70, 38.25, 41.20, 42.61, 46.65, 51.63, 52.85, 55.11, 56.34, 57.42, 60.72, 61.81, 70.05, 72.07, 74.05, 76.93, 81.73, 84.61, 87.46, 89.31.	20.98, 27.81, 29.78, **33.40**, 36.70, 38.24, 41.22, 42.69, 46.67, 51.66, 52.83, 55.16, 56.25, 57.46, 60.75, 61.82, 70.07, 72.04, 74.04, 76.94, 81.73, 84.55, 87.40, 89.26.	20.90, 27.71, 29.72, **33.43**, 36.60, 38.22, 41.23, 42.59, 46.59, 51.59, 52.77, 55.12, 56.19, 57.46, 60.64, 61.74, 70.01, 72.07, 74.02, 76.81, 81.73, 84.54, 87.38, 89.25.	20.95, 27.83, 29.68, 33.60, 36.57, 38.16, 41.16, 42.72, 46.65, 52.78, 55.11, 56.20, 57.44, 60.58, 61.71, 72.13, 76.90, 87.34, 89.17.
YAP	-	35.18.	24.08, 26.94, 34.30, 34.70, 35.89, 41.86, 49.46, 61.17, 67.58.	23.99, 26.88, 34.18, 34.60, 35.18, 35.85, 41.82, 49.41, 61.09, 67.54.	24.01, 26.96, **34.29,** 34.55, 35.87, 41.87, 49.36, 61.05, 67.56.
YAM	-	-	-	29.13.	29.10.
Al_2O_3	-	-	25.63, 30.81, 40.70, 43.44, 44.20.	25.57, 30.73, 40.65, 43.34, 44.13.	25.52, 30.70, 40.65, 43.45, 44.25.
Ce_2O_3	-	28.58, 47.51.	28.64, 47.69.	28.57, 47.54.	28.68, 47.68.

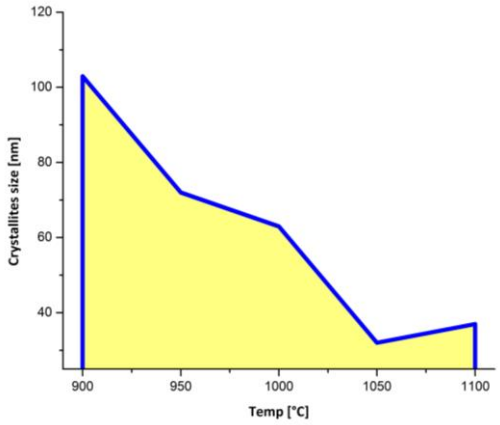

Fig. 2. *Variation of crystallite average size of the YAG:Ce samples as a function of sintering temperature*

Figure 3 presents the strain of the network as a function of the temperature, showing a direct proportional decrease with the temperature increase, which is explained by the decrease of the stress in the network as a result of the removal of the secondary phases from the final product.

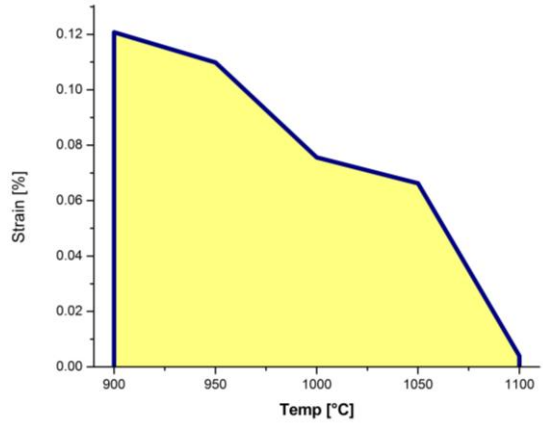

Fig. 3. *Strain variation of the YAG:Ce crystalline samples as a function of sintering temperature*

Further annealing of the powder over 1000 °C shows an increase of diffraction peak intensity due to the improved purity and crystallinity. The largest and sharpest peaks can be observed for phosphor powder treated at 1100 °C. The presence of cerium ions is only observed in the annealed samples up to 1050 °C, due to the incomplete transformation process. For the sintered sample at 1100 °C, the complete substitution of $Y^{3+}$with Ce^{3+} does not disturb the crystalline structure of the samples, appearing only a small change in the lattice parameters due to the difference in the ionic radii. The lattice parameters of the YAG:Ce were found to be 12.0028 Å.

In terms of qualitative analysis, in the energy-dispersive X-ray spectrum in Figure 4 we can see peaks that correspond to the atoms of O (O(K) at 0.53 keV), Al (Al(K) at 1.49 keV), Y (Y(L) at 1.92 keV) and Ce dopant (Ce(L) at 4.8 keV). The quantitative analysis was based on the use of atomic percentages, from EDX data, for calculating the molecular formula of the yttrium based phosphor sample. The final composition was calculated and corresponds to theoretical $Y_{2,81}Ce_{0,13}Al_{5,02}O_{12,04}$ formula, which suggests a good crystallinity and is very close to that of the target materials.

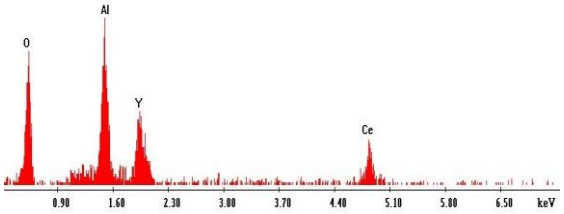

Fig. 4. *EDX spectrum of a representative YAG:Ce phosphor powder*

Moreover, the FTIR spectra (Fig. 5) for a YAG:Ce sample annealed at 1100 °C confirms the existence of Ce-O bond in the crystalline network.

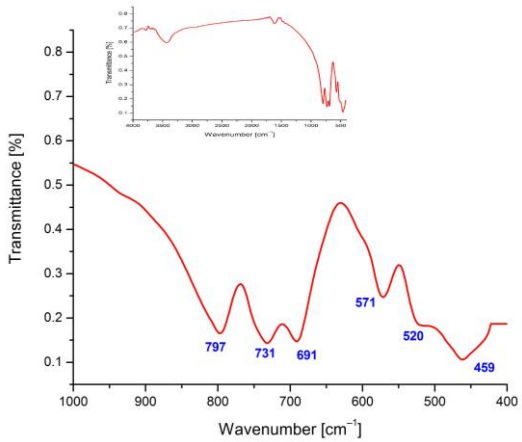

Fig. 5. *FTIR spectrum for YAG:Ce phosphor powder*

It is observed that the spectrum consists of significant absorption bands at the lowest frequencies (below 800 cm^{-1}), that has been assigned to the vibrations mode of the M-O bonds from the garnet structure. The bands centered at 797 and 691 cm^{-1} occur from the stretching vibrations of the Al-O; the peak from 732 cm^{-1} is assigned to Y-O, while the peak from 571 cm^{-1} is assigned to Y-O-Al bonds. The

presence of the dopant in the sample was observed in the bands centered at 520 and 459 cm^{-1} which can be attributed to the vibration mode of the Ce-O bonds from the garnet crystalline network [20]. The bands attributed to O-H bonds (3440 and 1636 cm^{-1}) are due to water absorption. No organic residue was observed in the spectrum.

Obtaining particles with spherical surface and at nanoscale is necessary to avoid scattering phenomena and to improve optical properties. Figure 6 shows SEM micrographs for precursor samples and treated at temperatures between 900 and 1100 °C. The SEM micrograph for the precursor sample (Fig. 6 [1]) confirms the XRD observations of amorphous compound formation. The samples treated at temperatures up to 1050 °C (Fig. 6 [2]-6 [5]) present irregular particles with a heterogeneous distribution, thus confirming that the process is incomplete. The sintered sample at 1100 °C (Fig. 6 [6]), exhibits particles with spherical shape and smooth surface. An average particle size of about 40-60 nm was determined.

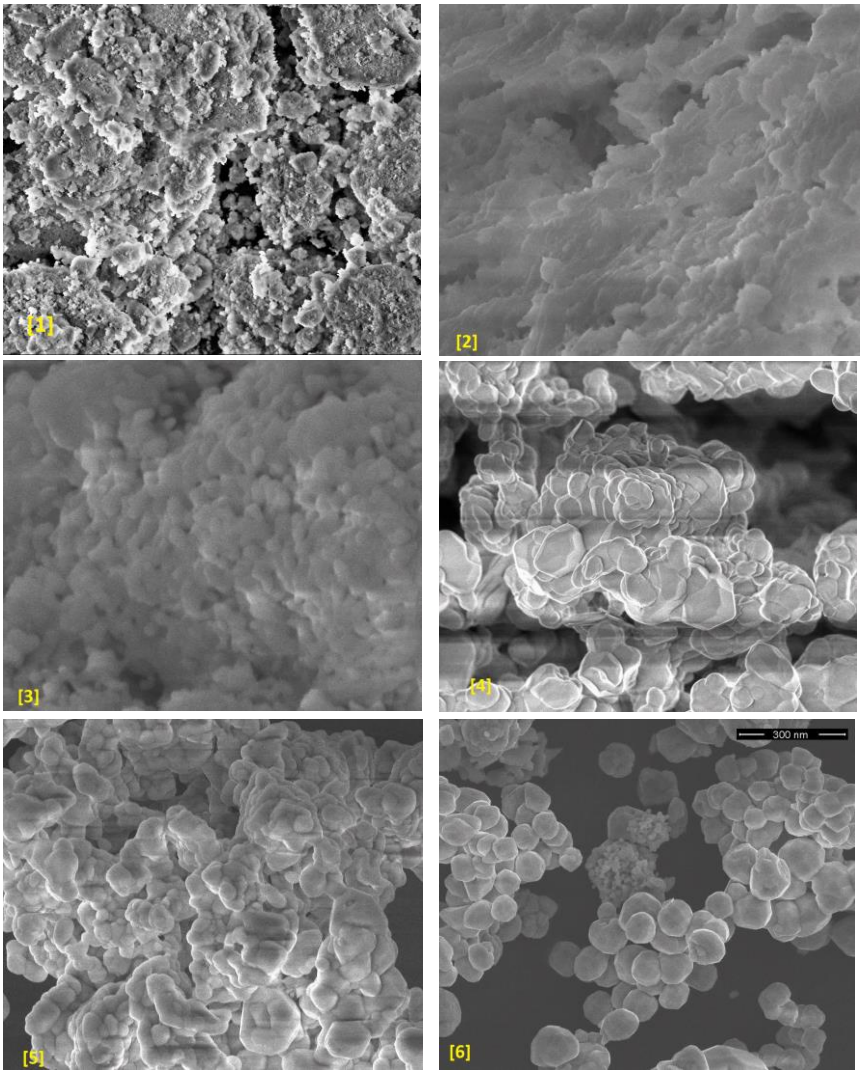

Fig. 6. *SEM micrograph of the YAG:Ce phosphor samples sintered at different temperature: (1)-precursor, (2) sintering at 900 °C, (3) sintering at 950 °C, (4) sintering at 1000 °C, (5) sintering at 1050 °C, (6) sintering at 1100 °C*

4. Conclusion

Using a modified sol-gel method we synthesized a yellow garnet phosphor. The oxides and the acetylacetone were used in the process as raw materials and as chelating agent, respectively. CTAB and DMSO were used for morphology control. The thermal treatment was studied from the structural and morphological point of view. An amorphous precursor (at 900 °C) and transition to crystalline

phases (by annealing over 900 °C) was confirmed by the XRD diagrams. In the sample sintered at high temperature, the formation of YAG phases was observed. Only for phosphor annealed at 1100 °C YAG is the single-phase present. For the samples sintered at 900-1050 °C, the coexistence of Al_2O_3, Ce_2O_3, YAM, YAP, and YAG phases was determined. The existence of intermediate phases due to the incomplete process was also observed in the variance of the network strain. We noticed that the average particle size increases with increasing temperature for the samples sintered at 900-1100 °C. Using the EDX analysis, the main atoms were identified and the $Y_{2,81}Ce_{0,13}Al_{5,02}O_{12,04}$ molecular formula was established. The presence of the dopant in the crystalline structure was evidenced by EDX and FTIR analyses. Peaks were observed in the FTIR spectrum, which can be assigned to the vibration mode of the M-O bonds from the garnet molecule. SEM micrographs come to confirm the XRD observation. The amorphous form of the precursor was observed, with irregular particles variation and heterogeneous distribution for the sample treated at 900-1050 °C and nanoparticles with spherical shape and smooth surface for the samples after treatment at 1100 °C.

Acknowledgments

This work was supported by UEFISCDI in the Partnership Framework: PN-III-P2-2.1-PTE-2016-0145 (Project No. 46PTE/2016), PN-III-P2-2.1-PED-2016-0123 (Project No. 119/2017), PN-II-PT-PCCA-2013-4-0366 (Project No. 208/2014) and by National Basic Funding Program TEHNOSPEC - Project No. PN1632/2016.

This work was supported by a grant of the Ministry of National Education and Scientific Research, RDI Program for Space Technology and Advanced Research-STAR, project number 639/2017.

This paper is part of the Vasilica (Şchiopu) Ţucureanu's PhD thesis, at Transilvania University of Braşov, Department of Materials Science, coordinated by Prof. dr. eng. Daniel Munteanu, to whom I am grateful for all the support and guidance.

References

[1]. Kim T., Lee J., *Template-free Synthesis and Characterization of, Template-Free Synth. YAGCe NanoPhosphor* Bull. Korean Chem. Soc., 35, p. 2917-2921, 2014.

[2]. Panatarani C., Joni I. M., *Challenging and development of phosphors for lighting applications*, AIP Conf. Proc., 1712, 020003(1-5), 2016.

[3]. Pust P., Schmidt P. J., Schnick W., *A revolution in lighting*, Nat. Mater., 14, p. 454-458, 2015.

[4]. Zhang L., Lu Z., Zhu J., Yang H., Han P., Chen Y., Zhang Q., *Citrate sol-gel combustion preparation and photoluminescence properties of YAG:Ce phosphors*, J. Rare Earths., 30, p. 289-296, 2012.

[5]. Ryu H. Y., *Analysis on the luminous efficiency of phosphor-conversion white light-emitting diode*, J. Opt. Soc. Korea., 17, p. 22-26, 2013.

[6]. Jang M. S., Choi Y. H., Wu S., Lim T. G., Yoo J. S., *Material properties of the Ce^{3+}-doped garnet phosphor for a white LED application*, J. Inf. Disp., 17, p. 117-123., 2016.

[7]. Haaheim J., DenBaars S., *A History of Solid State White Lighting the Evolution of GaN Nanowires, and New Potentials for White Light Generation Using InGaN Nanowires*, Dep. Electr. Comput. Eng. Univ. Calif. – St. Barbar, p. 1-15, 2002.

[8]. Lee H. M., Cheng C. C., Huang C. Y., *The synthesis and optical property of solid-state-prepared YAG:Ce phosphor by a spray-drying method*, Mater. Res. Bull., 44, p. 1081-1085, 2009.

[9]. Chou C. S., Wu C. Y., Yeh C. H., Yang R. Y., Chen J. H., *The optimum conditions for solid-state-prepared $(Y_{3-x}Ce_x)Al_5O_{12}$ phosphor using the Taguchi method*, Adv. Powder Technol., 23, p. 97-103, 2012.

[10]. Zhang X., Jin C., Zhang Y., Jia N., He W., *Synthesis of spherical yttrium aluminum garnet via a mixed solvothermal method*, RSC Adv., 4, p. 57452-57457, 2014.

[11]. Yixuan R., Li G., Junguo R., *Effect of PEG Addition on the Properties of YAG:Ce Phosphor Synthesized via a Homogeneous Precipitation Method*, Rare Met. Mater. Eng., 44, p. 2100-2104, 2015.

[12]. Wang B., Qi H., Han H., Song Z., Chen J., Shao J., *Structural, luminescent properties and chemical state analysis of YAG:Ce nanoparticle-based films*, Opt. Mater. Express, 6, p. 155-165, 2016.

[13]. Tucureanu V., Matei A., Mihalache I., Danila M., Popescu M., Bita B., *Synthesis and characterization of YAG:Ce,Gd and YAG:Ce,Gd/PMMA nanocomposites for optoelectronic applications*, J. Mater. Sci., 50, p. 1883-1890, 2015.

[14]. Trifonov Y. G., Kuznetsova D. E., Dosovitskii G. A., Omarov A. Y., Novoselov R. A., Tarasovskii V.P., *Preparation of Aluminum-Yttrium Garnet Luminscent Ceramic Alloyed with Cerium*, Refract. Ind. Ceram., 56, p. 271-275, 2015.

[15]. Palmero P., Traverso R., *Co-precipitation of YAG powders for transparent materials: Effect of the synthesis parameters on processing and microstructure*, Materials (Basel), 7, p. 7145-7156, 2014.

[16]. Ma R., Lu B., Cao H., Hu J., Zhang X., Qiu Q., Zheng R., Luo Z., Xue B., *Preparation and characterization of YAG:Ce thin phosphor films by pulsed laser deposition*, Int. J. Appl. Ceram. Technol, p. 1-9, 2017.

[17]. Kaithwas N., Dave M., Kar S., Bartwal K. S., *Structural features of Ce doped YAG nanoparticles synthesized by modified sol-gel method*, Phys. E., 44, p. 1486-1489, 2012.

[18]. He X., Liu X., Li R., Yang B., Yu K., Zeng M., Yu R., *Effects of local structure of Ce^{3+} ions on luminescent properties of $Y_3Al_5O_{12}$:Ce nanoparticles*, Sci. Rep., 6, p. 1-11, 2016.

[19]. Chung D. N., Dinh N. N., Hieu D. N., Duong P. H., *Synthesis of cerium-doped yttrium aluminum garnet nanopowder low-temperature reaction combustion method*, VNU J. Sci. Math, 28, p. 53-60, 2012.

[20]. Tucureanu V., Matei A., Avram A., *Synthesis and characterization of YAG:Ce phosphors for white LEDs*, Opto-Electronics Rev., 23, p. 239-251, 2015.

[21]. Hess N. J., Maupin G. D., Chick L. A., Sunberg D. S., McCreedy D. E., Armstrong T. R., *Synthesis and crystallization of yttrium-aluminium garnet and related compounds*, J. Mater. Sci., 29, p. 1873-1878, 1994.

[22]. Matei A., Tucureanu V. Tincu B., Popescu M., Romanita C., Cernica I., Dumitrescu L. G., *Experimental aspects for CeO_2 nanoparticles synthesis and characterization*, Sci. Conf. Dr. Sch., SCDS-UDJG 2017, p. 123-123, 2017.

THE ANNALS OF "DUNAREA DE JOS" UNIVERSITY OF GALATI
FASCICLE IX. METALLURGY AND MATERIALS SCIENCE
Nº. 1 - 2017, ISSN 1453-083X

EXPERIMENTAL ASPECTS FOR CeO_2 NANOPARTICLES SYNTHESIS AND CHARACTERIZATION

Alina MATEI[1*], Vasilica ŢUCUREANU[1,2], Bianca Cătălina ŢÎNCU[1], Marian POPESCU[1], Cosmin ROMANIŢAN[1,4], Ileana CERNICA[1], Lucia Georgeta DUMITRESCU[3]

[1]National Institute for Research and Development in Microtechnologies, IMT-Bucharest
[2]Transilvania University of Brasov, Department of Materials Science
[3] Transilvania University of Brasov, Product Design and Environment Faculty
[4]Faculty of Physics, University of Bucharest
[*]Corresponding author: alina.matei@imt.ro

ABSTRACT

In recent years, cerium oxide (CeO_2, or ceria) became a versatile nanostructured material because of its unique properties derived from the low dimensionality and high surface area. It was also extensively studied due to its practical performances in many scientific and industrial applications, such as fuel cells, luminescent materials, gas sensors, insulators, white LEDs, etc.

In this paper, the research focused on the synthesis and characterization of cerium oxide powder manufactured by the co-precipitation method, using inorganic cerium salt ($Ce(NO_3)_3$) and the precipitating agent (NaOH). In order to optimize the CeO_2 particles synthesis process, the parameters of the process were monitored to obtain the quantitative precipitate and to optimize the heat treatment. The precursors type and concentration used, reaction temperature and time, the pH of reaction medium and order of the precipitating agent addition are the main factors influencing the particle size and morphology of cerium oxide nanoparticles.

The physico-chemical properties of the cerium oxide nanoparticles were determined by Fourier transform infrared spectroscopy (FTIR), X-ray diffraction (XRD), and scanning electron microscopy (SEM), energy dispersive X-ray analysis (EDX). The FTIR spectrum of the CeO_2 particles calcinated at 550 °C, in normal atmosphere, exhibits a strong band at 482 cm^{-1} corresponding to Ce-O stretching vibration. The XRD pattern confirmed the crystalline nature of the CeO_2 nanoparticles with a cubic structure and average crystallite size around 15 nm. Moreover, EDX analysis confirms the presence of the Ce and O atoms corresponding to the theoretical formula. The morphology and microstructure were studied using SEM analysis.

KEYWORDS: cerium oxide, nanoparticles, synthesis, powders

1. Introduction

Cerium is a rare earth element, belonging to the lanthanide group, whose elements are arranged into an [Xe] $4f^15d^16s^2$ type electronic configuration, that can exist both free or in the oxide form [1-3]. Cerium oxide, also known as ceria or ceric oxide, is an excellent semiconductor material that has two valence states of Ce^{3+} (Ce_2O_3) and Ce^{4+} (CeO_2). It has the ability to switch very easily and reversibly between these oxidation states, with the possibility of rapidly forming, filling, and moving oxygen vacancies within the material [4–6].

From the two characteristic forms, CeO_2 is considered the most stable with a fluorite cubic structure, which contains eight coordinate cerium centers surrounded by a cube of eight oxide ions that are tetrahedrally coordinated into four cerium centers. Moreover, this material does not show any known crystallographic change from room temperature up to its melting point (2700 °C) [8, 9, 20].

According to the literature, cerium oxide has become an intensely studied material due to its

interesting features (size, morphology, specific surface area, dispersion state, oxygen storage capacity, oxygen deficiency and electronic conductivity) and its applicability in many areas of practical and modern technology, such as gas sensors, electrochemical devices, insulators, hybrid solar cells, protective products against sunlight exposure (for ultraviolet radiation absorption), ceramic biomaterials, polishing materials, white light emission, etc. [10–16].

Over the years, a considerable interest in enhancing the practical activity of cerium oxide is due to the excellent physical and chemical properties of CeO_2 nanoparticles, which are based on known and extensive synthesis methods. Thus, research has shown that many methods have been proposed to synthesize CeO_2 nanoparticles with promising control of properties, such as hydrothermal, mechanical processing, spray pyrolysis, sol-gel, solvothermal, thermal decomposition and precipitation methods [2, 8, 17, 18]. However, each of the applied methods is evidenced both by advantages and disadvantages for each particular process, the several disadvantages referring to the use of some toxic reagents and solvent, high reaction parameters and the necessity of requiring capping or / and stabilizing additives during the reaction [6, 19].

From the known chemical methods, co-precipitation synthesis is the most appropriate and simple method for obtaining oxide materials with a limited size distribution of particles and is widely applicable. It is considered a reliable method due to the advantages of a light synthesis condition. And because of certain concentration conditions and pH it can precipitate double salts, with complex stoichiometry. And also, by sintering the reactants with the monophasic amorphous structure, nanocrystalline powders with homogeneous chemical composition are obtained. In general, the physico-chemical characteristics of cerium oxide nanoparticles (size, morphology, type of intrinsic and / or extrinsic defect, crystal structure) largely depend on their synthesis procedures [7, 14, 19].

The objective of this paper was to synthesize cerium oxide nanoparticles by co-precipitation chemical method, which is a very simple method, accessible and with a small amount and cheap raw materials, in order to obtain pure CeO_2 powder for various practical applications.

The physico-chemical properties of cerium oxide nanoparticles were determined by Fourier transform infrared spectroscopy (FTIR), X-ray diffraction (XRD), scanning electron microscopy (SEM) and energy dispersive X-ray analysis (EDX).

2. Experimental details for the CeO_2 powder synthesis and characterization

In our experiments, cerium (III) nitrate ($Ce(NO_3)_3$), sodium hydroxide (NaOH), deionized water (H_2O DI), ethanol (C_2H_5OH) were used for the synthesis of cerium oxide nanoparticles. All chemicals were of reagent grade and used without further purification. In a typical synthesis, the cerium nitrate solution with 0.1M concentration was prepared and continuously stirred with a magnetic stirrer at 80 °C for 2 h. Then, the NaOH solution with a concentration of 1M was added dropwisely to the precursor solution and stirring was maintained for 3 hours at the same temperature, until a yellow precipitate was formed. The formed precipitate was left in repose for several minutes, after that it was filtered and washed alternatively with deionized water and ethanol for purification and removal of the secondary compounds.

After this step, the precipitate was further pre-sintered at 80 °C for 3 hours, these conditions being necessary for the complete conversion to CeO_2.

The sintering of the dried sample was carried out in a calcination furnace at a rate of 5 °C/min up to a temperature of 550 °C for 3 hours, in order to obtain a slightly light yellowish powder of CeO_2.

The structural characteristics for the sample in powder form were determined by Fourier Transform Infrared spectrometry (FTIR), in which IR spectra were recorded using a Bruker Tensor 27 spectrometer, in the wavenumber range of 4000-400 cm^{-1} by averaging 64 scans with a resolution of 4 cm^{-1} using the KBr pellet method.

The average crystallite size, crystalline phase and lattice parameters of the sample in powder form were analyzed by the X-ray diffraction (XRD) method using a 9 kW rotating anode SmartLab diffraction system (Rigaku Corporation, Japan) equipped with a $CuK\alpha_1$ tube and a multilayer mirror (λ = 1.5406 A). The experimental profile was recorded in grazing incidence XRD (GIXRD) with the incidence angle equal to 0.25°, while the detector was performed in the 2θ range from 20° to 90°.

The elemental analysis of the sample was carried out using energy-dispersive X-ray spectroscopy (EDAX, Smart Insight AMETEK). In addition, energy dispersive X-Ray (EDX) spectroscopy is attached to the scanning electron microscopy technique.

The morphology and microstructure were studied using a Field Emission Scanning Electron Microscope (FE-SEM). The SEM image was taken using an FEI Nova NanoSEM 630, with ultra-high resolution at high and low voltage in high vacuum of

1.6 nm @ 1 kV. For increasing the SEM images quality, the sample in powder form was dispersed in ethanol, dripped onto the silicon wafer surface and then, a gold layer was vaporized onto the sample surface.

3. Results and discussions

3.1. FTIR analysis

The FTIR spectrum of synthesized CeO_2 nanoparticles pre-sintered at 80 °C and calcined at 550 °C, in normal atmosphere, is presented in Figure 1.

The feature in FTIR spectrum of pre-sintered precipitate presents bands in the range of 4000 -1300 cm^{-1} which can be attributed to nitrate species vibration from raw materials and hydroxyl from water absorption. After calcinations, the peaks from this region were significantly changed with the increase of the heat-treatment temperature. The spectrum of CeO_2 nanoparticles calcined at 550 °C, clearly showed three peaks centered at 3446, 1638 and below 700 cm^{-1}. The bands at 3446 cm^{-1} and 1638 cm^{-1} can be attributed to the stretching mode of O-H bonds from absorption during the processing step of FTIR analysis [8, 18].

The strong band centered at 491 cm^{-1} can be assigned to the presence of C-O stretching vibration mode from CeO_2 molecules.

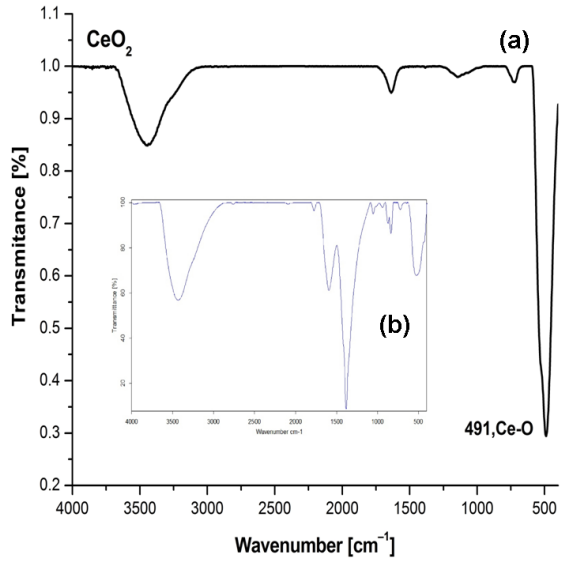

Fig. 1. *FTIR spectrum of the CeO_2 powder: a) pre-sintered at 80 °C, b) sintered at 550 °C*

3.2. XRD analysis

The XRD pattern of the CeO_2 nanoparticles was carried out by X-ray diffraction in the range of 2θ between 20° to 90° as shown in Figure 2.

XRD was also used to check the purity and crystallinity of CeO_2 nanoparticles, and to estimate the average crystalline size.

The sample exhibits typical peaks corresponding to the CeO_2 crystalline planes with Miller indices of (111), (200), (220), (311), (222), (400), (331), (420), (422) for a series of characteristic peaks located at 2θ = 28.3°, 33.1°, 47.4°, 56.3°, 59.0°, 69.3°, 76.6°, 79.0°, 88.3°, respectively [9, 14]. All the diffraction peaks of the sample were indexed to the cerianite (Ce) symmetric structure with cubic structure (lattice parameters are a = b = c = 5.4154 Å), belonging to Fm-3m space group no. 225 [DB no. 00-900-9008]. No peak of other crystalline impurities (i.e: Ce_2O_3) was detected, thus indicating the high purity and good crystallinity of the cerium oxide sample.

Using the full width at half maximum (FWHMs) of the diffraction peaks, the average size of the crystallites was estimated through Debye Scherrer's formula:

$$D = K\lambda/(\beta \cos \theta)$$

where: D is the crystallite size; K is the shape coefficient (0.94), λ is the radiation wavelength (1.54 A), β is the line broadening at half the maximum intensity (FWHM) in radians, and θ is the Bragg diffraction angle obtained from 2θ value corresponding to the maximum intensity peak (in radians).

Based on this formula, the average crystallite size of the CeO_2 powder sample was found to be around 11.5 nm.

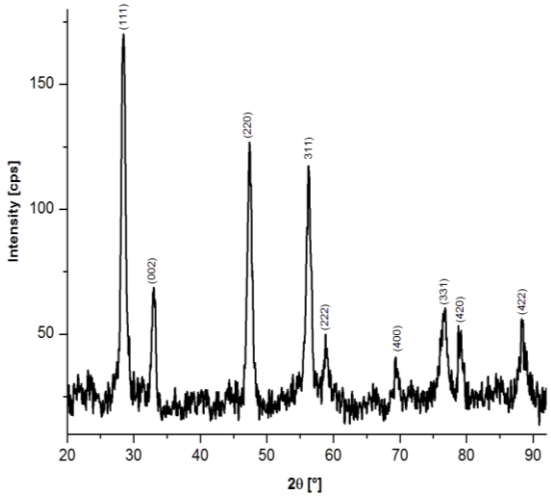

Fig. 2. *XRD pattern of the CeO_2 powder*

3.3. EDX analysis

In order to achieve a qualitative study, EDX analysis was performed as presented in Figure 3.

EDX provided information on the elemental analysis or chemical characterization of the powder sample, which further confirmed that the synthesized CeO_2 was pure and consisted in Ce and O. In the energy-dispersive X-ray spectrum (Figure 3), we can see peaks that correspond to the atoms of oxygen (O(K) at 0.53 keV) and cerium (Ce(L) at 4.84 keV and Ce(M) at 0.88 keV).

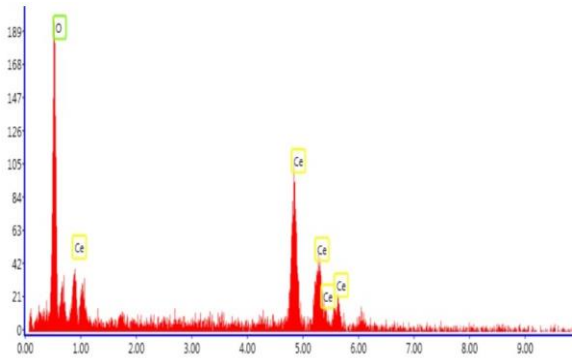

Fig. 3. *EDX spectrum of the CeO_2 powder*

This analysis also reveals the weight and atomic percentage of each component present in the synthesized sample as shown in Table 1. The quantitative analysis was based on the use of atomic percentages for calculating the molecular formula of the cerium oxide sample. The final composition was calculated and corresponds to the theoretical $Ce_{1.017}O_{1.983}$ formula, suggesting a good crystallinity of the material, being very close to that of the desired material [10].

Table 1. *Weight and atomic percentage of the elements present in the CeO_2 powder from EDX data*

Element	Wt%	At%
OK	18.2	66.08
CeL	81.8	33.92

3.4. Surface morphology

The surface morphology and size details of the CeO_2 nanoparticles were studied through the SEM image in Figure 4.

The SEM image displays the existence of crystalline particles with the sizes in the range of 15 to 30 nm. Spherical shapes of CeO_2 nanoparticles and a slightly tendency for agglomeration were confirmed. A homogeneous distribution of spherically synthesized CeO_2 nanoparticles was observed. This result is consistent with the crystallite size calculation by Scherrer formula from the XRD analysis.

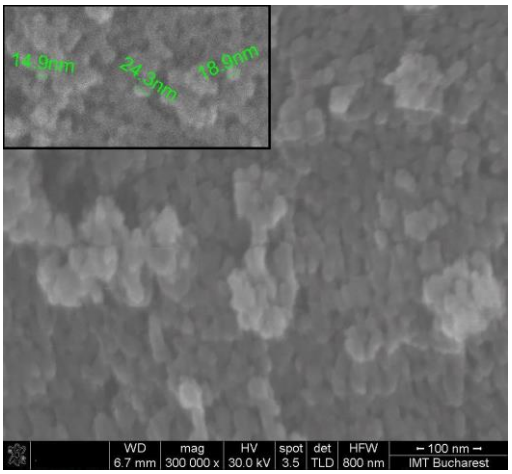

Fig. 4. *SEM micrograph of the CeO_2 powder*

4. Conclusion

CeO_2 nanoparticles were synthesized by the chemical precipitation method and the parameters and optimal synthetic conditions were established.

The influence of process conditions on the structural and morphological properties of synthesized particles has been investigated.

The FTIR spectrum indicated a strong band at 491 cm^{-1} due to the presence of Ce-O stretching vibration mode of CeO_2.

The results obtained from XRD and SEM confirm the crystalline nature of the synthesized sample and the nanoscale size of the crystallite (particle).

XRD pattern shows the formation of the fluorite type structure, with cubic symmetry characteristic for ceria, without other crystalline impurities. The average crystallite size of CeO_2 powder was calculated around 11.5 nm.

EDX spectrum indicates that the particle is composed only of Ce and O and it confirms the theoretical formula and the purity of the sample.

SEM image displays the existence of crystalline particles with the sizes in the range of 15 to 30 nm, but also spherical shapes of the particles with clumped distribution.

The co-precipitation method was preferred in cerium oxide nanoparticle synthesis because by optimizing the reaction conditions and calcination temperature, lower crystallite (particle) size was obtained. Moreover, the desired properties of CeO_2 nanoparticles make it a promising material in order to develop applications in the environmental field. The

particles thus obtained have demonstrated their usefulness and were subsequently used for the synthesis of ion-doped garnet phosphorus and cerium-doped aluminum phosphate, for optoelectronics ("*Influence of Sintering Temperature on the Structure of the Yttrium Based Phosphor Nanoparticles*" – the paper presented to SCDS-UDJG 2017 and awarded the First price), as well as for the development of applications within the TEHNOSPEC project –No. PN1632/2016.

Acknowledgments:

This research was supported by the National Basic Funding Programme TEHNOSPEC – Project No. PN1632/2016.

This work was supported by a grant of the Ministry of National Education and Scientific Research, RDI Program for Space Technology and Advanced Research-STAR, project number 639/2017.

This paper is part of Vasilica (Şchiopu) Ţucureanu's PhD thesis, at Transilvania University of Braşov, Department of Materials Science, coordinated by Prof. dr. eng. Daniel Munteanu.

References

[1]. Balavi H., Samadanian-Isfahani S., Mehrabani-Zeinabad M., Edrissi M., *Preparation and optimization of CeO_2 nanoparticles and its application in photocatalytic degradation of Reactive Orange 16 dye*, Powder Technol., 249, p. 549-555, 2013.

[2]. Hu C., Zhang Z., Liu H., Gao P., Wang Z. L., *Direct synthesis and structure characterization of ultrafine CeO_2 nanoparticles*, Nanotechnology, 17, p. 5983-5987, 2006.

[3]. Yang Z., Woo T. K., Baudin M., Hermansson K., Yang Z., Woo T. K., *Atomic and electronic structure of unreduced and reduced CeO_2 surfaces: A first-principles study*, J. Chem. Phys., 120, p. 7741-7751, 2004.

[4]. Luches P., Valeri S., *Structure, Morphology and Reducibility of Epitaxial Cerium Oxide Ultrathin Films and Nanostructures*, Materials, 8, p. 5818-5833, 2015.

[5]. Babitha K. K., Sreedevi A., Priyanka K. P., Boby Sanu, Thomas Vargehese, *Structural characterization and optical studies of CeO_2 nanoparticles synthesized by chemical precipitation*, Indian J. of Pure & Applied Physics, 53, p. 596-603, 2015.

[6]. Charbgoo F., Bin Ahmad M., Darroudi M., *Cerium oxide nanoparticles: green synthesis and biological applications*, Int. J. Nanomedicine, 12, p. 1401-1413, 2017.

[7]. Lin K. S., Chowdhury S., *Synthesis, Characterization and Application of 1-D Cerium Oxide Nanomaterials: A Review*, Int. J. Mol. Sci., 11, p. 3226-3251, 2010.

[8]. Suresh R., Ponnuswamy V., Mariappan R., *The role of oxidizing agents in the structural and morphological properties of CeO_2 nanoparticles*, Materials Science in Semiconductor Processing, 21, p. 45-51, 2014.

[9]. Farahmandjou M., Zarinkamar M., Firoozabadi T. P., *Synthesis of Cerium Oxide (CeO_2) nanoparticles using simple co-precipitation method*, Revista Mexicana de Fisica, 62, p. 496-499, 2016.

[10]. Zamiri R., Ahangar H. A., Kaushal A., Zakaria A., Zamiri G., Tobaldi D., Ferreira J. M., *Dielectrical Properties of CeO_2 Nanoparticles at Different Temperatures*, PLoS ONE10(4): e0122989, p. 1-11, 2015.

[11]. Tucureanu V., Matei A., Mihalache I., Danila M., Popescu M., Bita B., *Synthesis and characterization of YAG: Ce, Gd and YAG: Ce, Gd / PMMA nanocomposites for optoelectronic applications*, J. Mater. Sci., 50, p. 1883-1890, 2015.

[12]. Tucureanu V., Matei A., Avram A. M., *Synthesis and characterization of YAG:Ce phosphors for white LEDs*, Opto-Electronics Rev. 23, p. 239-251, 2015.

[13]. Schiopu V., Matei A., Dinescu A., Danila M., Cernica I., *Ce, Gd codoped YAG nanopowder for white light emitting device*, J. Nanosci. Nanotechnol., 12, p. 1-5, 2012.

[14]. Liu Y. H., Zuo J. C., Ren X. F., Yong L., *Synthesis and character of cerium oxide (CeO_2)*, Metabk 53, p. 463-465, 2014.

[15]. Farahmandjou M., Zarinkamar M., *Synthesis of nano-sized ceria (CeO_2) particles via a cerium hydroxy carbonate precursor and the effect of reaction temperature on particle morphology*, J. Ultrafine Grained and Nanostructured Materials, 48, p. 5-10, 2015.

[16]. López-Mena E. R., Carlos R., Martinez-Preciado H. A., Elías-Zuñiga C. A., *Simple Route to Obtain Nanostructured CeO_2 Microspheres and Simple Route to Obtain Nanostructured CeO_2 Microspheres and CO Gas Sensing Performance*, Nanosclae Research Letters, 12, 2017.

[17]. Mazaheri M., Aminzare M., Sadrnezhaad S. K., *Synthesis of CeO_2 Nanocrystalline Powder by Precipitation Method*, Proceeding ECERS Conference, p. 655-658, 2009.

[18]. Ketzial J. J., Nesaraj A. S., *Synthesis of CeO_2 nanoparticles by chemical precipitation and the effect of a sur factant on the distribution of particle sizes*, J. Processing Research, 12, p. 74-79, 2011.

[19]. Stankic S., Suman S., Haque F., Vidic J., *Pure and multi metal oxide nanoparticles: synthesis, antibacterial and cytotoxic properties*, J. Nanobiotechnology., 14, p. 1-20, 2016.

[20]. Farruhk M. A., *Functionalized Nanomaterials*, Publisher: InTech, ISBN 978-953-51-2856-4, Print ISBN 978-953-51-2855-7.

THE ANNALS OF "DUNAREA DE JOS" UNIVERSITY OF GALATI
FASCICLE IX. METALLURGY AND MATERIALS SCIENCE
Nº. 1 - 2017, ISSN 1453-083X

OBJECT ORIENTED ARCHITECTURE FOR PRODUCT INFORMATION SYSTEM ENGINEERING

Bilel RAHALI[1], Alaa ABOU HARB[2]
[1]Doctoral School of Engineering and Management of Technological Systems, Polytechnic University of Bucharest, Romania, e-mail: bilel.rahalii@gmail.com
[2]Doctoral School, Faculty of Materials Science and Engineering, Polytechnic University of Bucharest, Romania, e-mail: alaaabouhareb84@hotmail.com

ABSTRACT

The product information system is an organizational device for regulating the creation, circulation, use and evolution of the information assets of the product definitions. It refers to all the information that defines how the product is designed, manufactured and used.

Product information systems have become a critical element for the enterprises to support their process of product offer definition.

The company SOTACIB itself assembles these production elements (from the basic composition phase to the final phase). Our application provides a computerized management system for the technical data of the product manufacturing. Its objective is to support the development activities of the cement product by preparing atomized powders such as grinding, controlling the parameters of the slip, by sieving and final atomization. An UML modeling of the system is developed in the context of a driven approach centered on a proposed architecture.

KEYWORDS: UML, Product Information System, TDMS

1. Introduction

The information system of a company is a communication link both inside the company and outside. The systematic vision of the company sets up the information system at the interface between, on the one hand, the operating system responsible for production and responding to the purpose of the company and, on the other hand, maintains the chosen objectives [1].

The operating system of the company contains two key processes that are decisive for the achievement of the company's objective:

1 - a first process of "definition of the product offer", whose function is to define and maintain the products that the company releases on the market. Enterprise Resource Planning (ERP) information systems play an important role in supporting this process.

2 - a second process of "production of supply" This process begins when a customer expresses his need and therefore places an order. In this case, the company must provide a quality product as soon as possible. This process requires the installation of a PDM (product data management) information system. We refer to this second enterprise information system in this article. Thus, the objective of this work is the setting up of UML for the modeling of an information system for the preparation of cement. Indeed, with the complexity of the product offer and in a concurrent engineering context, the mastery of technical information has become a crucial and difficult subject: crucial because any failure in the management of information is translated immediately by non-qualities but also difficult due to the dynamics of the system [2, 3].

2. Development of the approach

The manufacturing process goes through several stages: after studying the needs of the customer, the product is defined and the preparation is made. The production takes place according to precise conditions, which are controlled at all the stages. The preparation of cement passes through several stages: choice of raw materials, grinding, control of color, control of the parameters of the slip, sieving and atomizing the slip. In the control room, engineers

drive the factory from their screens where all the information is displayed. At each stage of the transformation of the material, samples are automatically taken and analyzed very rigorously.

To construct a computer system that manages the manufacturing process, the SIP context is used, which implies different needs than those present in traditional management applications. The data managed are more complex (graphic, text, etc.), the data models are richer (with strong semantics and involve a rich dynamic with several levels of abstraction: instance, class, model).

This information system is developed by the object - oriented approach which has shown its results in research work on engineering application development [4].

3. System Modeling

The development of the product information system is based on an object - oriented architecture as part of an approach driven by the use cases centered on an architecture and iterated in an iterative and incremental way.

This tool is based on a PIS package that brings together all the business objects: manufacturing, product definition and user's need as it can be seen in Fig. 1 [5]. Our modeling is centered on the "manufacturing" business object that describes the technical data of the manufacturing process.

3.1. Description of Collaboration Diagrams

In analysis, UML creates the use cases by means of collaborations between the objects coming from the domain of the application [6, 7]. Collaboration diagrams show interactions between objects (class instances and actors, which allow us to represent the context of an interaction, because we can specify the states of the objects that interact with each other). Collaboration diagrams that present the functions "Define Product", "Grind" and the "Sift" function are shown in Fig. 2, Fig. 3 and Fig. 4.

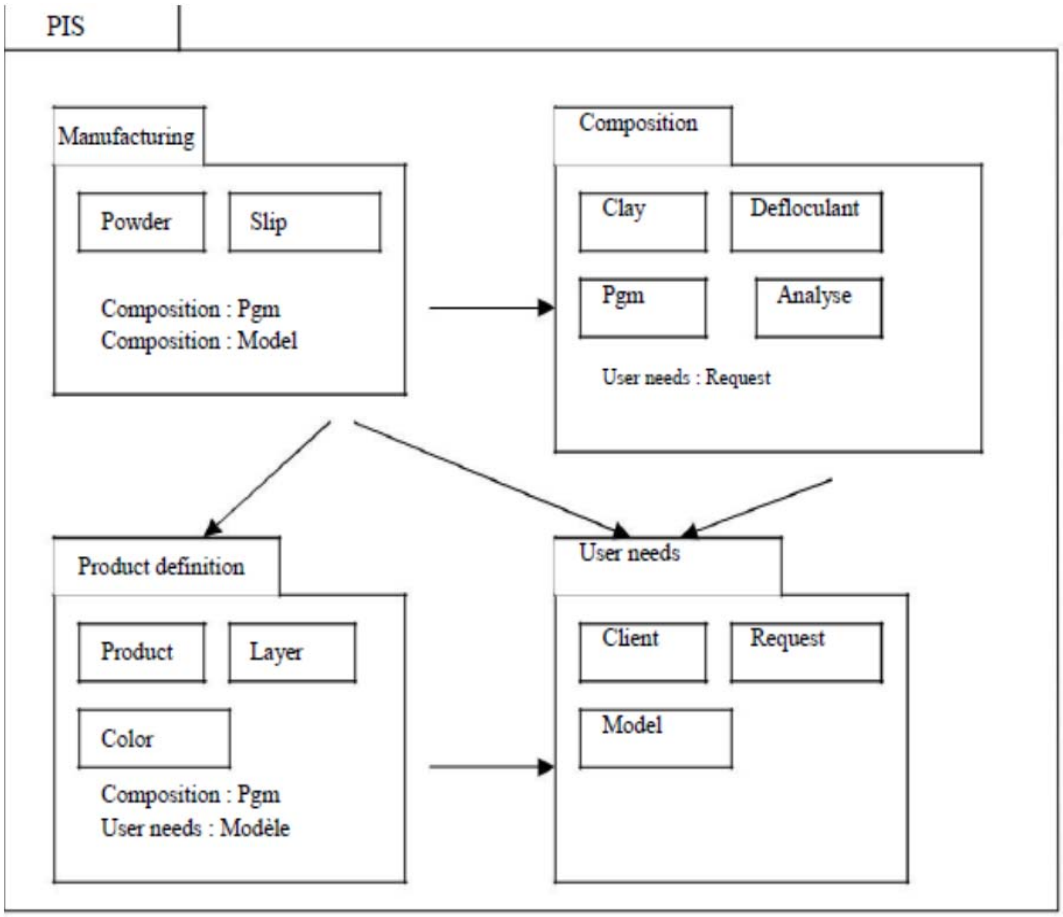

Fig. 1. *Representation of the PIS package for the cement*

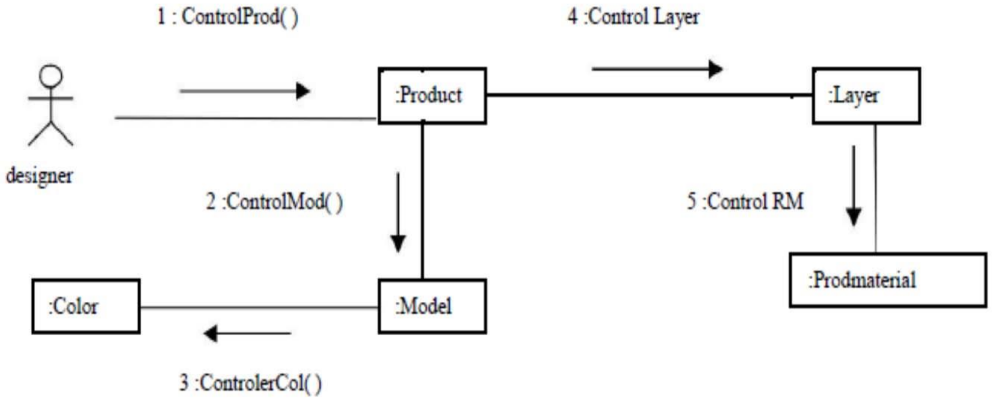

Fig. 2. *Collaboration diagram «Product definition»*

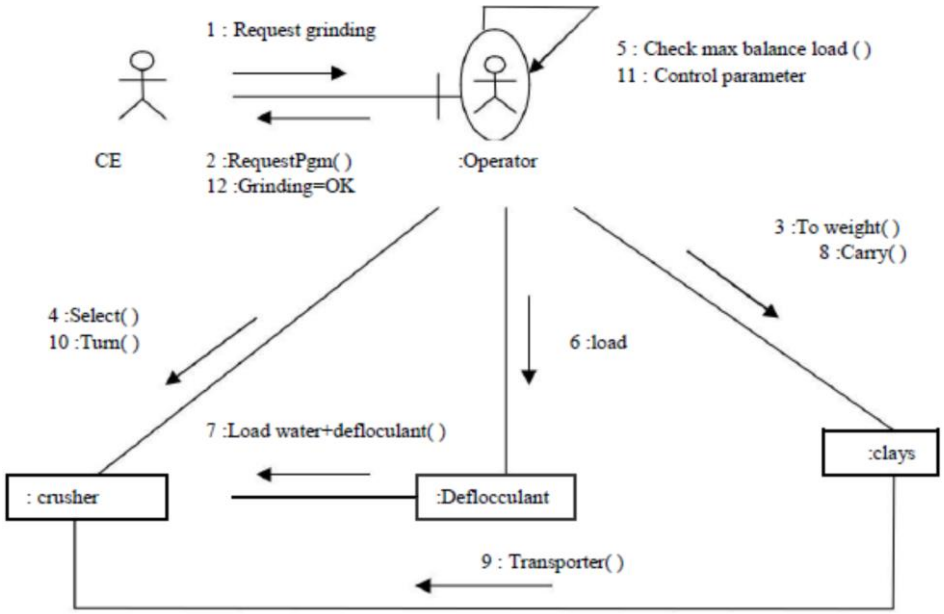

Fig. 3. *Collaboration diagram «Grind»*

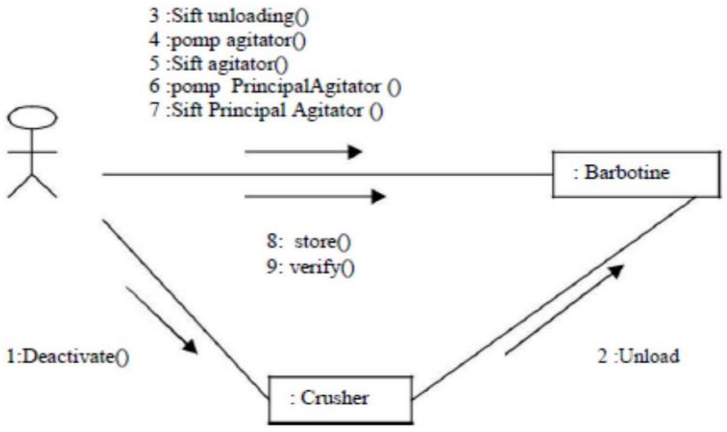

Fig. 4. *Collaboration diagram «Sift»*

3.2. Class Diagram

The class diagram is a schema used to present the classes and interfaces of the systems as well as the different relationships between them. This diagram is a part of the static part of UML because it disregards the temporal aspects. The class diagram of our application is shown in Fig. 5 [8, 9].

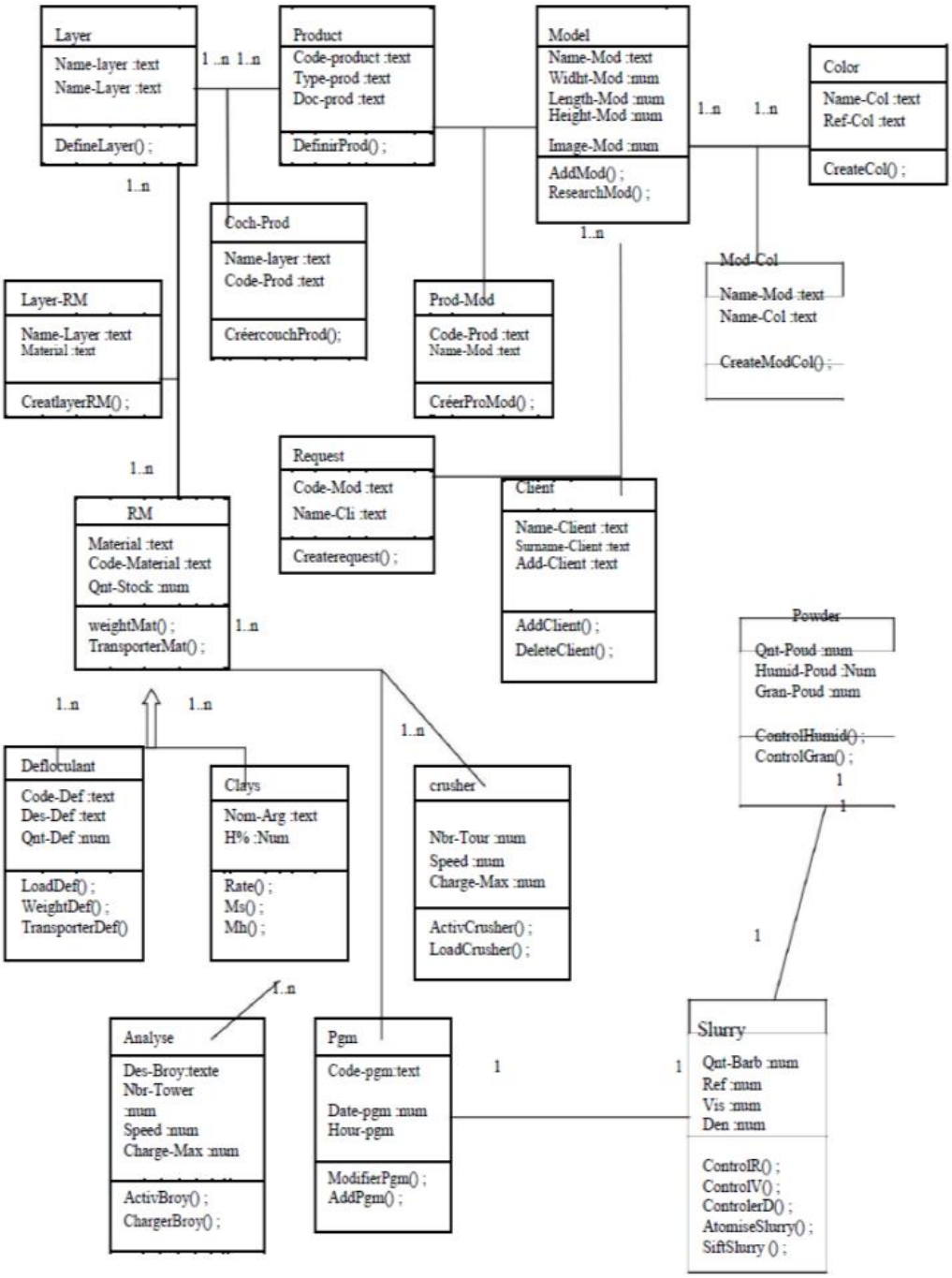

Fig. 5. *Class Diagram for Business Object "Manufacturing"*

4. Conclusion

This work is part of a research study on product information systems that use the UML modeling language. In this paper we have succeeded in developing an object- oriented architecture for the engineering of product information systems and more

specifically of the technical data management system (TDMS) for the manufacture of cement product.

The developed TDMS allows us to structure, secure and share access to information for the cement product and on the other hand to ensure both the accuracy of the production records and the visibility of the process Technical change management.

References

[1]. Projet E. J. Wait Ait, *Advanced Information technology for design and manufacturing*, WP2 definition, 1997.
[2]. Arasti M. R., *Aide à l'élaboration de stratégies technologiques cohérentes avec la stratégie globale de l'entreprise*, Thèse de doctorat de l'Institut National Polytechnique de Grenoble 1999.
[3]. Bourdichou P., *L'ingénierie simultanée et la gestion d'informations*, Ed. Hermès Paris, 1994.
[4]. Lilia Gzara, *Les patrons pour l'ingénierie des systèmes d'information produit*, Thèse pour obtenir le grade de Docteur, Institut National Polytechnique de Grenoble.
[5]. Jacobson I., Christerson M., Jonson P., Overgard G., *Object oriented software Engineering: A use case driven approach*, Addison Wesley, 1992.
[6]. Michel Lai, *UML, la notion unifiée de modélisation objet*, 1998.
[7]. Dounia Mansouri, *Architecture orientée objet de type SIAD pour l'élaboration de contenus pédagogiques*, département d'informatique, 2002.
[8]. Pernelle P., Theroude F., Courtois A., *Mise en oeuvre et utilisation des systèmes de gestion de données techniques dans les petites et moyennes entreprises*, Proc. IDMMC 2000, Montréal, 16-19 mai 2000, Presses Internationales Polytechnique.
[9]. Tessier C., *La pratique des méthodes en informatique de gestion*, les éditions d'organisation, Paris, 1995.

THE ANNALS OF "DUNAREA DE JOS" UNIVERSITY OF GALATI
FASCICLE IX. METALLURGY AND MATERIALS SCIENCE
Nº. 1 - 2017, ISSN 1453-083X

INVESTIGATION OF MECHANICAL PROPERTIES AND CORROSION BEHAVIOUR FOR 1010 CARBON STEEL PIPES USED FOR STEAM BOILERS

Alaa ABOU HARB[1], Ion CIUCA[2], Bilel RAHALI[3], Roxana-Alexandra GHEŢA[4]

[1]Doctoral School, Faculty of Materials Science and Engineering, Polytechnic University of Bucharest, Romania, e-mail: alaaabouhareb84@hotmail.com
[2]Faculty of Materials Science and Engineering, Polytechnic University of Bucharest, Romania, e-mail: ion.ciuca@medu.edu.ro
[3]Doctoral School, Faculty of Materials Science and Engineering, Polytechnic University of Bucharest, Romania, e-mail: bilel.rahalii@gmail.com
[4]Doctoral School of Engineering and Management of Technological Systems, Industrial Engineering Department, Polytechnic University of Bucharest, Romania, e-mail: roxana_gheta@yahoo.com

ABSTRACT

Depending on the conditions of their use, most equipment gets deteriorated in time. In this paper the corrosion rate (CR) was verified by using the experiment of weight loss (WL) of specimens from steam boiler pipes (SBP) made of 1010 carbon steel with a thickness of 4 mm. CR was calculated by specimens' weight loss in the corrosive environment at 25 °C in 5% NaCl - 10% H_2O_2 solution which reproduces the environment in the plant during specific times.

The mechanical properties which were verified include hardness test and tensile test. The results that have been obtained through tensile curves and hardness properties on specimens 1 and 2 were compared to a non-service specimen (3) made of 1010 carbon steel. It is concluded that there was an increase in the properties of tensile and a decrease of hardness for both specimens by comparing them with a non-service specimen. Due to overheating, a deposition of layers of lime (CaO) on the pipes was caused. It is noticed that the decrease of the mechanical properties leads to increased corrosion.

KEYWORDS: steam boilers pipes, carbon steel, corrosion rate, weight loss, hardness properties, tensile stress

1. Introduction

Over the years, the chemical engineers always provided the best information for corrosion and proper use of materials in the chemical industry and its operations.

Many scientists and researchers worked hard in this domain to answer the important question: how does corrosion occur [1].

Corrosion is a degradation of a metal by electrochemical changes that occur in the presence of the surrounding environment, which lead to the occurrence of the corrosion, namely to. a change in the mechanical properties of a metal [2, 3].

Corrosion usually begins on the stages which can be shortened by the following steps:

1. Interaction between the base metal and the corrosive environment.
2. Growth of oxidation layer and its penetration in the base metal [4].

Boiler is the heat transferring used in the production of steam (wet, toasted). We can use this steam in the power generation, heating, etc.

The main problems of corrosion that occurs in boilers are: oxidation, hydrogen damage, stress corrosion cracking, fatigue and chemical corrosion [5].

The pipes of boilers erode during the passage of water or steam inside and heated by the outside fire. Therefore, the failure can be classified into internal failure represented by the fatigue and external failure represented by oxidation, hydrogen damage, erosion and stress corrosion cracking [6, 7].

Pipe failure occurs in different parts of the boiler and the following statistics were collected: 40% in water wall tubes, 30% in super heater tubes, 15% in re - heater tubes, 10% in economizers, 5% in cyclones [8, 9].

Our aim in this research is to investigate the corrosion processes which occur in the pipes of the boiler and to study the influence of mechanical properties on corrosion.

2. Materials and methods

2.1. Specimens of experiment

Specimens for boiler tubes (horizontal and vertical boiler) were selected and numbered as follows: specimen 1 is the standard tube (non-service specimen) for the horizontal and vertical boiler (for comparison), specimen 2 is the tube that was in service for the horizontal boiler and specimen 3 is the tube that was in service for the vertical boiler, all with 4mm thickness.

The chemical composition of the 1010 carbon steel was obtained by spectral analysis device (Spectro Max) and is shown in Table 1.

2.2. Testing

Specimens with dimensions of 20 × 20 mm^2 and 4 mm in thickness were used for the weight loss measurement.

All samples have been metallographically prepared on SiC fine paper of different grit (1200 grit) followed by cleaning in distilled water, acetone and drying in hot air.

In order to evaluate the material mechanical properties, the tensile strength and yield strength have been analyzed by using a 300 KN servo hydraulic universal testing machine.

The specimens were subjected to hardness measurement, which was determined on several regions by Rockwell hardness (HRA) testing method.

3. Results and discussion

3.1. Structural characterization

Figure 1 shows the schematics of the samples used.

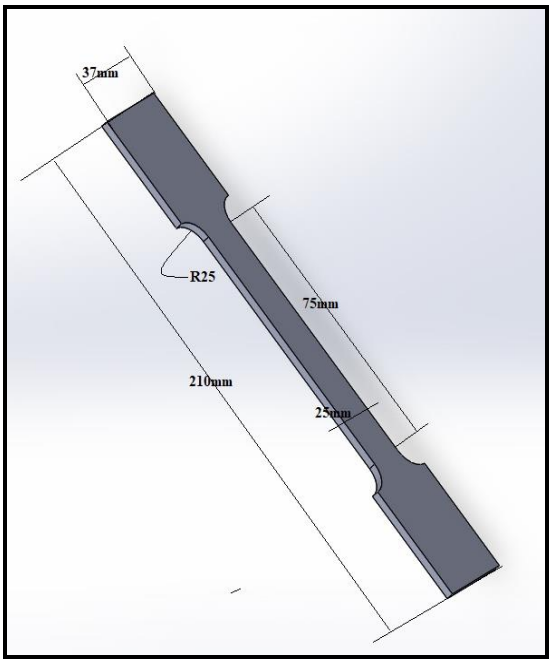

Fig. 1. *Tensile specimens used in the research*

In Figure 2 the physical tensile specimens which were used in the research are presented.

The Load - Displacement curves of the specimen are shown in Fig. 3 and the bar chart shown in Fig. 4 shows the comparison of the tensile parameters obtained from testing and the non-service specimen.

Table 1. *Chemical composition (wt. %)*

No.	C%	Si%	Mn%	P%	S%	Cr%	Ni%
1	0.094	0.076	0.004	0.01	0.404	0.088	0.09
2	0.150	0.078	0.0038	0.018	0.413	0.111	0.09
3	0.085	0.104	0.0085	0.0086	0.375	0.107	0.081

Fig. 2. *Macroscopic images of the 1010 samples used in the mechanical tests: 1) non-service specimen, 2) service horizontal boiler specimen and 3) service vertical boiler specimen*

It is noted that there is an increase in tensile properties for both specimens 2 and 3, by comparing them with specimen 1.

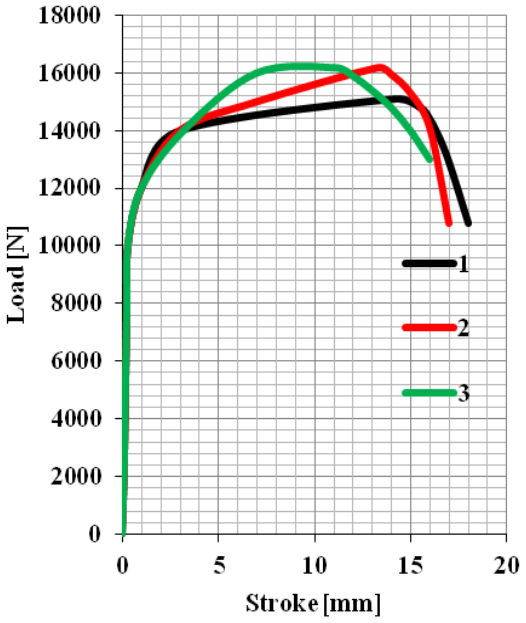

Fig. 3. *The load - displacement curves of the tested specimens: 1) non-service specimen, 2) horizontal boiler specimen and 3) vertical boiler specimen*

The hardness tests have been achieved on different regions, and they showed an approximate value of 48.6 HRA for specimen 1, 48 HRA for specimen 2 and 48.1 HRA for specimen 3.

It is noted that there is a decrease in hardness properties for both specimens 2 and 3, by comparing them with specimen 1.

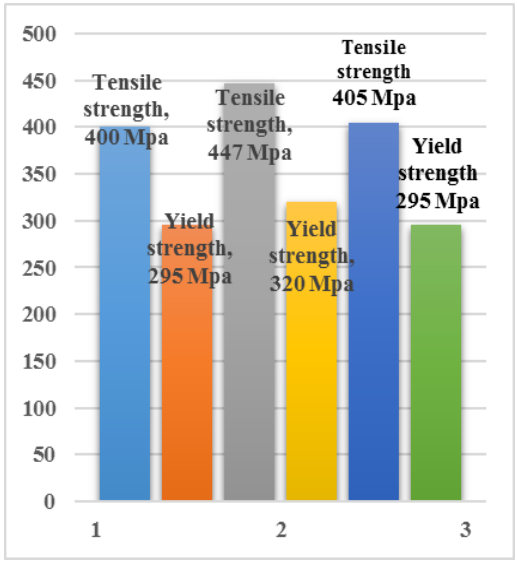

Fig. 4. *The tensile strength and yield strength of the tested specimens: 1) non-service specimen, 2) horizontal boiler specimen and 3) vertical boiler specimen*

It is noticed a decrease of mechanical properties (hardness and tensile stress) through the chart for both specimens. This makes the metal more susceptible to corrosion such as stress corrosion cracking and pitting corrosion under high temperature and high pressure. So, it is required a type of metal which has high mechanical properties to protect it from the corrosion.

In searching for the suitable metal, it is found that there is a type of carbon steel able to work in this condition.

ASTM A210 [10] is a carbon steel pressure tube with very good mechanical properties, which can be successfully used in this application.

In Table 2 are shown the chemical properties of ASTM A210 carbon steel pressure tube.

Table 2. *Chemical composition (wt. %)* [10]

ASTM	C%	Si%	Mn%	P%	S%
A210	0.27	0.1	0.93	0.048	0.058

In Table 3 are shown the mechanical properties of ASTM A210 carbon steel pressure tube.

Table 3. *Mechanical properties* [10]

ASTM	Tensile strength [Mpa]	Yield strength [Mpa]
A210	415	255

3.2. Corrosion results

The tests were carried out at 25 ºC in chemical solution of 5% NaCl - 10% H_2O_2 which simulates the environment in the factory during specific times.

Using a hand grinding wheel machine, the surface of the specimens was polished. After that, surface preparations were carried out by wet grinding with a series of SiC papers to 1200 grit followed by cleaning in distilled water, with acetone and air drying.

A solution of 5% NaCl - 10% H_2O_2 in distilled water was used, to simulate the environment in the factory during specific times (every 24 h, three times) at 25 °C, whereas the concentration of solution represents the work environment.

The weight loss was monitored by measuring the initial and final mass with an analytical balance (Sartorius, model TE 153S) with a precision of 0.001 g.

We can determine the corrosion rate [11] using the following equations (1) and (2).

$$R = \frac{K \cdot W}{A \cdot T \cdot D}(mm/year) \quad (1)$$

$$W = m_i - m_f\,(mg) \quad (2)$$

where:

R: Corrosion rate (mm/year);
K: 87.6 (conversion constant);
W: weight loss (mg);
A: area (cm^2);
T: time (h);
D: density (g/cm^3);
m_i: initial mass;
m_f: final mass.

In Fig. 5 is presented a macroscopic image of a specimen used in the weight loss experiments.

Fig. 6 represents the variation of corrosion rate within time for all specimens, where all measurements have been repeated three times.

Fig. 5. *Macroscopic image of the tested specimen in the corrosive environment during the weight loss analysis*

It is noted that the corrosion rate increases in the first 24 hours, and it starts to decrease during the following hours (Fig. 6).

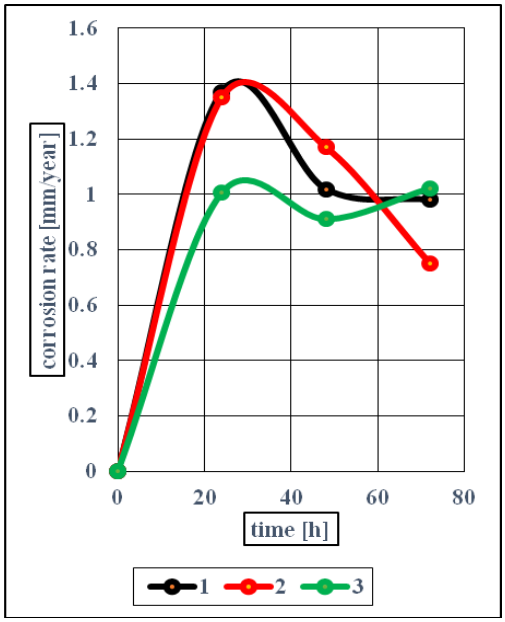

Fig. 6. *Time - corrosion rate curves of the tested specimens: 1) non-service specimen, 2) horizontal boiler specimen and 3) vertical boiler specimen*

4. Conclusion

The mechanical tests have highlighted that specimens2 and 3 present higher tensile when compared to a non-service specimen 1.

Furthermore, by making a comparison between specimens 2 and 3 and a non-service specimen 1, we notice a variation in hardness: the non-service specimen 1 has higher hardness.

The weight loss tests have indicated that the interaction which occurs in the corrosive media at room temperature leads to materials deterioration. The corrosion rate increases in the first 24 hour, and it starts to decrease during the following hours.

It is noticed that in the following hours, there is an increase in corrosion rate for both specimens 2 and 3, by comparing them with specimen 1.

This leads to the formation of a protective layer on the materials surface, inhibiting thus the corrosion process, but this leads to increasing pipe breakdown by overheating due to the low conductivity of the oxidation layer.

So, as a final conclusion it can be said that 1010 carbon steel is not a proper material for SBP fabrication and should be replaced by ASTM A210 carbon steel pressure tube that will improve its usage in this application.

By comparing A210 type and 1010 used, it is noticed an increase rate of manganese in A210 (up to 0.93%), that improves tensile properties in high temperature and pressure.

It is noticed a decrease rate of sulfide in A210 (up to 0.058%), that protects the metal from breakage in the corrosive environment.

References

[1]. ***, www.outokumpu.com.
[2]. Talbot D., Talbot J., *Corrosion Science and Technology*, Materials Science and Technology, CRC Pres., 1998.
[3]. Anthony U., Ikenna M., Ufuma O. B., Ezemuo D. T., *Corrosion Rates and its Impact on Mild Steel in Some Selected Environments*, Journal of Scientific and Engineering Research, 3(1), p. 34-43, 2016.
[4]. Marcus P., *Introduction to the Fundamentals of Corrosion*, Corrosion: Fund-Amentals, Testing, and Protection, vol. 13A, ASM Handbook, ASM International, p. 3-4, 2003.
[5]. Ahmad Z., *Principles of Corrosion Engineering and Corrosion Control*, Boiler Corrosion, Chapter 11, p. 576-608, 2006.
[6]. Al-hajri M., Al-muaili F., Andijani I., Mobin M., Muaili F., *Corrosion of boiler tubes some case studies*, published in the Proceeding Of 4th SWCC Acquired Experience Symposium held at Jeddah, p. 739-763, 2005.
[7]. Bayer G., Larkin E., Zamanzadeh M. *Failure analysis and Investigation methods for boiler tube failures*, Matco Associates, Inc. 4640 Campbells Run Road Pittsburgh, Pennsylvania 15205, 2007.
[8]. Jonas O., *Boiler Tube Sampling and Inspection Procedures*, Recommended Practices, Water Chemistry Control. Jonas, Inc., Wilmington, DE, 1992.
[9]. Mobin M., Malik A. U., Al-Hajri M., *Investigations on the Failure of Economizer Tubes in a High-Pressure Boiler*, J. Fail. Anal. And Preven., 8, p. 69-74, 2008.
[10]. ***, ASM metals handbook, vol. 1, *Properties and Selection: Irons, Steels, and High-Performance Alloys*, Sep 2005.
[11]. Mc Naughon, Kenneth J., the Staff of Chemical Engineering, *Controlling Corrosion in Process Equipment*, Materials Engineering II, McGraw – hill Publication Company, 1980.

THE ANNALS OF "DUNAREA DE JOS" UNIVERSITY OF GALATI
FASCICLE IX. METALLURGY AND MATERIALS SCIENCE
Nº. 1 - 2017, ISSN 1453-083X

THE QUALITY OF METAL PRODUCTS MADE ON CNC MACHINES

Nela PUŞCAŞ (POPESCU)
"I. N. Socolescu" Technical College of Architecture and Public Works, Bucharest, Romania,
12 Occidentului Street, sector 1
e-mail: netapops@yahoo.com

ABSTRACT

Contemporary market must provide products that adapt to customer needs, which requires large investments and long-term employment. Producers have to take care of the buyers' different way of thinking. The quality of products and services is an important economic indicator. The paper presents studies and research in the field of bending of metal parts (thickness between 1 and 3 mm) on CNC machines. This paper tries to provide answers to the many problems arising in the companies due to the quality of the economic goods. In the technological flow of the achievement of a metal product, bending is very important, the quality and conformity of the product depending on this operation. The paper proposes laborious research and studies on determining the drawings of metal parts with the thickness between 1 and 3 mm, considering that other variables such: the temperature variation during the processes of punching and bending, tool usage, the tolerance between the surfaces of the bending tools, the vibrations of the machines, their usage and the roughness of the sheet metals may influence the quality and precision of the products. The calculation of the drawing (the geometry in plane of the piece) becomes important because it must include the deformation caused by the bending operation. Bending coefficients $K_î$ must compensate for deviations from the final dimensions of the metal parts, because of the many variables that can adversely affect their execution. The bending coefficient $K_î$ is determined by experimental tests and measurements.

KEYWORDS: bend metallic component; quality, conformity, other variables, CNC machines

1. Introduction

The research was made in multiple stages in two companies, on machines with different CNs. In the first stage were determined the bending coefficients K_i for metal marks with a thickness between 1 and 3 mm, on the following machines with CN:

- Stamping machine TC 200R;
- Bending Machine type SAFAN.

The bending coefficients resulted after the tests and measurements determined the extension of the research on other machines with CN. The second stage of the research introduced a variety of possibilities used to determine the drawings (flat patterns) of the components. The machines used to create the metal components were:

- Stamping machine TruPunch 3000R with CN;
- Bending Machine ERM 30135.

The drawings were calculated in four ways:

a) The drawing of the single part calculated using the bending coefficient K_{Ai} resulted in the first stage;

b) The drawing calculated mathematically on neutral fiber;

c) The drawing calculated on neutral fiber using the coefficients K_{Ei} obtained from the table;

d) The drawing calculated by the bending machine software.

The purpose of the research is to determine the optimal bending coefficient for the components to be obtained with the highest precision. The bending coefficients $K_î$ obtained after the experimental determinations were highlighted tabularly. They can be introduced in the computer aided design program (CAD - Computer Aided Design) for the metal components to be processed using CN machines (CAM - Computer aided - manufacturing). The input of the research for manufacturing components that

follow the deviation of measures highlighted the importance of the quality of metallic marks.

2. Technical requirements

The global economic system allowed the debut of ISO 9000 standards and the instruction of real professionals, which had a powerful impact in the commercial trades between countries [1]. There was a significant leap in quantity and quality in commercial trades, determining a new international economic order [2]. The quality of products and benefits became a priority due to the degree of utility and the need of maximizing the consumer satisfaction. The study and research conducted and presented in this essay focuses on the manufacturing of metal marks made of OL37 with 2.5 mm thickness. The quality and precision of the samples obtained are affected by the presence of variables caused by the machines that perform various activities and also by the tools used and elements that create a system (machine / tool) for achieving the desired purpose [3]. These variables are not included in the software used for the computer aided design and manufacturing [3].

2.1. Semi-manufactured cutting

The calculation of the drawings is important because it contains also the deformations created during the bending process. The metal marks made of metal sheet with g = 2.5 mm were manufactured using the stamping machine TruPunch 3000R. Three types of samples with a gradual degree of complexity were manufactured. For each type of drawing, four types of calculations were used. For the component "L support" (Fig. 1), 4 types of samples were suggested, depending on the drawings (flat patterns) calculated. The bending coefficient (K_i) obtained has been included in the calculation of the drawings as seen in Fig. 2, Fig. 3, Fig. 4 and Fig. 5.

The drawing of sample no. 1 image 25-1-L was calculated using the bending coefficient resulted from the previous research $K_{Aî}$ = 0.52 mm / bending on a 90-degree angle**.**

$$\begin{aligned} L_1 &= \ell_1 - g + \ell_2 - g + K_{Ai} \\ L_1 &= 20 - 2.5 + 30 - 2.5 + 0.52 \\ L_1 &= 45 + 0.52 \\ L_1 &= 45.52mm \end{aligned} \quad (1)$$

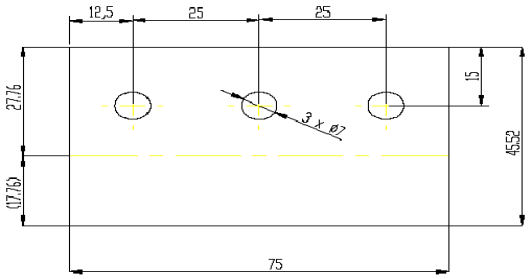

Fig. 2. *The drawing of sample no. 1 (L Support)*

Sample no. 2 image 25-2-L has the drawing calculated from the neutral fiber [5].

$$\begin{aligned} L_2 &= \ell_1 + \ell_2 + \ell_\varphi \\ L_2 &= 20 - 2\times g + 30 - 2\times g + \frac{\pi \times 90^0}{180^0}(r + 0.45\times g) \\ L_2 &= 20 - 2\times 2.5 + 30 - 2\times 2.5 + 1.57(2.5 + 0.45\times 25) \\ L_2 &= 40 + 1.57\times 3.625 \\ L_2 &= 40 + 5.69125 \\ L_2 &= 45.69125mm \end{aligned} \quad (2)$$

For the drawing of sample no. 2, the following information was used: φ= 90º; r = 2.5 mm; x = 0.45 [8]; g = 2.5 mm.

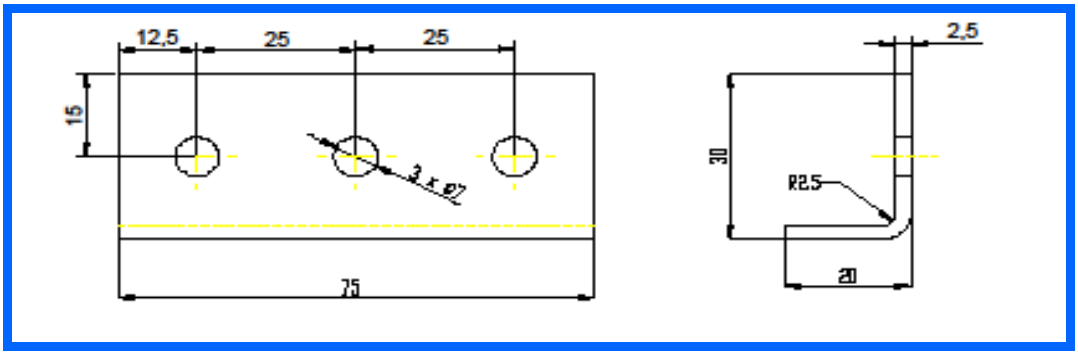

Fig. 1. *L Support (Sample: no. 1, no. 2, no. 3, no. 4)*

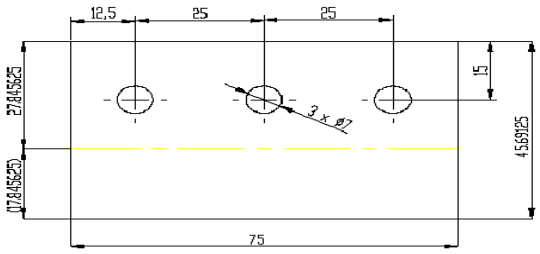

Fig. 3. *The drawing of sample no. 2 (L Support)*

For the drawing of sample no. 3 image 25-3-L, the drawing of the neutral fiber was calculated using the bending coefficient K_{E3} = - 4.4 mm / bending at a 90-degree angle, depending on the thickness of the material g = 2.5 mm and the radius of the bending punch R = 2mm.

$$\begin{aligned} L_3 &= \ell_1 + \ell_2 + K_{E3} \\ L_3 &= 20 + 30 - 4.4 \\ L_3 &= 50 - 4.4 \\ L_3 &= 45.6mm \end{aligned} \quad (3)$$

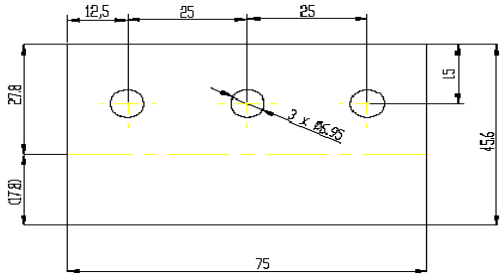

Fig. 4. *The drawing of sample no. 3 (L Support)*

The drawing of sample no. 4 image 25-4-L was calculated by the software of the bending machine with CN (Numerical Command) [4].

$$\begin{aligned} L_4 &= \ell_1 - g + \ell_2 - g + K_{soft} \\ L_4 &= 20 - 2.5 + 30 - 2.5 + 0.52 \\ L_4 &= 45.52mm \end{aligned} \quad (4)$$

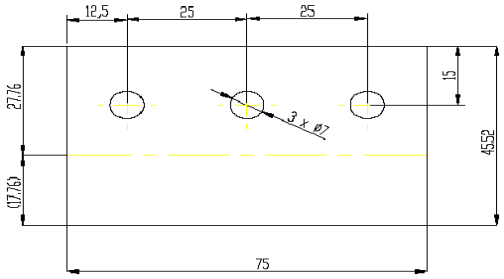

Fig. 5. *The drawing of sample no. 4 (L Support)*

The profile of the component "U Support" is presented in Fig. 6. The 4 types of samples depending on the drawing calculated are described in Fig. 7, Fig. 8, Fig. 9 and Fig. 10.

The drawing of sample no. 5 image 25-1-U (Fig. 7) was calculated using the bending coefficient K_{Ai} resulted in the first stage of the research K_{Ai} = 0.52 mm / bending at a 90-degree angle.

$$\begin{aligned} L_5 &= \ell_1 - g + \ell_2 - 2 \times g + \ell_3 - g + 2 \times K_{Ai} \\ L_5 &= 20 - 2.5 + 40 - 2 \times 2.5 + 20 - 2.5 + 2 \times 0.52 \\ L_5 &= 35 + 35 + 1.04 \\ L_5 &= 71.04mm \end{aligned} \quad (5)$$

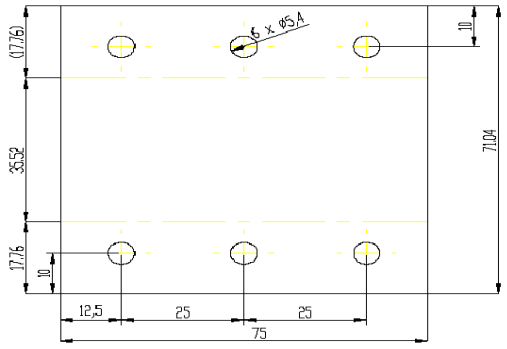

Fig. 7. *The drawing of sample no. 5 (U Support)*

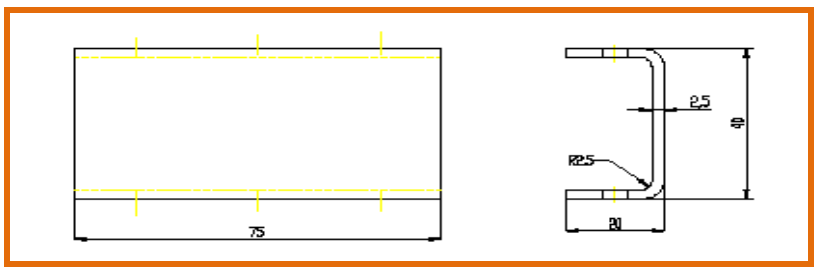

Fig. 6. *U Support (Sample: no. 5, no. 6, no. 7 and no. 8)*

For sample no. 6 image 25-2-U (Fig. 8) the drawing was calculated on neutral fiber [5].

$$\begin{aligned} L_6 &= \ell_1 + \ell_2 + \ell_3 + 2\times\ell_\varphi \\ &= 20 - 2\times g + 40 - 4\times g + 20 - 2\times g + 2\times \frac{\pi\times 90^0}{180^0}(r + 0.45\times g) \\ &= (20-5)\times 2 + 40 - 4\times 2.5 + 3.14\times(2.5 + 0.45\times 2.5) \\ &= 30 + 30 + 3.14\times(2.5 + 1.125) \\ &= 60 + 3.14x3.625 \\ &= 60 + 11.3825 \\ &= 71.3825.mm \end{aligned} \quad (6)$$

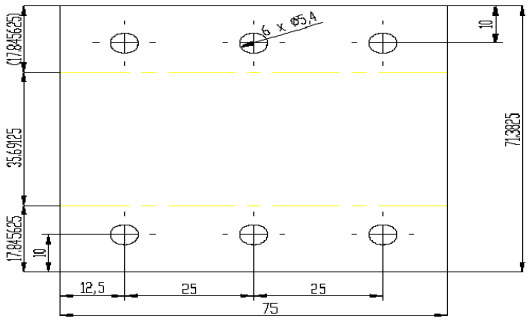

Fig. 8. *The drawing of sample no. 6 (U Support)*

The drawing of sample no. 7 image 25-3-U was calculated according to the coefficient de K_{E3} = -4.4 mm / bending at a 90-degree angle (Fig. 9).

$$\begin{aligned} L_7 &= \ell_1 + \ell_2 + \ell_3 + 2\times k_{E3} \\ L_7 &= 20 + 40 + 20 - 2\times 4.4 \\ L_7 &= 80 - 8.8 \\ L_7 &= 71.2mm \end{aligned} \quad (7)$$

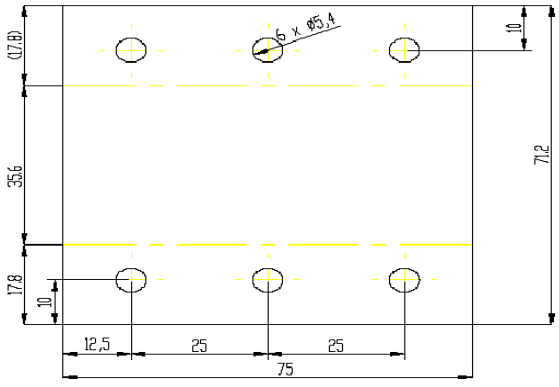

Fig. 9. *The drawing of the sample no. 7 (U Support)*

The drawing of the sample no. 8 image 25-4-U was calculated by the software of the bending machine with C.N (Fig. 10).

$$\begin{aligned} L_8 &= \ell_1 - g + \ell_2 - 2\times g + \ell_3 - g + 2\times k_{soft} \\ L_8 &= 20 - 2.5 + 40 - 2\times 2.5 + 20 - 2.5 + 2\times 0.52 \\ L_8 &= 35 + 35 + 1.04 = 71.04mm \end{aligned} \quad (8)$$

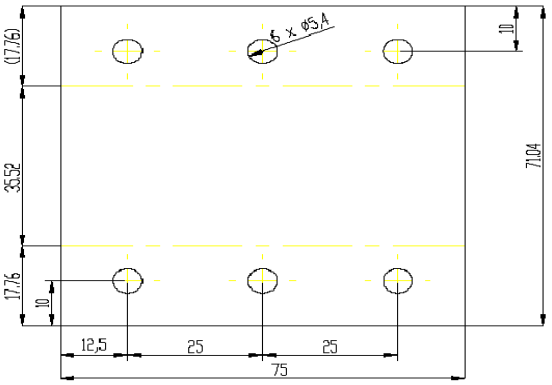

Fig. 10. *The drawing of the sample no. 8 (U Support)*

The profile of the "Ω Support" component is described in Fig. 11 and the drawings were calculated in four ways (Fig. 12, Fig. 13, Fig. 14, Fig. 15).

The drawing of the sample no. 9 image 25-1-Ω (Fig. 12) was calculated using the bending coefficient $K_{Aî}$ = 0.52mm/ bending at a 90-degree angle [5].

$$\begin{aligned} L_9 &= \ell_1 - g + \ell_2 - 2\times g + \ell_3 - 2\times g + \ell_4 - 2\times g + \ell_5 - g + 4\times K_{Ai} \\ L_9 &= 25 - 2.5 + 25 - 2\times 2.5 + 25 - 2\times 2.5 + 25 - 2\times 2.5 + 25 - 2.5 + 4\times 0.52 \\ L_9 &= 45 + 60 + 2.08 \\ L_9 &= 107.08mm \end{aligned} \quad (9)$$

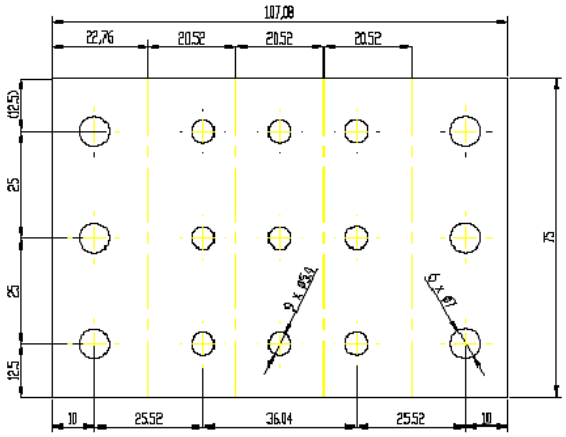

Fig. 12. *The drawing of sample no. 9 (Ω Support)*

The drawing of sample no. 10 image 25-2-Ω (Fig. 13) was calculated mathematically on neutral fiber according to the thickness of the material and the radius of the bending punch.

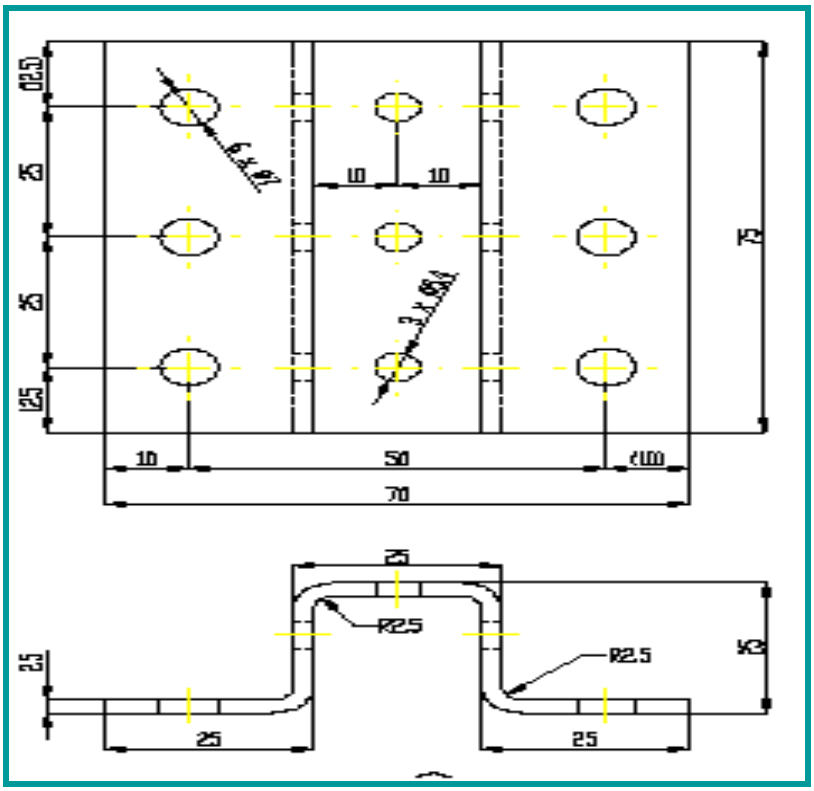

Fig. 11. *Ω Support (Sample: no. 9, no. 10, no. 11 and no. 12)*

$$L_{10} = \ell_1 + \ell_2 + \ell_3 + \ell_4 + \ell_5 + 4 \times \ell_\varphi$$
$$L_{10} = 25 - 2 \times g + 25 - 4 \times g + 25 - 4 \times g + 25 - 4 \times g + 25 - 2 \times g + 4 \times \frac{\pi \times 90^0}{180^0}(r + 0.45 \times g) \quad (10)$$
$$L_{10} = (25-5) + (25-10) \times 3 + 25 - 5 + 3.14 \times 2 \times (2.5 + 0.45 \times 2.5)$$
$$L_{10} = 40 + 45 + 6.28 \times 3.625$$
$$L_{10} = 85 + 22.765$$
$$L_{10} = 107.765.mm$$

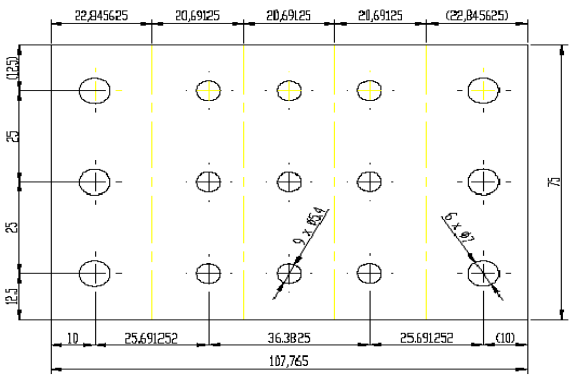

Fig. 13. *The drawing of sample no. 10 (Ω Support)*

The drawing of sample no. 11 image 25-3-Ω (Fig. 14) was calculated on neutral fiber according to the bending coefficient K_{E3} = -4.4 mm / bending at a 90-degree angle.

$$L_{11} = \ell_1 + \ell_2 + \ell_3 + \ell_4 + \ell_5 + 4 \times k_{E3}$$
$$L_{11} = 25 + 25 + 25 + 25 + 25 - 4x4.4 \quad (11)$$
$$L_{11} = 125 - 17.6$$
$$L_{11} = 107.4mm$$

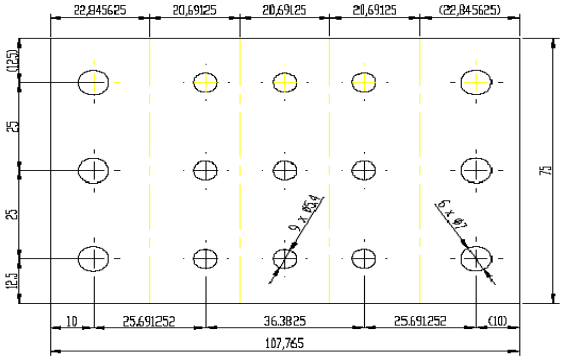

Fig. 14. *The drawing of sample no. 11 (Ω Support)*

The drawing of sample no. 12 image 25-4-Ω (Fig. 15) was calculated by the software of the bending machine with CN.

$$L_{12} = \ell_1 - g + \ell_2 - 2\times g + \ell_3 - 2\times g + \ell_4 - 2\times g + \ell_5 - g + 4\times k_{soft}$$
$$L_{12} = 25 - 2.5 + 25 - 2\times 2.5 + 25 - 2\times 2.5 + 25 - 2\times 2.5 + 25 - 2.5 + 4\times 0.5225 \quad (12)$$
$$L_{12} = 45 + 60 + 2.09$$
$$L_{12} = 105 + 2.09$$
$$L_{12} = 107.09mm$$

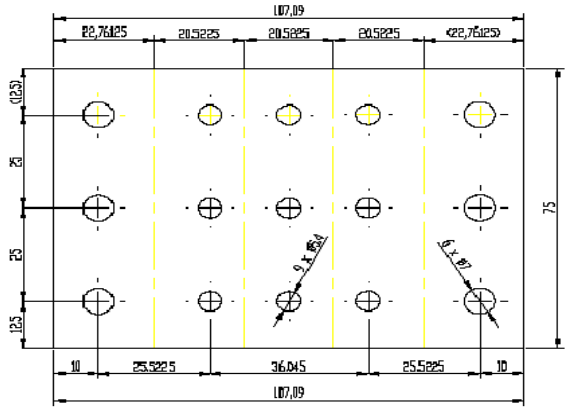

Fig. 15. *The drawing of sample no. 12 (Ω Support)*

The final data was centralized in Table 1. There are differences between the drawings and these differences increase gradually, depending on the complexity and the number of the bent component [6].

2.2. Measuring the benchmarks of the samples after stamping

The samples cut using the stamping machine TruPunch 3000R (table 2) were measured using the digital calipers Mitutoyo that has a precision of ± 0.01 mm. The stamping precision according to the specifications of the machine TruPunch 3000R is ± 0.1mm. From every type of sample five pieces were executed.

2.3. Bending semi-manufactured materials

The bends of the stamped samples were done through the bending process. The company where the research was made had an important processing center equipped with numerical controlled machines and the necessary tools and devices. The resulted benchmarks, consistent with the execution image, depend on the user's experience and professionalism.

Table 1. *The drawings calculated using the four methods*

Sample name (g = 2.5 mm)	The drawing determined by tests and measurements K_{Ai}	The drawing calculated on neutral fiber	The drawing calculated on neutral fiber with K_{E3} coefficient	The drawing calculated by the software of the bending machine
Sample no. 1÷4 - L support	45.52 mm	45.69125 mm	45.6 mm	45.52 mm
Sample no. 5÷8 - U support	71.04 mm	71.3825 mm	71.2 mm	71.04 mm
Sample no. 9÷12 - Ω support	107.08 mm	107.765 mm	107.4 mm	107.09 mm

Table 2. *The drawings calculated using the four methods*

Sample	Image	Nominal benchmark (mm)	Sample no. 1 (mm)	Sample no. 2 (mm)	Sample no. 3 (mm)	Sample no. 4 (mm)	Sample no. 5 (mm)
Sample no. 1	25-1-L	45.52	45.53	45.58	45.53	45.54	45.54
Sample no. 2	25-2-L	45.69125	45.71	45.7	45.71	45.71	45.7
Sample no. 3	25-3-L	45.6	45.61	45.62	45.63	45.61	45.63
Sample no. 4	25-4-L	45.52	45.52	45.57	45.57	45.56	45.53
Sample no. 5	25-1-U	71.04	71.05	71.03	71.09	71.01	71.05
Sample no. 6	25-2-U	71.3825	71.31	71.38	71.38	71.3	71.3
Sample no. 7	25-3-U	71.2	71.2	71.16	71.16	71.16	71.16
Sample no. 8	25-4-U	71.04	71.05	71.03	71.09	71.01	71.05
Sample no. 9	25-1-Ω	107.08	106.98	107.09	107.08	107.11	107.09
Sample no. 10	25-2-Ω	107.765	107.7	107.76	107.79	107.78	107.75
Sample no. 11	25-3-Ω	107.4	107.36	107.4	107.4	107.42	107.34
Sample no. 12	25-4-Ω	109.09	107.02	107.1	107.1	107.1	107.07

The fields of elastic and plastic deformation are a product of bending. The plastic and elastic deformation of the semi-manufactured material is produced only in the area near the bending line [7]. The tools used for the bending process were chosen according to the type of material, the thickness of the metal sheet and the configuration of the component, which positively influenced the quality and precision of the execution. For the calculation of the drawing was taken into consideration the type of punch and die used. A punch with R = 2 mm and a die with an opening V = 16 mm [9] were selected. The bending was done freely without calibration. The sequence of the bending operations used to create the benchmark "L Support" is described in Fig. 16.

The components created were measured and the data was centralized in Table 4. The deviations and the nominal benchmarks were also calculated in order to choose the most optimal option. The limits for the linear deviations are according to Table 3.

Fig. 16. *Bending samples no. 1, 2, 3, 4*

Table 3. *Maximum deviations to linear dimensions except for countersinks*

Execution	Benchmark 0.5 mm up to 3 mm	Benchmark 3mm up to 6 mm	Benchmark 6 mm up to 30 mm	Benchmark 30 mm up to 120 mm
Smooth	±0.05	±0.05	±0.1	±0.15
Medium	±0.1	±0.1	±0.2	±0.3
Rough	±0.2	±0.3	±0.5	±0.8
Coarse	-	±0.5	±1	±1.5

Table 4. *Deviations from the nominal benchmarks of sample 1, 2, 3, 4*

L Support	Component no.1 (mm)		Component no.2 (mm)		Component no.3 (mm)		Component no.4 (mm)		Component no.5 (mm)	
Nominal benchmark (mm)	20	30	20	30	20	30	20	30	20	30
Sample no. 1	19.86	30.19	20.04	30.07	19.86	30.5	19.98	30.10	19.79	30.2
Deviations from the nominal benchmarks (mm)										
	-0.14	+0.19	+0.04	+0.07	-0.14	+0.5	-0.02	+0.20	-0.21	+0.20
Sample no. 2	19.93	30.35	19.89	30.33	19.86	30.42	19.93	30.34	19.89	30.34
Deviations from the nominal benchmarks (mm)										
	-0.07	+0.35	-0.11	+0.33	-0.14	+0.42	-0.07	+0.34	-0.11	+0.34
Sample no. 3	19.92	30.27	19.86	30.31	19.80	30.42	19.88	30.30	19.93	30.30
Deviations from the nominal benchmarks (mm)										
	-0.08	+0.27	-0.14	+0.31	-0.20	+0.42	-0.12	+0.30	-0.07	+0.30
Sample no. 4	19.88	30.22	19.93	30.19	19.96	30.16	19.94	30.20	19.97	30.19
Deviations from the nominal benchmarks (mm)										
	-0.12	+0.22	-0.07	+0.19	-0.04	+0.16	-0.06	+0.20	-0.03	+0.19

For type "U Support" reference points, the benchmarks after the bending process and the deviations from the nominal benchmarks were centralized in Table 5. Fig. 17 describes the bending operations.

Table 5. *Deviations at nominal benchmarks for samples 5, 6, 7, 8*

U Support	Piece no. 1 (mm)			Piece no. 2 (mm)			Piece no. 3 (mm)			Piece no. 4 (mm)			Piece no. 5 (mm)		
Nominal benchmark (mm)	20	40	20	20	40	20	20	40	20	20	40	20	20	40	20
Sample no. 5	19.77	40.17	19.98	19.84	40.35	19.88	19.95	40.20	19.93	19.92	40.25	20.01	19.92	40.23	19.98
Deviations from the nominal benchmarks (mm)	-0.23	+0.17	-0.02	-0.16	+0.35	-0.12	-0.05	+0.20	-0.07	-0.08	+0.25	+0.01	-0.08	+0.23	-0.02
Sample no. 6	19.93	40.45	19.93	19.87	40.31	20.00	19.98	40.15	20.17	19.42	41.00	19.95	19.69	40.75	19.69
Deviations from the nominal benchmarks (mm)	-0.07	+0.45	-0.07	-0.13	+0.31	0	-0.02	+0.15	+0.17	-0.58	+1	-0.05	-0.31	+0.75	-0.31
Sample no. 7	19.99	40.33	19.99	19.95	40.29	20	19.98	40.36	20	19.98	40.36	19.92	19.95	40.25	20.02
Deviations from the nominal benchmarks (mm)	-0.07	+0.33	-0.01	-0.05	+0.299	0	-0.02	+0.36	0	-0.02	+0.36	-0.08	-0.05	+0.25	+0.02
Sample no. 8	19.89	40.53	19.87	19.98	40.56	19.95	20.01	40.51	19.93	19.99	40.56	19.98	20.04	40.54	19.97
Deviations from the nominal benchmarks (mm)	-0.07	+0.53	-0.13	-0.02	+0.56	-0.05	+0.01	+0.51	-0.07	-0.01	+0.56	-0.02	+0.04	+0.54	-0.03

Fig. 17. *Bending samples no. 5, 6, 7, 8*

The benchmarks obtained after bending the reference points type "Ω Support" were centralized in Table 6. The sequence of the bending operations is described in Fig. 18.

Table 6. *Deviations at nominal benchmarks for samples 9, 10, 11, 12*

Ω Support			Sample no. 9	Deviations from the nominal benchmarks (mm)	Sample no. 10	Deviations from the nominal benchmarks (mm)	Sample no. 11	Deviations from the nominal benchmarks (mm)	Sample no. 12	Deviations from the nominal benchmarks (mm)
Piece no.1	Nominal benchmark	25	24.80	-0.20	24.92	-0.08	24.82	-0.18	24.94	-0.06
		25	25.02	+0.02	24.97	-0.03	24.93	-0.07	25.14	+0.14
		25	24.96	-0.04	25.67	+0.67	25.56	+0.56	24.96	-0.04
		25	25.17	+0.17	25.08	+0.08	24.87	-0.13	25.00	0.00
		25	24.95	-0.05	24.92	-0.08	24.85	-0.15	24.95	-0.05
Piece no.2	Nominal benchmark	25	24.98	-0.02	24.94	-0.06	24.79	-0.21	24.86	-0.14
		25	25.11	+0.11	24.93	-0.07	25.05	+0.05	25.19	+0.19
		25	25.05	+0.05	25.86	+0.86	25.63	+0.63	25.28	+0.28
		25	25.11	+0.11	25.04	+0.04	24.92	-0.08	25.02	+0.02
		25	24.89	-0.11	24.98	-0.02	24.81	-0.19	24.90	-0.10
Piece no.3	Nominal benchmark	25	24.96	-0.04	24.95	-0.05	24.88	-0.12	24.88	-0.12
		25	25.04	+0.04	25.08	+0.08	24.98	-0.02	25.10	+0.10
		25	24.98	-0.02	25.90	+0.90	25.65	+0.65	25.12	+0.12
		25	24.98	-0.02	24.87	-0.13	24.88	-0.12	25.11	+0.11
		25	24.90	-0.10	24.93	-0.07	24.88	-0.12	24.90	-0.10
Piece no.4	Nominal benchmark	25	24.97	-0.03	24.91	-0.09	24.92	-0.08	24.91	-0.09
		25	25.13	+0.13	25.55	+0.55	24.89	-0.11	25.07	+0.07
		25	24.75	-0.25	25.96	-0.96	25.49	+0.49	25.17	+0.17
		25	25.11	+0.11	25.12	+0.12	25.09	+0.09	25.07	+0.07
		25	25.04	+0.04	24.91	-0.09	24.88	-0.12	24.89	-0.11
Piece no.5	Nominal benchmark	25	25.19	+0.19	24.92	-0.08	24.90	-0.10	24.89	-0.11
		25	25.34	+0.34	25.13	+0.13	25.10	+0.10	25.04	+0.04
		25	24.12	-0.88	25.18	+0.18	25.42	+0.42	25.33	+0.33
		25	25.3	+0.30	25.10	+0.10	25.10	+0.10	25.01	+0.01
		25	25.14	+0.14	25.06	+0.06	24.92	-0.08	24.81	-0.19




Fig. 18. *Bending samples no. 9, 10, 11, 12*

3. Conclusion

1. From the analysis and the comparison of the results obtained, it may be concluded that the dimensions of the stamped samples are between the accepted limits of the stamping machine tolerance TruPunch 3000.

2. The deviations from the nominal benchmarks are caused by the vibrations that occur during the stamping process, but also by the tools used during this process.

3. The stamping machine TruPunch 3000R is extremely capable and very productive, the transfer speed on axis Ox is 90 m/min and on axis Oy is 60 m/min [10]. The vibrations that occur during the stamping process are inevitable, but the usage of the tools also influences the quality in execution of the components.

4. The high speed in changing the tools, the movement route of the index on high routes, (the metal sheet has the surface of 1500 x 3000 mm^2) and the forces created during the stamping process that can reach up to 20 KN are factors that produce vibrations even if the machine is strongly constructed [10].

5. A negative influence in the execution of components using the stamping machine is the uneven appearance of the surfaces of the metal sheets due to lamination, as this has an uneven thickness.

6. After the samples were bent, the deviations from the nominal benchmarks were significant. We suggest determining the optimal bending coefficient by using an algorithm, which is the subject of another essay.

References

[1]. Bacirov I. C., Juran J. M., *A man for history quality - Quality Assurance*, number 74, S.U.A., 2013.
[2]. Zaharia R. M., Braileanu T., *Uniunea Europeana și economia globala, suport de curs*, Universitatea Ioan Cuza, Centrul de Studii Europene, Iasi, 2007.
[3]. Tempea I., Dugaesescu I., Neacsa M., *MECANISME - Notiuni teoretice si teme de proiect rezolvate*, Editura PRINTECH, Bucuresti, 2006.
[4]. Trumpf GmbH + Co., *Workbook – Fundamentals TC 500R and TC 200R*, Edition 03/99, Ditzingen, 1999.
[5]. Lucretiu R., *Sheet – Bending*, Biblioteca digitala, Bucuresti, 2011.
[6]. ***, www.sm-tech.ro/boschert-gizelis.htm.
[7]. Stancioiu A., Popescu Gh., Girniceanu Gh., *Fiability & Durability*, nr. 2/2009, Editura "Academica Brancusi", Targu Jiu, 2009.
[8]. ***, Color-metal.ro/indoirea-tablelor.
[9]. ***, www.eurostampsrl.it/en/offer-request.
[10]. ***, *Manual for the use and maintenance of your machine* – Manual Synchro.

THE ANNALS OF "DUNAREA DE JOS" UNIVERSITY OF GALATI
FASCICLE IX. METALLURGY AND MATERIALS SCIENCE
Nº. 1 - 2017, ISSN 1453-083X

ANALYSIS OF FACTORS WITH CONSIDERABLE ACTION ON RECYCLING WEEE FOCUSED ON METALS RECOVERY

Anişoara CIOCAN
"Dunarea de Jos" University of Galati
e-mail: aciocan@ugal.ro

ABSTRACT

From an economic point of view, the driving force of rapid technological development of WEEE recycling solutions is the recovery of valuable metals, until not long ago just on copper and gold. Nowadays many other metals have become the target of WEEE recycling. From this point of view, the importance of WEEE recycling results from the analysis of factors with considerable action on this process. This paper highlights the necessity of WEEE recycling by analyzing the following key issues regarding the recovery of valuable metals. The study was mainly focused on the following aspects: electronic waste is a significant source of base and precious metals, and also of scarce metals; many of the metals which are essential in the manufacture of EEE; the availability of metals necessary in the production of EEE constantly decreases; supply shortages for many elements obtained from natural resources; worldwide ore reserves are limited and unequally distributed; in the world, the production of essential metals in the construction of a mobile phone is dominated by a few companies; the extraction of many metals in a ore deposit is co-dependent on other factors.

KEYWORDS: WEEE, recycling, valuable metals, recovery, economic factors

1. Introduction

The rapid progress of electronics and telecommunications industry over the past few years has focused on meeting the increasingly demanding requirements of consumers across the world for performing and multifunctional devices. The electronic industry has been steadily developing and growing both in market size, as well as in models and suppliers of devices. The smartphone can be given as example (Figure 1) [1].

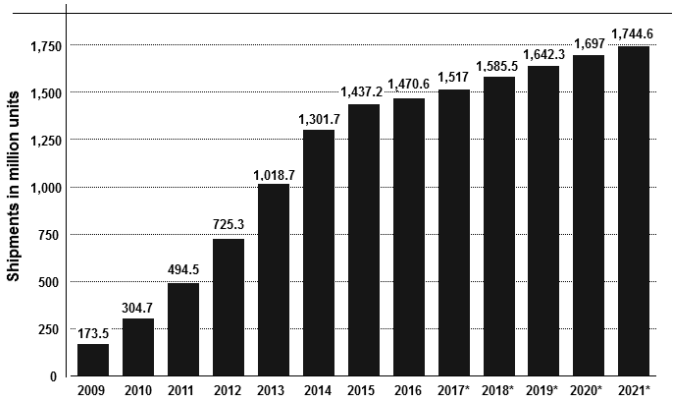

Fig. 1. *Global smartphone shipments, forecasted from 2010 to 2021 (in million units). Observation: The statistic depicts the forecast total unit shipments of smartphones worldwide from 2009 to 2016 with data forecasted for 2017 to 2021* [1]

This evolution has led to a very high growth in both the number of metals needed to produce increasingly complex devices and the number of devices that meet market requirements (Figure 2 and Figure 3).

Technological innovation and intensive marketing forced the acceleration of the EEE replacement process. These aspects, correlated with the quantity of EEE on the market and the evolution of equipment life, have led to a huge increase in the amount of generated waste (Table 1).

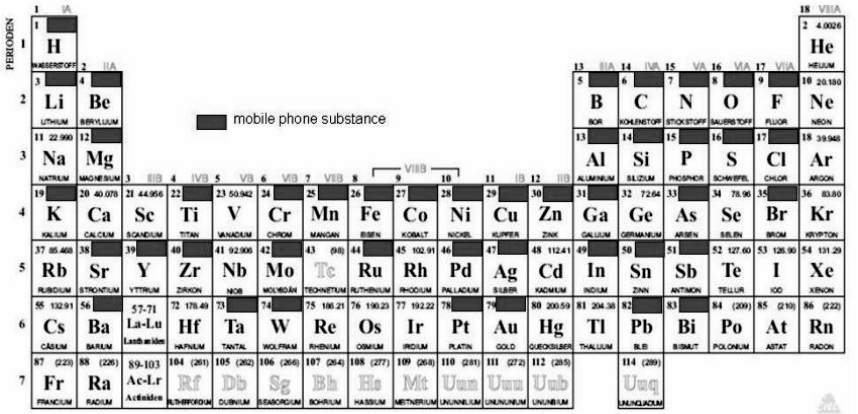

Fig. 2. *Elements used at mobile phone fabrication* [2]

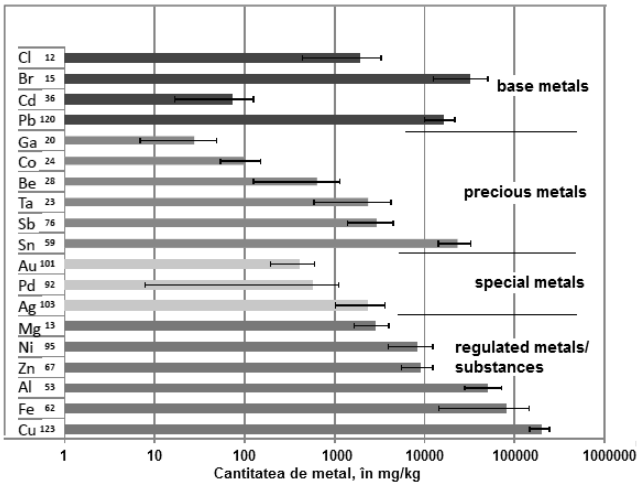

Fig. 3. *Evaluation of datasets on the content of printed circuit boards 1995-2013* [3]

Table 1. *Total quantity of generated electronic waste* [4]

Year	E-waste generated (Mt)	Population (billion)
2010	33.8	6.8
2011	35.8	6.9
2012	37.8	6.9
2013	39.8	7.0
2014	41.8	7.1
2015	43.8	7.2
2016	45.7	7.3
2017	47.8	7.4
2018	49.8	7.4

The electronic waste becomes a valuable resource of metals, especially for those that are precious and scarce [5-7].

WEEE are an excellent resource for metals because they contain many rare and very valuable elements from the periodic table. As a result, these are considered as "urban mining deposits". The literature notes that WEEE have valuable metals in higher concentration than ores, even though over the years, manufacturers have gradually reduced the content of these metals to reduce the cost of the equipment. So, the gold content in WEEE is greater than 4 to 80 times and also, the copper content is 30 to 40 times higher in relation to their concentration in natural resources. As example the gold: content in ores is ~5 g/t Au; content in WEEE is 200-250g/t Au in PC circuit boards, 300-350 g/t Au in cell phones and respectively 2000 g/t PGM in automotive catalysts [2].

2. Highlight and discussion of factors important for WEEE recycling

The recycling of end-of-life devices must be analyzed from an economic and environmental perspective. The disposal of WEEE in landfills essentially impedes to reintroduce the metals from their composition in the production cycle of new products. Lost metals must be replaced by those extracted from ores, and thus natural resources in the earth's crust would be quickly exhausted. Moreover, the operations specific to primary mining and extractive metallurgy are accompanied by significant consumption of material and energy resources and by damage to the environment [7]. Consequently, at end-of-life the EEEs need to be collected and introduced into environmentally sound recycling streams where technologies with maximal recovery efficiency are applied.

The importance of recycling WEEE for metal recovery is highlighted by the analysis of factors with significant action on the process. The key factors of WEEE recycling related to metal recovery are the following:

- importance of metals for electronic industry;
- availability and security of the metal supply;
- existence and availability of substitutes for the considered metal;
- consequences of deficit for certain metals;
- strategic importance of the application in which metal is used;
- impact of recycling on the environment;
- benefits of DEEE recycling.

For electronic industry, the increasing demand for metals can be assessed as high or moderate. The supply risks must be evaluated in relation to the regional concentration of mining operations. Moreover, the deficit must be assessed by comparing data on resource, production and demand. The restrictions for recycling are assessed by the nature of requests. The metals are necessary in many devices but in low quantity. As a result, the metals are dissipated in more types of devices. There are physical or chemical limitations on recycling. Many countries do not have adequate technologies and/or recycling infrastructure because they do not have financial incentives for these operations.

Electronic wastes, in particular printed circuit boards, are significant source of base and precious metals, and also of scarce metals. In agreement, United Nations Environment Program - UNEP, U.S. Congress, U.S. Department of Defense, Resource Efficiency Knowledge Transfer Network of the United Kingdom, German Environmental Agency have named many of the important elements for EEE manufacture as *strategic, rare, special or critical metals* [8]. This characterization is based on the economic, social and political importance of metals and the applications in which they are used. Furthermore, according to these criteria, metals from EEE can be arranged in a series in relation to themselves. This allows for the prioritization of metals that must be recovered from electronic waste. In agreement with UNEP's strategy regarding resource efficiency / sustainable consumption and production, the list of critical metals in EEE includes: indium (In), germanium (Ge), tantalum (Ta), magnesium (Mg), niobium (Nb) and tungsten; PGM or platinum group metals, such as ruthenium (Ru), platinum (Pt) and palladium (Pd)], tellurium (Te), cobalt (Co), lithium (Li), gallium (Ga) and RE (rare earths) [9]. In the case of mobile phones, antimony, beryllium, palladium, indium and platinum especially must be considered [6].

In high-performance electronic equipments, the metals named critical perform essential functions. For these metals, there are few replacement materials or these have not been found yet to meet the requirements. For example, palladium or platinum have no substitution alternatives and their huge dispersion in various products makes recovery much expensive and difficult. The possibility of supplying these metals can sometimes be limited. This leads to significantly higher prices and also to difficulties to ensure the amount necessary for current production, with negative economic and social consequences [10]. By common agreement, the countries members EU, Japan and USA have considered that the supply of some of these metals would be endangered in the very near future [8]. A study made by the Öko-Institut for UNEP about the situation of critical metals used in the EEE industry pointed out that tellurium, indium and gallium are the most problematic elements in the short term (the prospect

for the next five years); on a medium-term perspective, rare earth elements, lithium, tantalum, palladium, platinum and ruthenium are crucial; on long term, by 2050, germanium and cobalt will come to be critical (Figure 4) [8, 9].

The majority of important reserves of ores (with sufficient concentration of the element of interest from which are produced the metals necessary for the EEE industry) have been intensively exploited and as a result their availability in nature is constantly decreasing (Table 2). As example, in Figure 5 is shown the situation of gold from primary mining. The depletion of mineral resources requires the extraction of metals from poor ores. In this situation, even with performing technologies, the energy consumption is higher and the pollutants are emitted in larger quantities.

The quantity of metals that can be ensured from natural resources is limited. Electronics industry has a significant impact on metal demand. The total amount of metals with important role in the construction of new equipment used in emerging technologies has a relatively large proportion (Table 3).

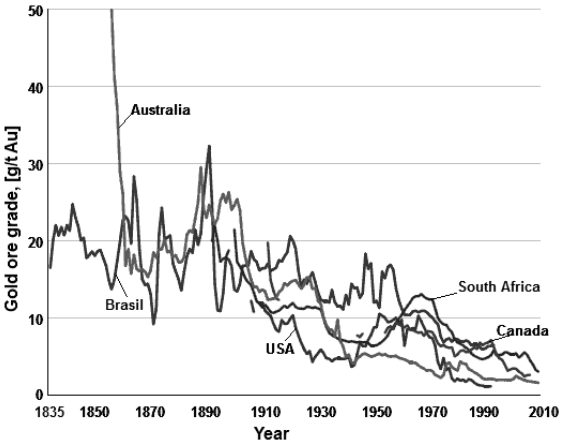

Fig. 5. *Evolution of gold ores in the period 1830 - 2010* [8]

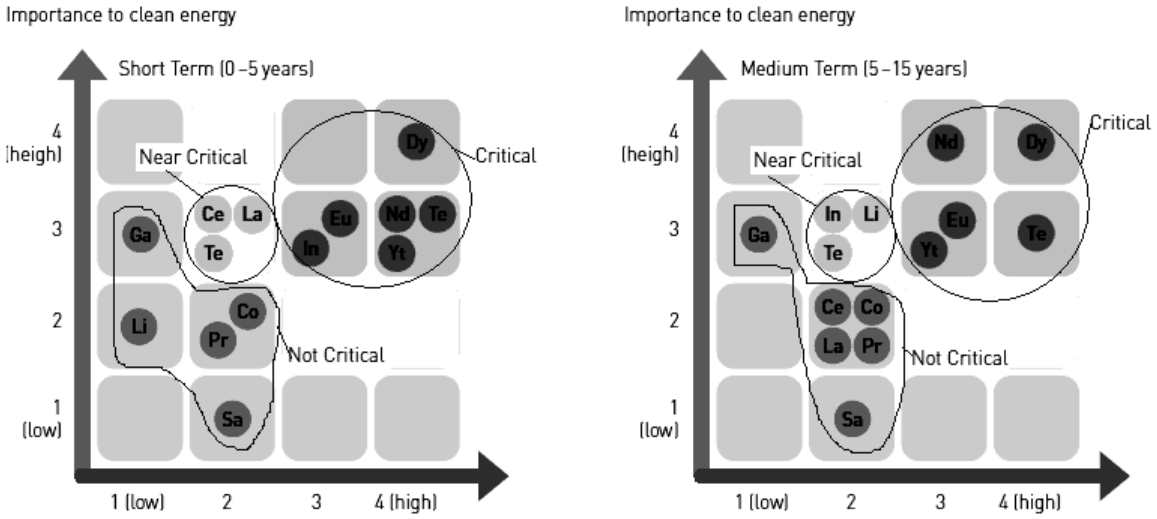

Fig. 4. *Critical levels of some elements, according to U.S. Department of Energy for 2010* [8]

Table 2. *Availability of rare and expensive metals from natural resources (if the consumption and the production of critical metals is maintained at current rate)* [11]

Number of years left	Elements
100-1000	Cr, Al, P, Se, Pt, Ta, earth metals (La, Ce, Pr, Nd, Sm, Eu, Gd, Tb, Dy, Ho, Er, Yb, Lu)
50-100	Ni, Cu, Cd, Tl, U
5-50	Zn, Ge, Ga, As, Rh, Ag, In, Sn, Sb, Hf, Au

Table 3. *Global demand for metals used for manufacturing EEE and the quantity produced* [12]

Element	World mine production*, [tons/year]	Demand for EEE*, [tons/year]	Demand related to mine production, [%]
Ag	20,000	6,000	30
Au	2,500	250	10
Pd	215	32	15
Pt	220	13	6
Ru	30	6	20
Cu	16,000,000	4,500,000	28
Sn	275,000	90,000	33
Sb	130,000	65,000	50
Co	58,000	11,000	19
Bi	5,600	900	16
Se	1,400	240	17
In	480	380	79
*rounded quantities. Source: USGS Mineral commodity summaries 2007			

The depletion of raw material reserves coupled with the increased demand of technological metals makes predictable the supply deficit for many elements (Table 4) [12]. For example, by estimation, the abundance of indium in the Earth's crust is evaluated only at 0.24 ppm. For this vital element for LCD screens, solar cells and semiconductors, the natural resources can be estimated to disappear in about 13 years [8].

Over the years, the worsening of the deficit in accordance with the accelerated growth of metals demand has reflected indirectly on their price (Figure 6).

On the other hand, the availability of critical metals is influenced by how ores deposits are geographically distributed. In the world, the regions where ore resources are concentrated are non-uniformly distributed (Figure 7). For four metals, important in electronic industry, the situation is as follows: 89% of antimony production is located in China; 89% of beryllium production is located in the United States; 44% of palladium production is established in Russia; 75% of platinum is produced in South Africa along with a significant supply of palladium [13].

Table 4. *Estimates of the demand for various scarce and valuable technological metals and their compounds used in emerging (sustainable) technologies* [12]

Element	**Production[1)], [t]**	**ETRD*, [t]**		**Indicator****	
		2006	**2030**	**2006**	**2030**
Gallium	152[5)]	28	603	0.18[1)]	3.97[1)]
Indium	581	234	1,911	0.40[1)]	3.29[1)]
Germanium	100	28	220	0.28[1)]	2.20[1)]
Neodymium[6)]	16,800	4,000	27,900	0.23[1)]	1.66[1)]
Platinum[7)]	255	Very little	345	0	1.35
Tantalum	1,384	551	1,410	0.40[1)]	1.02[1)]
Silver	19,051	5,342	15,823	0.28[1)]	0.83[1)]
Cobalt	62,279	12,820	26,860	0.21[1)]	0.43[1)]
Palladium[7)]	267	23	77	0.09[1)]	0.29[1)]
Titanium	7,211,000[3)]	15,397	58,148	0.08	0.29
Copper	15,093.00	1,410,000	3,696,070	0.09	0.24
Ruthenium	29[4)]	0	1	0	0.03
Niobium	44,531	288	1,410	0.01	0.03
Antimony	172,223	28	71	<0.01	<0.01
Chromium	19,825,713[2)]	11,250	41,900	<0.01	<0.01

*ETRD = Emerging Technologies Raw Material Demand;
**Example of calculation for Ga: Indicator 2006 = 28/152 = 0.18; Indicator 2030 = 603/152 = 3.97.
[1)]Data updated by the BGR based on new information [2)]chromite; [3)]concentrate from ore; [4)]consumption; [5)]estimates of global production in China and Russia; [6)]rare earth elements; [7)]platinum group metals

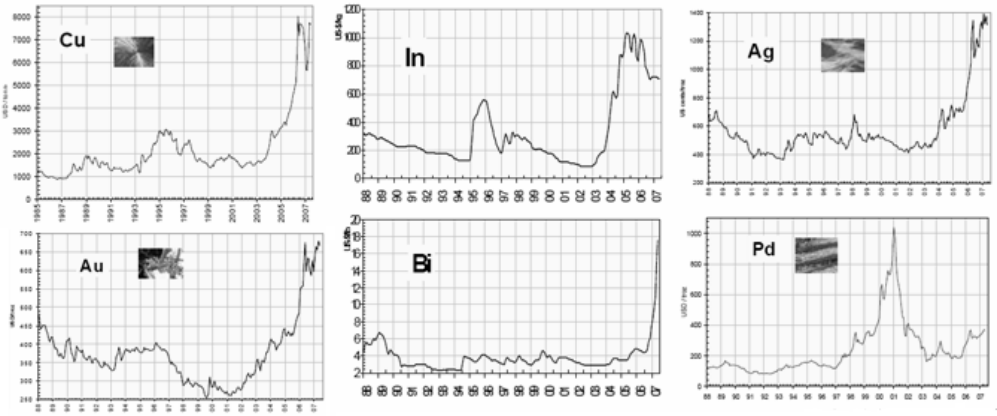

Fig. 6. *Variation of price for some metals over the years* [12]

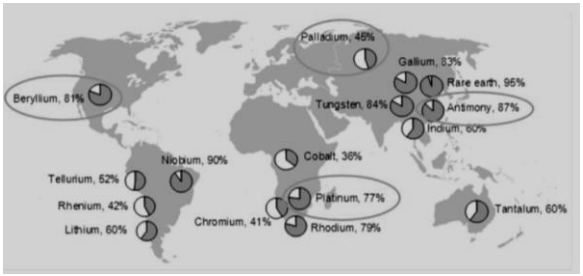

Fig. 7. *Regions with dominant production of primary metals used in mobile phones manufacturing* [14]

The mineral reserves are dynamic, being strongly influenced by technical, economic and political realities. The global resources for some metals and the countries with dominant reserves are given in Table 5.

In addition, with the concentration of natural reserves in certain geographic regions, the availability and security of some metal supplies are conditioned also by an essential aspect. In the world the production of metal is dominated by a few companies (Table 6). Consequently, both supply and price may, in certain circumstances, depend on their behavior.

Table 5. *World reserves of antimony, beryllium, palladium and platinum* [15]

Critical metal	Global reserves in the world, [ktons]	Country with dominant reserves	
		Number 1	Number 2
Antimony	2,100	China (87%)	Bolivia (3%)
Beryllium	80	USA (81%)	China (11%)
Palladium*	100	Russia (45%)	South Africa (39%)
Platinum*	-	South Africa (77%)	Russia (11%)

*World reserves of Pt and Pd combined with rare earth metals

Table 6. *Companies controlling the production of some metals important for electronic industry* [15]

Metals in mobile phones	Share of world production	Country	Mining company, (mine)
Critical metals			
Antimony	82-87%	China	Hsikwangshan Twinkling Star (Hsikwangshan)
Beryllium	81-90%	USA	Brush Wellman (Delta)
Palladium	45-65%	Russia	Norilsk (Norilsk)
Platinum	77-80%	South Africa	Amplants-Implats-Lonnin (Bushveld)
Other metals			
Lithium	60-80%	Chile	Sociedad Quimica y Minera de Chile SA-Soquimich (Salar d'Atacama)
Niobium	90%	Brazil	Companhia Brasileira de Metallurgia e mineraçao CBMM (Araxa)
Rare earth metals	85-95%	China	Baotou Iron and Steel Company (Bayan Obo)
Tantalum	60-70%	Australia	Sons of Gwalia (Woogina)
Tungsten	75-84%	China	Jianxi Tungsten (Minnetals)

Many of the metals, indispensable to the production of EEE, are usually required in very small quantities in an electronic device. But, overall, the huge number of EEE products requires high quantity of these metals. Approximately 80% (or even more) of the cumulative primary production of several technological metals (Ru, Rh, Pd, Os, Ir, Pt, Ga, In or rare earth elements) has been requested in a relatively recent period, being extracted intensively after 1980 [2, 16]. This must be correlated with a period of great progress in electronic industry (Figure 8).

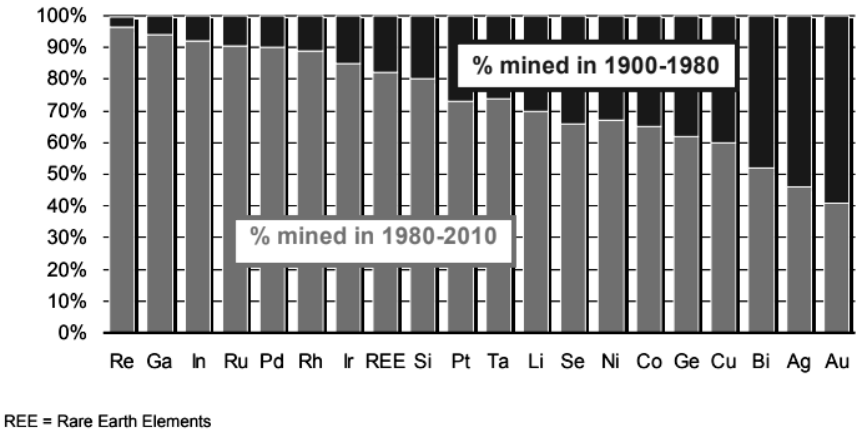

Fig. 8. *Mine production of technological metals: comparison between periods 1900-1980 and 1980-2010* [17]

From the metallurgical point of view, the extraction of many metals in a deposit is often co-dependent on others that are economically viable for exploitation [14]. For a polymetallic ore, the interdependence between minor metals with base metals that coexist in the same ore is explained by the tool called "Metal Wheel". This is a graph which illustrates the complex interactions between metals and when it is possible to recover some critical metals from an economic and thermodynamic point of view from other ores [15]. For example, the production of zinc and lead is associated with obtaining gold and silver. Moreover, other metals important for electronics industry, like indium, cobalt or germanium, result from secondary streams of the metallurgical process for obtaining base metals. Antimony can be obtained directly from its minerals, but also as a secondary metal at the extraction of copper, lead or silver. Platinum and palladium are rarely extracted from native ores that predominantly contain platinum group elements. These are generally together in some ores and are often associated in ores with copper, silver or nickel and obtained as secondary metals in nonferrous metals industry.

These co-dependencies make the production of minor metals sensitive to the factors that have influence on the base metals. The non-intended decisions referred to the production of common metals may have consequences on minor metals. This situation is specific to critical metals used in electronic industry. For example, the EU legislation restricts the use of hazardous substances in electrical and electronic equipment (RoHS Directive 2002/95/EC). For compliance with legislation, the lead alloys have been substituted by safer alternatives. The diminishing of lead production by mining has negative effects on the supply of other metals necessary in electronics industry [15].

3. Conclusion

The electronic devices contain a complex of metals: precious metals (Ag, Au, Pd), base metals and special metals (Cu, Ni, Co, Sn, Al, Fe, Ti, Ta, Bi), metals of concern (Be, Pb, Cd, As, Sb, Cr, In etc.). Recycling is a significant source for the supply of many of the metals and provides numerous benefits such as: resource conservation, energy savings, reduced volumes of waste, reduced emissions associated with primary materials production. In the past years, the WEEE recycling industry had a simple objective: recovery of copper and gold. Today the sustainable recycling is focused on recovering rare or special metals for electronic industry. A comprehensive analysis of the metals from EEE devices made possible the identification of factors with considerable action on recycling WEEE focused on valuable metals recovering. Using data collected from literature, were identified the opportunities and barriers regarding the importance of metals from electronic products. The result of the analyses highlights the metals which should be recovered from WEEE by recycling based on the following indicators: availability and security of the metal

resources; existence of substitutes for the considered metal; consequences of deficit for certain metals; geographical distribution of resources and of important companies for their production.

References

[1]. *,** https://www.statista.com/statistics/263441/global-smartphone-shipments-forecast.
[2]. Caffarey M., *Recycling Electronic End of Life Materials*, SERDC, www.serdc.org, October 2012.
[3]. Rotter V. S., Flamme S., Münster F. H., Ueberschaar M., Chancerel P., *Recovery of Critical Metals - Towards a Paradim Shift in WEEE Recycling*, ISWA World Congress Viena, 2003.
[4]. Baldé C. P., Wang F., Kuehr R., Huisman J., *The global e-waste monitor – 2014*, United Nations University, IAS – SCYCLE, Bonn, Germany, 2015.
[5]. Rotter V. S., Flamme S., Münster F. H., Ueberschaar M., Chancerel P., *Recovery of Critical Metals – Towards a Paradim Shift in WEEE Recycling*, ISWA World Congress Viena, 2003.
[6]. Evans C., Renz R., McCullough E., Lawrence S., Pavlenko N., Suter S., Brundage A., Hecht J., Lizas D., Bailey P., *Case Study on Critical Metals in Mobile Phones. Final Report*, http://www.oecd.org/env/waste/smm-casestudies.htm.
[7]. Dodson J. R., Hunt A. J., Parker H. L., Yang Y., Clark J. H., *Elemental sustainability: Towards the total recovery of scarce metals*, Chemical Engineering and Processing, 51, p. 69-78, 2012.
[8]. Reuter M. A., Hudson C., Van Schaik A., Heiskanen K., Meskers C., Hagelüken C., *Metal Recycling: Opportunities, Limits, Infrastructure, A Report of the Working Group on the Global Metal Flows to the International Resource Panel.*, UNEP, www.unep.org, 2013.
[9]. Buchert M., Schüler D., Bleher D., *Sustainable Innovation and Technology Transfer Industrial Sector Studies. Critical Metals for Future Sustainable Technologies and their Recycling Potential*, United Nations Environment Programme & United Nations University, July 2009.
[10]. *,** *EurActiv*, *EU Starts Screening Raw Materials 'Critical List'|EU – European Information on Sustainable Dev.*, http://www.euractiv.com/en/sustainability/eu-starts-screening-raw-materials-critical-list/article-187791, 2009.
[11]. Rhodes C., *Short on reserves: the planet's metal reserves could be running out sooner that we think. We need to start recycling them urgently*, Chem. Ind. 16, 2008.
[12]. Hagelüken C., *Metal Recovery from e-scrap in a global environment. Technical capabilities, challanges and experience gained*, 6th session of OEWG Basel Convention, 7 sept. 2007.
[13]. ***, *A Sustainable Materials Management Case Study: Critical Metals and Mobile Devices*, OECD, http://www.oecd.org, 2011.
[14]. ***, *Case Study on Critical Metals in Mobile Phones. Final Report OECD*, https://www.oecd.org.
[15]. ***, *Materials Case Study 1: Critical Metals and Mobile Devices*, Working Document OECD Environment Directorate, OECD, https://www.oecd.org, 2010.
[16]. Hagelüken C., Meskers C., *Technology challenges to recover precious and special metals from complex products*, http://ewasteguide.info, 2009.
[17]. Hagelüken C., Meskes C. E. M., *Complex life cycles of precious and special metals*. Linkages of Sustainability, T. Graedel, E. Van der Voet (eds.) MIT Press, 2010.

MANUSCRISELE, CĂRŢILE ŞI REVISTELE PENTRU SCHIMB, PRECUM ŞI ORICE CORESPONDENŢE SE VOR TRIMITE PE ADRESA:

MANUSCRIPTS, REVIEWS AND BOOKS FOR EXCHANGE COOPERATION, AS WELL AS ANY CORRESPONDANCE WILL BE MAILED TO:

LES MANUSCRIPTS, LES REVUES ET LES LIVRES POUR L'ECHANGE, TOUT AUSSI QUE LA CORRESPONDANCE SERONT ENVOYES A L'ADRESSE:

MANUSCKRIPTEN, ZIETSCHRITFTEN UND BUCHER FUR AUSTAUCH SOWIE DIE KORRESPONDENZ SID AN FOLGENDE ANSCHRIFT ZU SEDEN:

After the latest evaluation of the journals by the National Center for Science Policy and Scientometrics (**CENAPOSS**), in recognition of its quality and impact at national level, the journal will be included in the B^+ category, 215 code (http://cncsis.gov.ro/userfiles/file/CENAPOSS/Bplus_2011.pdf).

The journal is already indexed in:

SCIPIO-RO: http://www.scipio.ro/web/182206

EBSCO: http://www.ebscohost.com/titleLists/a9h-journals.pdf

Google Academic: https://scholar.google.ro

The papers published in this journal can be viewed on the website of "Dunarea de Jos" University of Galati, the Faculty of Engineering, pages: http://www.sim.ugal.ro, http://www.imsi.ugal.ro/Annals.html.

Name and Address of Publisher:
Contact person: Elena MEREUȚĂ
Galati University Press - GUP
47 Domneasca St., 800008 - Galati, Romania
Phone: +40 336 130139
Fax: +40 236 461353
Email: gup@ugal.ro

Name and Address of Editor:
Prof. Dr. Eng. Marian BORDEI
Dunarea de Jos University of Galati, Faculty of Engineering
111 Domneasca St., 800201 - Galati, Romania
Phone: +40 336 130208
Phone/Fax: +40 336 130283
Email: mbordei@ugal.ro

AFFILIATED WITH:

- THE ROMANIAN SOCIETY FOR METALLURGY
- THE ROMANIAN SOCIETY FOR CHEMISTRY
- THE ROMANIAN SOCIETY FOR BIOMATERIALS
- THE ROMANIAN TECHNICAL FOUNDRY SOCIETY
- THE MATERIALS INFORMATION SOCIETY (ASM INTERNATIONAL)

Edited under the care of the FACULTY OF ENGINEERING

Annual subscription (4 issues per year)

Editing date: 15.03.2017
Number of issues: 200
Printed by Galati University Press (accredited by CNCSIS)
47 Domneasca Street, 800008, Galati, Romania